Imperial College London

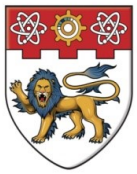

NANYANG TECHNOLOGICAL UNIVERSITY

EXPLORING NEW BIOPROCESS CONSIDERATIONS FOR CARDIOMYOGENESIS OF EMBRYONIC STEM CELLS

TEO AILING

DEPARTMENT OF CHEMICAL ENGINEERING

SCHOOL OF CHEMICAL AND BIOMEDICAL ENGINEERING

2014

EXPLORING NEW BIOPROCESS CONSIDERATIONS FOR CARDIOMYOGENESIS OF EMBRYONIC STEM CELLS

TEO AILING

Department of Chemical Engineering (Imperial College)

School of Chemical and Biomedical Engineering (NTU)

A thesis submitted to the Imperial College London and the Nanyang Technological University in partial fulfilment of the requirement for the degree of

Doctor of Philosophy

Acknowledgments

First, I would like to express my utmost gratitude to my supervisors, Assistant Professor Mayasari Lim of Nanyang Technological University and Professor Athanasios Mantalaris of Imperial College for their extensive guidance and support. Under their supervision, I have learnt and grown as a researcher.

I would also to thank Professor Mary Chan (NTU) and Professor Alexander Bismarck (Imperial) for giving me the opportunity to join this joint Imperial-NTU PhD programme.

Next, I would like to thank the colleagues in my research groups for their generous help and advice. They include Cao Xue (NTU), Dr Amir Morsehdi (NTU), Dr David Yeo (Imperial), Dr Supacharn Tangviriyasirikul (Imperial), Anastasia Georgiou (Imperial), Idtisak Paopo (Imperial), Dr Iliana Fauzi (Imperial), Thi Thu Thao Vu (NTU) and all other people whom I have worked together with.

I also greatly appreciate the advice and help from my collaborators, Assistant Professor Zhou Yufeng and Wang Jen-chieh, in the ultrasound studies.

Last but not least, I would like to acknowledge the financial support from Nanyang Technological University – Imperial College joint PhD programme and Singapore National Research Foundation (Technion Seed Grant) that enabled me to carry out the various studies.

Statement of Originality

This is a statement to certify that the content of this thesis is my own work. I attest that the intellectual content of this thesis is the product of my work and that all assistance received in the preparation for this thesis have been acknowledged.

- Ailing Teo

Copyright Declaration

Abstract

Ex vivo cardiomyocytes production from pluripotent stem cells is highly attractive as a future clinical therapy for cardiovascular diseases. Scaled-up 3-dimensional cell culture can be used to produce clinically relevant cell numbers but requires numerous bioprocess design considerations. In this thesis, we employed hydrogel encapsulation of mouse embryonic stem cells (mESCs) to study various novel design parameters that could be used for large-scale cardiomyocyte production. First, we demonstrated that our novel rotary, perfused bioreactor provided a dynamic and perfused environment that was superior to a commercial rotary wall bioreactor and conventional tissue culture vessels in terms of cell numbers and cardiac differentiation. With this novel bioreactor, we had also investigated the effects of pH on cardiomyogenesis. Cardiomyogenesis was found to be sensitive to different pH values, where slight fluctuations could cause significant changes to cell proliferation and cardiac differentiation. Last but not least, we utilised ultrasound as a novel mechanical stimulus for cardiac differentiation of mESCs and demonstrated its benefits in improving cardiomyocyte yield.

Contents

Nomenclature

2D	Two-dimensional
3D	Three-dimensional
AFP	Alpha-fetoprotein
ANOVA	Analysis of variance
AT1	Angiotensin II Type 1
ATN	Sacromeric α-actinin
BM-MSC	Bone marrow mesenchymal stem cell
BMP	Bone morphogenetic protein
cDNA	Complementary DNA
CPC	Cardiac progenitor cell
CSC	Cardiac stem cell
cTNI	Cardiac Troponin I
cTNT	Cardiac Troponin T
CVD	Cardiovascular disease
DMEM	Dulbecco modified Eagle's medium
dsDNA	Double stranded DNA
EB	Embryoid body
ECM	Extracellular matrix
ESC	Embryonic stem cell
FBS	Fetal bovine serum
HARV	High aspect rotating vessel
hESC	Human embryonic stem cells
HepG2-CM	HepG2 conditioned medium

HIF-2 α	Hypoxia induced factor – 2α
ICM	Inner cell mass
IMDM	Iscove's modified Dulbecco's medium
iPSC	Induced pluripotent stem cell
LIF	Leukemic inhibitory factor
LIUS	Low intensity ultrasound
MAPK	Mitogen activated pathway kinase
mESC	Murine embryonic stem cell
MHC	Myosin heavy chain
MSC	Mesenchymal stem cell
Oct-3/4	Octamer binding factor-3/4
PBS	Phosphate buffered saline
PCR	Polymerase chain reaction
RCCS	Rotary cell culture system
SSEA-1	Stage specific embryonic antigen 1
STLV	Slow-turning lateral vessel
TCP	Tissue culture polystyrene
TGF	Transforming growth factor
UC-MSC	Umbilical cord mesenchymal stem cell

List of tables

List of figures

Day 14, 18 and 21 of differentiation process. Bar represents significant difference of indicated sample from its respective control. * represents significant difference between the indicated sample and its previous time point. $p < 0.05$, $N = 3$...- 170 -

Summary

Cardiovascular disease is a leading cause of mortality globally with very limited resources for those requiring a heart transplant or suffering severe damages from myocardial infarct. Ex vivo generation of cardiomyocytes for cell replacement therapy is therefore an appealing opportunity for cardiac diseases. However, the ability to produce functional cardiomyocytes with clinically relevant numbers faces challenges and requires development of scalable processes and 3-dimensional (3D) cell cultures. This thesis aims to address key bioprocess considerations in for differentiating 3D cultures of pluripotent cells towards cardiomyocytes by using murine embryonic stem cells (mESCs) as a cell model and employing the strategy of hydrogel encapsulation.

First, design of the culture platform was considered since different bioreactor designs and feeding strategies will result in different hydrodynamic profiles, which impact availability of nutrients in the immediate macro- and micro-environment, thus affecting cardiomyogenesis. In this thesis, a novel rotary perfused bioreactor was used to determine how the different culture environments might impact cardiac differentiation of encapsulated mESCs. As a comparison, mESCs were also differentiated in the conventional tissue culture flasks and the commercial high-aspect rotary vessel (HARV) bioreactor. Higher cell numbers and viabilities were observed in the dynamic cultures (HARV and novel bioreactor) than the static flask cultures, showing the significance of uniform environment in 3D cultures of cells. Meanwhile, improved cardiomyogenesis was observed by earlier and higher expressions of cardiac genes such as myosin heavy chains and cardiac troponin T in the novel bioreactor's perfused

environment. From this study, it was shown that the novel bioreactor provided a dynamic and perfused environment that was favourable for cardiomyogenesis and shown to be conducive for producing cardiomyocytes with clinically relevant numbers.

Differentiation of ESCs appears to be rather sensitive to pH. Literature has shown that pH affected contractile properties of cardiomyocytes and stem cell fate. When encapsulated mESCs were cultured under different pH environment, lower proliferation and viability was observed at pH 6.8 than at pH 7.1 and 7.4. Meanwhile, a lower extent of cardiomyocyte differentiation and higher residual pluripotency occurred at pH 6.8. These showed the high sensitivity of mESCs in cardiac differentiation towards pH environment, where a slight pH fluctuation can cause drastic changes. Therefore, it is important to maintain a tight control on environmental parameters so as to ensure high cell yields and quality in a scaled-up production involving pluripotent stem cells.

To improve the yield and contractile properties of cardiomyocytes derived from cell sources, mechanical stimulation was incorporated. In the last chapter of this thesis, a novel application of ultrasound on cardiomyocyte differentiation from mESCs was studied. Low intensity ultrasound was found to enhance cardiomyocyte differentiation of mESCs greatly in both conventional 2D differentiation and 3D encapsulated cultures. Besides increasing cardiomyocyte yield, spontaneous endodermal differentiation was also inhibited by ultrasound. This translated to an increase in mesodermal selectivity during mESC differentiation, hence improving cardiomyocyte yield and purity. These findings strongly suggest the feasibility of using a novel application of ultrasound for improving cardiac differentiation from pluripotent cell sources.

In the effort to develop a scalable 3D bioprocess for generating cardiomyocytes, this thesis addressed three important aspects in an indefinite list of factors: (1) cell culture platforms, (2) pH environment, and (3) incorporation of a mechanical stimulus (i.e. ultrasound). These studied areas have shown their impact on cardiomyogenesis of mESCs and could be used as references to study and design an optimal bioprocess to produce cardiomyocytes of clinically relevant numbers and contractile properties from human pluripotent stem cells.

1 Introduction

Cardiovascular disease (CVD) is a leading cause of mortality in most developed countries and accounted for 30% of all deaths worldwide in 2008 [1]. Moreover, increased affluence and lifestyle habits in these developed countries will only aggravate current situation. For instance, current statistics of people suffering from obesity and having lack of healthy lifestyle in the United States predicted an increase in the number of people suffering from heart diseases and also an increased associated healthcare costs [2]. Among the mortality rates caused by CVDs, coronary heart disease was responsible for 42% of this population. In patients suffering from coronary heart disease, blood vessels become constricted due to causes such as fatty deposit. This limits blood supply to the heart and eventually causes myocardial ischemia. During myocardial ischemia, limited oxygen and nutrient supply to cardiac muscle cells results in cell death, causing infarction. The infarcted area then undergoes inflammation and forms collagenous scar tissue, which is void of cardiac muscle functionality such as muscle contraction and electrical conduction. This will result in decreased cardiac ventricular working capacity and increases the risk of heart failure. Till date, clinical interventions have yet to restore full functionality in the infarcted area. Patients who suffer from severe heart damage have to undergo heart transplantation for regaining full cardiac function. However, availability of suitable heart donors is very scarce. Therefore, there is a need to seek other clinical therapies which can allow patients to regain cardiac functionality and are relatively more accessible for the expanding number of patients.

Given the current advances in biotechnology and stem cell research, a promising therapy for cardiac regeneration is to obtain cellular products through cardiac tissue engineering for repairing the infarcted heart muscles. However, several

major challenges remain in the roadmap of using cardiac tissue engineering for CVD therapies. These challenges include generation of cellular products with clinically relevant cell numbers, cardiac properties and tissue integration. Therapeutic applications require a local administration of 10^8 – 10^9 of functional cardiomyocytes per treatment in order to replace the damaged ventricular cardiomyocytes in a post-infarct patient [3]. Conventional two-dimensional (2D) methods using tissue culture polystyrene (TCP) has been extensively used for producing cardiomyocytes but can be impractical and laborious for large-scale production. Moreover, cells cultured on TCP face high possibility of altered morphologies because of the adherence to hard surfaces. Such altered morphologies will result in unnatural cell behaviours that differ significantly from the three-dimensional (3D) *in vivo* environment. 3D culture systems have been developed to mimic the physical and structural components of the *in vivo* microenvironment, facilitating 3D cell-cell and cell-matrix interactions. Therefore, in cardiac tissue engineering, the goal is to design 3D environments that would bear greater resemblance to cardiomyocytes in the myocardium than 2D cultures [4, 5].

One major challenge in obtaining cellular products for clinical therapies is to obtain clinically relevant cell numbers readily. To achieve this, scalable platforms are usually needed and one of such platform is the bioreactors. Utility of bioreactors can also reduce inter-batch variability through uniform mixing and control and monitoring of culture parameters. Several studies have demonstrated the ability of bioreactor cultures to produce cardiomyocytes in numbers of 10^8 magnitude [6, 7]. During the development to obtain suitable bioreactor designs, different design parameters should first be considered. Hydrodynamics is an

important design factor that will affect cell fate through availability and distribution of soluble cues and physical stress in the culture environment.

Aside from the need to achieve clinically relevant cell numbers, the quality of differentiated cardiomyocytes must be ensured to be suitable for transplantation, i.e. high purity and ability to perform contractile function. Therefore, it will be necessary to maximise the yield of cardiomyocytes. Besides using chemical agents to enhance cardiomyogenesis, another approach is to utilise mechanical stimulation, which has been shown to aid cardiomyocyte differentiation by increasing cardiomyocytes numbers and improving contractile functions [8-10]. Mechanical stimulation can also be incorporated into the bioreactor design and this would provide an integrative approach.

1.1 Hypothesis and objectives

In the pursuit of developing a better cell culture platform for 3D cardiac tissue engineering from pluripotent cells, this thesis seeks to define parameters that would affect an optimal design of the bioprocess. Control of extracellular microenvironment is hypothesised to direct cell fate decisions; different design parameters that influence hydrodynamics, nutrient transport and even mechanical stimuli would affect yield and purity of cardiomyocytes from pluripotent cell sources. Such parameters includes, but are not limited to, the hydrodynamic flow within a culture vessel, the environmental pH and any physical stimulation on the cells.

This thesis aims to investigate how the three stated parameters can affect cardiomyogenesis from pluripotent embryonic stem cells. As these works involved a large-scaled cell culture environment and due to the ethical

considerations of using human embryonic stem cells, murine embryonic stem cells (mESCs) was adopted as a model to demonstrate the impact of various bioprocess parameters on cardiomyogenesis of pluripotent stem cells. mESCs had been extensively studied and were established in methods of clonegenity, ex vivo expansion and differentiation. However, for clinical applications, human ESCs (hESCs) or human induced pluripotent stem cells (IPSCs) should be used. Though mESCs and hESCs are both derived from the inner cell mass tissue of embryos, share the key pluripotent transcription factors (Oct-4, Nanog, Sox-2) and can differentiate to somatic cell lineages, they displayed fundamental species-specific differences in their *in vitro* growth characteristics and self-renewal signalling pathways [11, 12]. Human ESCs were found to share several defining features with the less-pluripotent murine epiblast stem cells (EpiSCs), emphasizing that conventional culture conditions may have yet been optimised to stabilise and propagate hESCs [13, 14]. Hanna et al. had successfully rewired hESC and human IPSCs to a more immature state, which was beneficial to clonogencity and ex vivo differentiation efficiency [14]. While more studies are being conducted to establish hESC model and to optimise its culture conditions, mESC was used as a more cost-efficient model to generate hypotheses on how the investigated bioprocess parameters will affect a large-scaled cardiac differentiation of human pluripotent cells.

In the next section (Chapter 2), different types of cells which can be used as sources for obtaining cardiomyocytes were reviewed. Selected bioreactor designs which are currently available and their nutrient transport considerations were also briefly discussed, and were followed by a brief overview on the usage of 3D substrates and physical stimulation for cardiomyogenesis. In Chapter 3, a novel

bioreactor, which incorporated rotary mixing and perfusion, was utilised to differentiate mESCs towards cardiomyocytes and its efficacy was compared to those of conventional TCP cultures and commercial rotary wall bioreactor, HARV. Thereafter sensitivity of ESC differentiation towards culture environmental parameters, specifically extracellular pH, was studied in Chapter 4. Through this, the importance of a bioprocess's ability to ensure uniformity and consistency in the cell culture environment would be demonstrated. Last but not least, the feasibility of using ultrasound to complement cardiomyogenesis was investigated to show its ability as mechanical stimuli in cardiac tissue engineering. Though ultrasound had been used for bone and cartilage regeneration, it has not been studied for cardiac regeneration. The effects of ultrasound on cardiomyogenesis of mESCs were reported for the first time in Chapter 5.

To apply tissue engineering and regenerative medicine for clinical therapies, much work is required to determine efficacy and safety of a stem cell product. The last chapter in this thesis would discuss the significance of the works presented in this thesis and the future developments that are required for translating these works to clinical applications.

2 Background

2.1 Cell sources for obtaining cardiomyocytes

Cardiomyocytes are terminal somatic cells and have limited proliferative capacity. Therefore, it is challenging to use cardiomyocytes to produce large cell numbers required for cardiac construct despite their functional utility. This means that there is a need to consider cell types with higher proliferative ability as sources to obtain cardiomyocytes for transplantation. Numerous studies have differentiated various cell types into cardiomyocytes *in vitro*, one such cell type is the adult skeletal myoblasts. Myoblasts, being precursors of myocytes, have higher proliferative capacities than cardiomyocytes and still contain contractile apparatus [15]. Since they can be extracted from patient's own tissue, it will allow autologous transplantation too. However, as myoblasts are from the skeletal muscle lineage, their integration into the myocardium environment results in problems like arrhythmias and fibrosis [16, 17].

Another potential source is progenitor cells from the cardiac lineage such as cardiac progenitor cells (CPCs) and cardiac stem cells (CSCs) [18, 19]. These cells appear promising as sources for cardiac regeneration due to their high cardiogenic lineage specificity and high self-renewal ability as immature progenitors [20-22]. However, studies suggested that their ability to cause cardiac regeneration might not be due to directed cardiomyogenesis of these transplanted progenitors but due to indirect mechanisms inducing endogenous regeneration of the host's myocardium [23] or residual myocardial tissue fragments from the isolation process [24]. Therefore, more studies are still required to determine their suitability. Moreover, isolation of CPCs and CSCs involves a complex process, posing limitations to obtain sufficient numbers readily for the production of cardiomyocytes.

Mesenchymal stem cells (MSCs) are adult stem cells, which are extensively studied for many tissue engineering applications. Common sources of MSCs include bone marrow and umbilical cord. MSCs from bone marrow (BM-MSCs) and umbilical cord (UC-MSCs) have demonstrated abilities to differentiate into adiopogenic, osteogenic, chondrogenic and cardiomyogenic lineages [25-27]. BM-MSCs have a distinct advantage of being able to inhibit inflammation and evade immune detection [28-31]. This can then prevent rejection and improve recovery during transplantation. However, extraction of BM-MSCs is highly invasive and painful, making it difficult to obtain sufficient numbers from donors. On the other hand, extraction of UC-MSCs is from the placenta or cord lining and thus is non-invasive. Despite the potential in using MSCs for cardiomyogenesis and its demonstrated safety and clinical benefits, both human and non-human MSCs have not produced significant yields of cardiomyocytes with contractile abilities [32-37]. Therefore, more studies are necessary to qualify the potential clinical benefit of MSCs for cardiac diseases.

The discovery of embryonic stem cells (ESCs) presents a highly proliferative and pluripotent cell source that seems promising to generate high cell numbers of all lineages. ESCs can spontaneously differentiate into cardiomyocytes *in vitro* [38]. An advantage of using ESCs is their equal differentiation potential towards cardiogenesis and vasculogenesis. This can be highly beneficial to regenerate a myocardium with vascular network [39, 40]. However, ESCs can also spontaneously differentiate into other undesired cell lineages, leading to teratoma formation. In overcoming this problem, cardiogenic cells can first be separated from other differentiated cells, thus increasing the purity of cardiomyocytes and vascular cells prior to transplantation [41, 42]. Nevertheless, utility of ESCs in

clinical application still raises issues in non-autologous transplantation, immune rejection, fibrosis, arrhythmia [43] and ethical concerns.

One discovery that arose as means to resolve the ethical concerns of using embryos to obtain ESCs is the induced pluripotent stem cells (IPSCs). Cardiomyogenesis of murine IPSCs was first reported in 2008 [44-46]. Subsequently, human IPSC-derived cardiomyocytes were also obtained and found to be similar to those derived from ESCs in their expression of cardiac genes and activity in action potentials [47, 48]. Utility of IPSCs also opens up possibilities for autologous transplantation. However, obtaining IPSCs from somatic cells requires stable transfection, where the most reliable method is viral transfection currently. Unfortunately, such viral transfection could lead to possible karyotypic abnormalities, undermining its clinical suitability. Non-viral transfection methods like transposons [49], protein- and mRNA-based delivery [50-52] and small molecules [53] have been developed but are less efficient. Moreover, utility of IPSCs, similar to ESCs, faces the possibility of teratoma formation upon transplantation in the presence of any residual pluripotent cells.

Many cell types can be considered for obtaining cardiomyocytes for regenerative clinical therapies. Each different source has their own advantages and limitations, as summarised in Table 2.1. In considering the possible cell sources, one must determine the desired quantity and quality of the final cell product. This means selecting suitable sources with the proliferative and differentiating capacities towards clinically relevant numbers, lineage specificity, and maturity of derived cardiomyocytes. With a suitable cell source and a systematic approach in bioprocess engineering, tissue engineering applications of cardiomyogenesis in clinical applications will then be achievable.

Table 2-1 Summary of pros and cons of discussed cell sources for obtaining cardiomyocytes

Cell source	*Pros*	*Cons*
Myoblasts	Contractile apparatus Autologous transplantation	Integration with host tissue
Cardiac progenitors	Lineage specificity	Difficult to extract
MSCs	Anti-inflammatory and anti-rejection abilities	Low cardiomyocyte yield Difficult to extract
ESCs	High proliferative capacity	Teratoma formation
iPSCs	High proliferative capacity	Teratoma formation Need for stable and safe transfection method

2.2 Utilising embryonic stem cells for cardiomyogenesis

2.2.1 Overview of embryonic stem cells

When an embryo is fertilised, gamete cells of the sperm and those of the embryo will join to form an initial cell called the zygote. The zygote next undergoes rapid replication and division into 2-, 4-, 8-, 16-cell ovum. Upon reaching 16-cell stage, cell compaction will start. A morula is then formed where the outer cells start to be more densely packed, forming a cavity and leaving some cells in the interior. Further cell expansion will form a blastocyst of 50-150 cells where the outer shell of cells is called trophectoderm and the interior cells called inner cell mass (ICM). ESCs are derived from the ICMs for ex-vivo uses. This process is briefly illustrated in Figure 2.1.

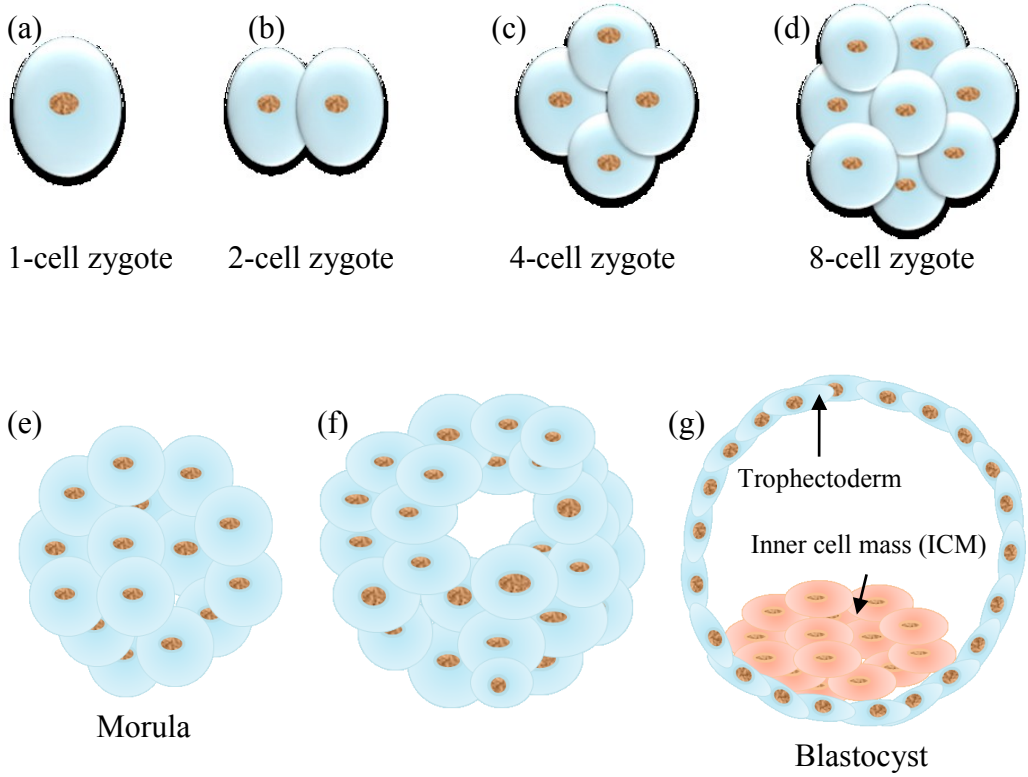

Figure 2-1 Development of fertilized embryo to blastocyst

ESCs are unique for two distinctive properties: (1) their pluripotency and (2) their ability for indefinite symmetrical self-renewal. Being derived from the blastocyst, a form of early stage developing embryo, ESCs are pluripotent, i.e. they have the ability to differentiate into all somatic cells in the body, as illustrated in Figure 2.2. This is different from the adult stem cells isolated from developed tissues. Adult stem cells are only multipotent, i.e. they have the ability to differentiate into cells of limited lineages and not all lineages. Together with ESCs' ability for unlimited self-renewal, ESCs' potential in regenerative therapies shows a distinct benefit potential over that of adult stem cells and other progenitors.

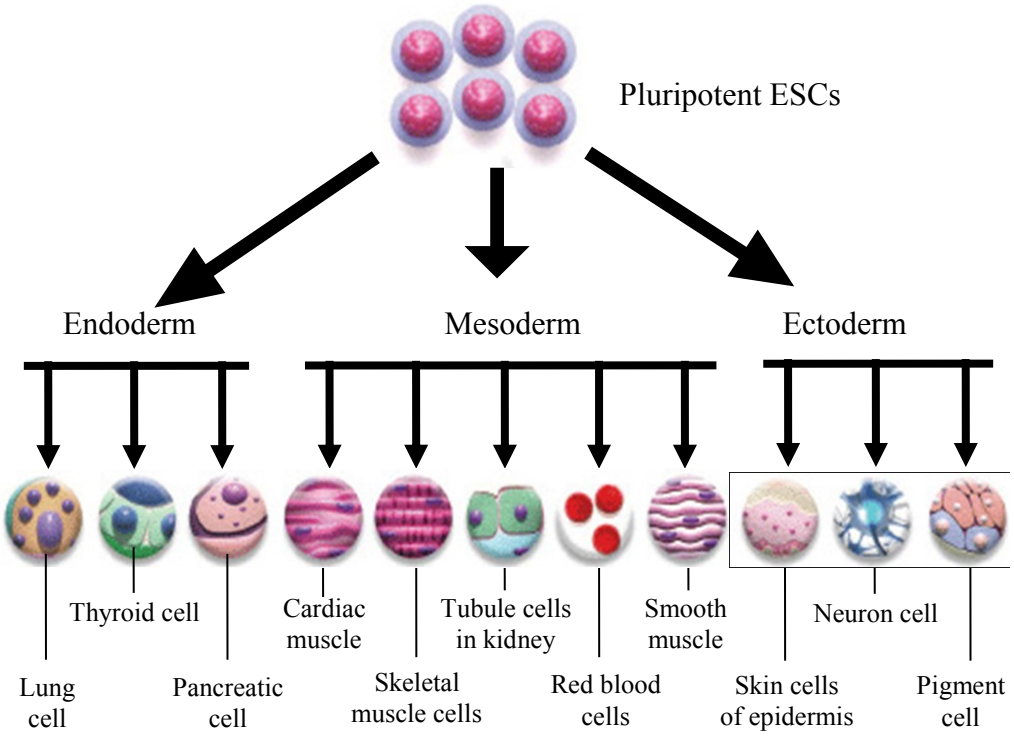

Figure 2-2 Examples of different somatic cells derived from pluripotent embryonic stem cells (Adapted from sigmaaldrich.com)

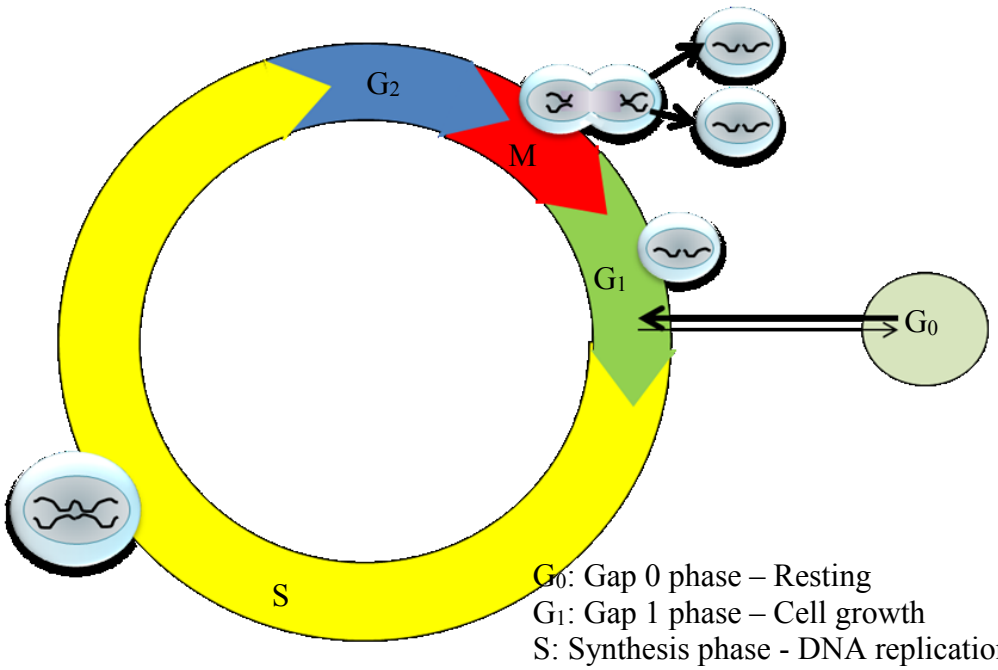

Figure 2-3 Cell cycle of embryonic stem cells, where synthesis phase is longer and gap phases are shorter than most somatic cells

The indefinite self-renewal property of ESCs can be attributed to the fact that ESCs do not require external stimulus to initiate DNA replication unlike differentiated somatic cells. As seen in cell cycle illustration (Figure 2.3), the G1 checkpoint is absent and S phase of DNA synthesis forms the bulk of ESCs' cycle. To ensure pluripotency during the indefinite self-renewal, assays have been developed based on genes or surface antigens associated with undifferentiated ESCs [54, 55]. Such markers include stage-specific embryonic antigen (SSEA) series, tumour rejection antigen (TRA) series, cluster of differentiation 9 (CD9), alkaline phosphatase activity, Nanog, and octamer binding factor 3/4 (Oct3/4).

Oct3/4 has been widely used to identify undifferentiated ESCs. It is expressed exclusively in blastomeres, early embryo cells, and cells of germline lineages

[56]. Oct3/4 plays a crucial role in determining and monitoring the cell fate of ESCs. For instance, it participates in activation and inhibition of different target genes to maintain ESCs in a proliferating and non-differentiating phenotype [57]. During gastrulation in vivo, it is down-regulated when ESCs differentiate to primitive ectodermal and trophectodermal cells [58]. Niwa et al. has also demonstrated the sensitivity of ESCs to expression levels of Oct3/4 [59]. When Oct3/4 expression is lower than the critical threshold of two-fold upregulation, differentiation into embryonic ectoderm and mesoderm will still occur.

2.2.2 Differentiation of embryonic stem cells towards cardiomyocytes

Being a pluripotent cell, ESC can differentiate into cells of all three lineages: (1) endodermal lineage, (2) mesodermal lineage, and (3) ectodermal lineage. To understand how ESCs can differentiate to cardiomyocytes amongst all cells, *in vivo* embryonic development can be used as a reference. During the blastocyst stage, the inner cell mass is surrounded by trophectoderm and primitive endoderm (as seen in Figure 2.4). The inner cell mass will start to differentiate to primitive ectoderm (epiblast). Meanwhile, the primitive endoderm differentiates to parietal and visceral endoderm, which are localised in the anterior region [60]. Soon after, primitive ectoderm cells of the epiblast lines over the distal visceral endoderm and triggers various signals for gastrulation stage [61]. During gastrulation, programmed migration of epiblast cells results in formation of a primitive streak along the embryo's posterior axis which will become mesendodermal cells [61, 62]. Mesendoderm is the precursor of mesoderm and endoderm and since cardiomyocytes are of mesodermal lineage, cardiac progenitors will also be formed here [63].

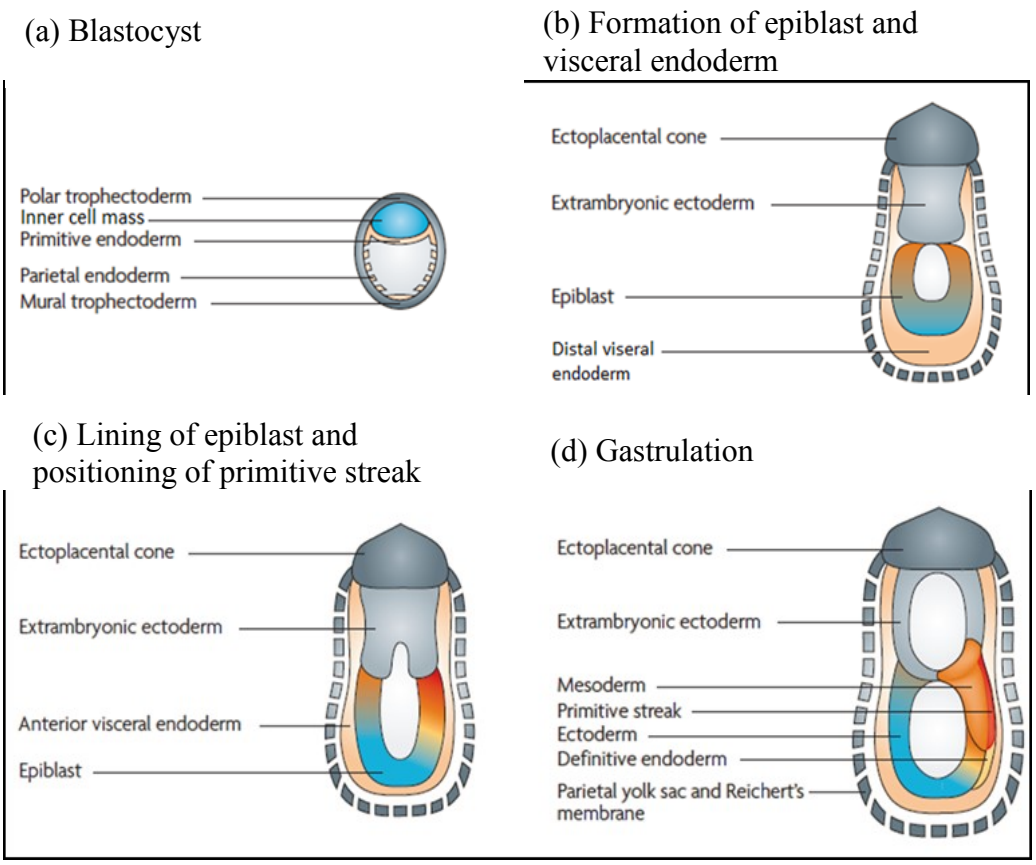

Figure 2-4 *In vivo* early post-implantation development of embryo (Adapted from Tam and Loebel, 2007 [61])

In general, there are four main steps in ESC differentiation towards cardiomyocytes: (1) commitment towards mesoderm, (2) specification towards cardiac progenitors, (3) differentiation towards cardiomyocytes and (4) maturation of differentiated cardiomyocytes. As reviewed by Rajala et al. [64], different gene expressions can be used to identify different stages of this process. During ESC's induction towards mesodermal lineage, transcription factors Brachyury-T and Mesp-1 can be used to identify the primitive streak mesodermal and cardiogenic mesodermal commitment respectively. Mesp-1 was found to promote mesoderm development towards cardiac specificity by binding to regulatory DNA sequences of promoters in the cardiac regulatory network and also by repressing key genes regulating other mesoderm derivatives [65, 66].

Nkx2.5 is a cardiac progenitor transcription factor that Mesp-1 targets to promote mesodermal specificity towards cardiac lineage. It can also be used to monitor ESC specificity towards the cardiac lineage. Last but not least, expressions of cardiac signalling or structural proteins can be used to check the extent of ESC differentiation to cardiomyocytes. Some examples of these markers are α-actinin, myosin heavy chains and cardiac troponin T. Figure 2.5 (as adapted from Cheung and Singha, 2011 [67].) briefly illustrates this differentiation pathway.

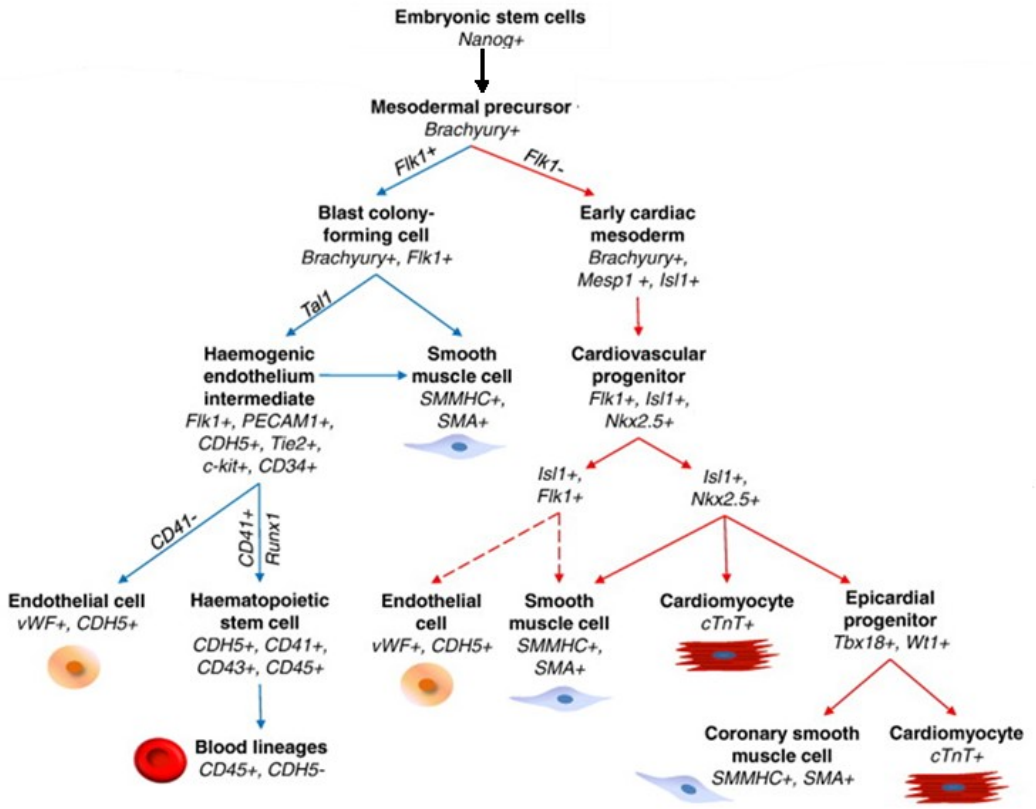

Figure 2-5 Schematic diagram of ESCs' differentiation pathway towards cardiomyocytes and other relevant cells of mesodermal lineage (Adapted from Cheung and Singha, 2011 [67])

To enhance *in vitro* cardiomyogenesis of ESCs, numerous studies have investigated different soluble factors which were favourable. Soluble factors provide biochemical signals which play a key role in influencing cellular pathways and cell fate. Transforming growth factors- β (TGF-β) and bone morphogenetic proteins (BMPs) are important in regulating early embryogenesis such as morphogenesis in embryo and induction of ventral mesoderm [68, 69]. It was also reported that these growth factors such as TGF-βs, BMPs and activins could increase cardiomyogenesis of both hESCs and mESCs, showing increased cardiac expressions and beating areas [70-75]. However, commercial growth factors are usually expensive for usage in large scale culture. Cocktails of factors produced by cultures of other cell lineages can also have similar benefits on cardiomyogenesis of ESCs. One instance is the viseral endoderm-like (END-2) cells. Co-culture with these cells or using their conditioned medium can contribute to efficient formation of cardiac progenitors from both hESCs and mESCs [76-79]. Another possible candidate is the liver cell line. Cultures of liver cancer cells (HepG2) were found to produce soluble factors that efficiently directed mESCs towards mesodermal lineage [79, 80], which could then increase cardiomyocyte differentiation.

Chemicals are preferred over growth factors due to their economic benefits for large scale cultures. Several chemicals have also been observed to promote cardiomyogenesis. They include DNA demethylating agents such as 5-aza-2'-deoxycytidine (decitabine) [81] and 5-azacytidine (azacitidine) [82] which increased the cardiac gene expressions of hESCs and mESCs respectively. Meanwhile derivatives of vitamin A and vitamin C were also used for cardiac differentiation of mESC [83-85]. Cardiogenol C is a small diaminopyrimidine

chemical which is a potent inducer of cardiomyogenesis. It was reported to increase cardiac myosin heavy chain (MHC) expression in mESCs [86]. It could also upregulate Wnt11 expression, which is involved in essential pathways regulating cardiac specification [87, 88].

Soluble factors have a significant impact on cardiomyogenesis via the biochemical cues they provide. However, their efficacy does not depend solely on the factor itself, but also on their availability to cellular microenvironment. In scaled-up cultures, the availability of nutrients and biochemical factors will be heavily influenced by hydrodynamic profiles in the culture vessels. Meanwhile, physical cues can also play a key role in determining cell fate of ESCs. Such physical cues can come from mechanical or electrical stimulation.

2.3 Utilising bioreactors for cardiomyogenesis

Conventional methods of *in vitro* cardiomyocyte differentiation from different cell sources are conducted in 2D plate cultures, involving the use of TCPs. Typically, cardiomyogenesis from these cells involve multi-step procedure. The cells first undergo proliferation to reach the required cell numbers and then differentiation toward the cardiomyogenic lineage. For instance, ESCs will be cultured as an adherent culture on TCP to expand till the required numbers. Thereafter, it will be suspended as aggregates to form embryoid bodies (EBs). Last but not least, these EBs will be replated on TCP for directed cardiomyocyte differentiation. TCP has a low area-volume ratio and restricts the cell densities achieved on these 2D platforms. Therefore, expansion to clinically relevant cell numbers will require handling large number of TCP plates. Being a multi-step procedure, this quantity of TCP plates will usually make such conventional differentiation process laborious and susceptible to high inter-batch variability. With current biotechnology advances, one can consider various possible bioreactor configurations in the scale up of tissue engineering applications to meet specific applications and user preferences.

2.3.1 Bioreactor configurations for cardiomyogenesis

One commonly studied configuration is the spinner flask system [6, 7, 42, 89]. There are currently a few different commercially available configurations such as the Sartorius 2L Biostat MD and Dasgip cellferm-pro system. A spinner flask generally consists of an impeller, as illustrated in Figure 2.6 (a). The impeller provides a mixing action, thus ensuring a well-mixed environment for cell culture. A well-mixed environment improves homogeneity of the cell population during proliferation, EB formation (when ESCs are used), and directed

differentiation. During spinner flask cultures, the cells are either suspended as substrate-free cellular aggregates or seeded on scaffolds [7, 42]. Advantages of this bioreactor design include ease in scale-up and readily available monitoring capabilities. However, there are concerns that the fast spinning impeller motion produces a high shear stress environment that can cause fatal cell damage and be detrimental to cardiomyogenesis.

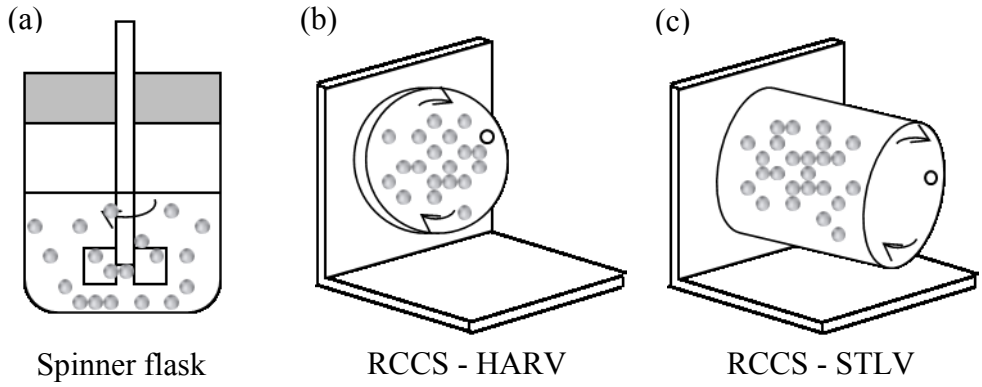

Figure 2-6 Diagrams of some commonly used configurations: (a) spinner flask, (b) RCCS - HARV, and (c) RCCS - STLV

Another common bioreactor configuration is the microgravity simulated rotating systems. The commercial available system is the rotary cell culture systems (RCCS) by Synthecon. Such system achieves homogenous mixing without using impellers. It was first designed by NASA to investigate the effects of microgravity on cells and tissues. Microgravity is simulated via vertical rotation of the culture vessel, resulting cells to be suspended in the vessel's central region. This rotating motion can also provide homogeneous mixing under an ultra-low shear stress environment. RCCS exists in two main configurations: the high-aspect rotating vessel (HARV, Figure 2.6 (b)) and the slow-turning lateral vessel (STLV, Figure 2.6 (c)). These two configurations produce minimal shear stress, thus will be suitable platforms for cell cultures requiring a low shear stress

environment. Cardiomyogenesis studies have also been conducted in RCCS [90-92], demonstrating that the utility of such systems is feasible. As environments of low shear stress with upper limits of 2.5 dyn/cm^2 are typically more favourable for cardiomyocyte maturation [8, 93-95], utility of RCCS have a great potential to produce clinically relevant cardiomyocyte numbers.

Apart from the two commercial bioreactor designs above, novel bioreactors have been developed by individual research groups for cardiomyogenesis. One distinct feature in several bioreactors is the incorporation of pulsatile flow [8, 9, 96-98]. Pulsatile flow can introduce mechanical stimulation or shear stress to cardiac constructs and enable directed cell differentiation or cardiomyocyte maturation. For instance, Hoerstrup et al. designed a bioreactor [96], as seen in Figure 2.7 (a), which used airflow ranging from 50 – 2000 ml/min to provide a systemic pressure of 10 – 240 mmHg for mechanical stimulation . First, controlled pulsed airflow was introduced into the chamber (1), expanding the silicone diaphragm (3). This would induce mechanical stimuli on the cellular construct seeded in position (5) when the expanded silicone diaphragm pushed the fluid though the channel (4) and cellular construct. Brown et al. [8] has also designed a pulsatile perfused bioreactor to provide physiological flow rate and shear stress through pulsatile fluid flow (illustrated in Figure 2.7 (b)). Cardiac construct was held in position (3) by being sandwiched between gaskets (2) and meshes (1) and was subjected to 1Hz pulsatile flow at 0.32 ml/min or 1.50 ml/min. Under these pulsatile flows, improved cardiomyocyte maturation was achieved as indicated by the low excitation threshold, higher maximum capture rate and contraction amplitude.

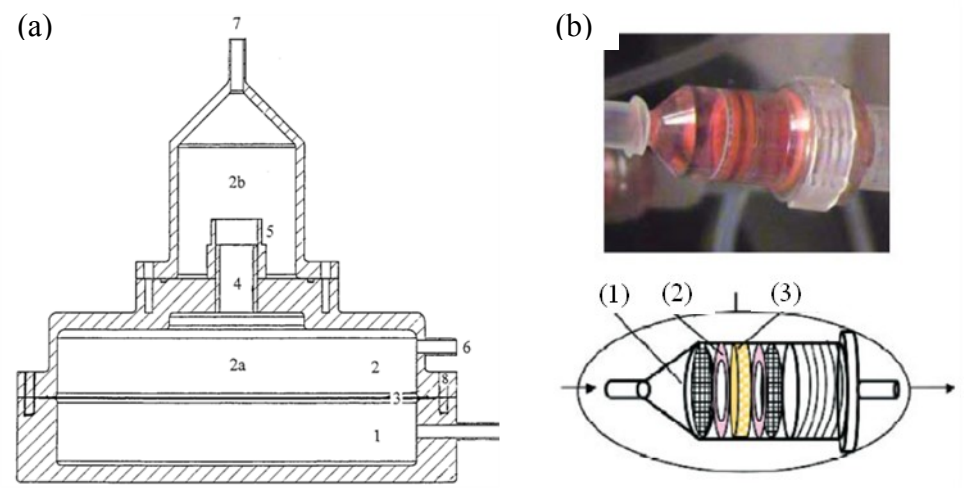

Figure 2-7 Novel bioreactors incorporating pulsatile fluid flow as mechanical stimuli on seeded cells, as designed by (a) Hoerstrup et al. [96], and (b) Brown et al. [8].

2.3.2 Mass transport within bioreactors

One main difference between bioreactor cultures and conventional flask cultures is the presence of hydrodynamic flow. Hydrodynamics will affect flow patterns within a culture vessel and will predicate the transport and availability of nutrients and soluble factors to the cells. In conventional flask culture, where the environment is a static condition with no hydrodynamic flow, transport of soluble factors is mainly via diffusion through the culture medium. Diffusion in static conditions is generally slow and will not be able to replenish the consumed factors at different localised areas of the cell culture. The lack of fluid flow will lead to concentration gradients within the bulk medium and localised extreme conditions, posing several control and monitoring challenges for large-scale cell production. To minimise non-homogeneous culture environments, improved uniformity in the culture vessel can be achieved by convective transport.

2.3.3 Bulk convective transport in bioreactors

In dynamic bioreactors, bulk fluid transport is facilitated by convection, providing a more homogeneous environment within the culture vessel. Under such conditions, more efficient transport of soluble factors can be achieved, leading to higher cell expansion and viabilities [92, 99]. In this well-mixed environment, the peripheral surface of cardiac constructs gave rise to more uniformly distributed cardiomyocytes [100]. Apart from higher cell numbers, viabilities and uniformity, cardiomyogenesis was also enhanced in well-mixed environments. For instance, cardiac genes like Nkx2.5 and α-myosin heavy chain gave a 27-fold and 9-fold increase in the horizontal rotary culture as compared to the static cultures [90]. Similarly, gene expressions of α-myosin heavy chain and atrial natriuretic factor were also higher in differentiating mESCs in rotating wall vessels than in static cultures [92].

Mixing will introduce different flow patterns inside the vessels, thus different methods of mixing will affect the flow patterns and the overall convective transport efficacy. Horizontal shaking used by shaker flask system were found to produce a lower mass transfer efficacy than spinner flasks [101]. Thus such systems may not be suitable for cultures having high oxygen demands, such as cardiomyocyte maturation. Agitation speed must also be optimised to be fast enough to eliminate concentration gradients but gentle enough to minimise any deleterious shear stress. Papadaki et al. has compared constructs of neonatal rat cardiomyocytes cultured in RCCS and spinner flasks [100]. They observed that though both bioreactor configurations provided homogeneous environments, the constructs in RCCS had higher cellularity levels (1.5 fold) and higher expression of Connexin-43 (3.5 folds) and creatin kinase-MM (2 folds) than those in spinner

flasks. This difference might be attributed to the higher shear stress in spinner flasks being detrimental to cardiomyogenesis. Similar to the agitation speed, the vertical rotating speed of RCCS must be optimised. The optimal speed should achieve microgravity and maintain the cells in the central zone to minimise any collision with the wall boundary of the vessel. Consolo et al. have shown that this speed is 25 rpm for hydrogel-encapsulated ESCs in HARV bioreactor [92]. Meanwhile, a rotation speed of 18 rpm is required for cells seeded in 600 μm microbeads and cultured in HARV [102].

Though convection can improve homogeneity of bulk fluid tremendously, the key solute transport within 3D construct is still molecular diffusion. The efficiencies of nutrient transport within constructs affect the cell's microenvironment and thus cell fate such as cardiomyogenesis. Diffusional limitations can cause heterogeneous cell distribution, and cells in regions distant from construct periphery may experience compromised cell viability due to limited nutrient supply. Despite homogeneity in bulk fluid, cardiac constructs in RCCS and spinner flasks only had a viable cellular region of up to 100 μm in thickness along the peripheral region [103, 104]. Meanwhile, their cores contained mostly apoptotic/dead cells, which demonstrated the consequences of diffusion constraints in oxygen supply. To model the effect of such molecular diffusion constraints, nutrient availability inside the 3D constructs can be estimated from a simple mass transfer simulation based on diffusion and consumption rates of oxygen and relevant metabolites. With reference to a hepatocyte spheroids model [105, 106], increasing spheroid sizes would enlarge the core area, which would experience oxygen levels below the critical survival threshold.

As such, the critical radius of the largest spheroid that could be formed is:

$$r = \sqrt{\frac{6\mathrm{DH}(\mathrm{P_{O2}} - \mathrm{P^*})}{\mathrm{O2\ consumption\ rate}}} \quad \ldots\ldots \text{Equation 2.1}$$

where D: Diffusion coefficient of oxygen within aggregate
H: Henry constant of oxygen from air to medium
P_{O2}: Partial pressure of oxygen in the air
P*: Critical pressure of oxygen for cell survival

2.3.4 Perfusion incorporation in bioreactors

Conventional flask cultures involve manual changing of medium, which is referred as fed-batch. The process of medium change involved sudden removal of metabolites and endogenous factors and sudden addition of nutrients. Between medium changes, there will be a gradual decrease in nutrients and a gradual build-up of metabolites. Thus fed-batch cultures will result in inconsistent environment throughout the culture period (Figure 2.8). On the other hand, perfusion enables a continuous supply and removal of nutrients and metabolites respectively, permitting a consistent environment during the whole culture period (Figure 2.8). The consistency will also allow better control of operational parameters like pH and oxygen. There are two classifications of perfusion: total and partial [107], as seen in Figure 2.9 (adapted from [108]). For total perfusion, the construct is typically homogenously and densely packed, such that the entire cross-sectional area is equally occupied. The perfused flow will then flow through this construct uniformly. Partial perfusion occurs in non-homogenously packed constructs or in constructs that are freely suspended in culture medium. In non-homogeneously packed constructs, there are channels with lower flow resistance, which will promote more fluid flow through these regions of lower resistance (i.e channels in constructs and regions unoccupied by suspended

constructs) while less fluid will flow through regions with higher flow resistance, resulting in a phenomenon of partial perfusion. Total and partial perfusion will result in different transport profiles and microenvironments within the cardiac construct, thus affecting cell numbers and cardiac differentiation.

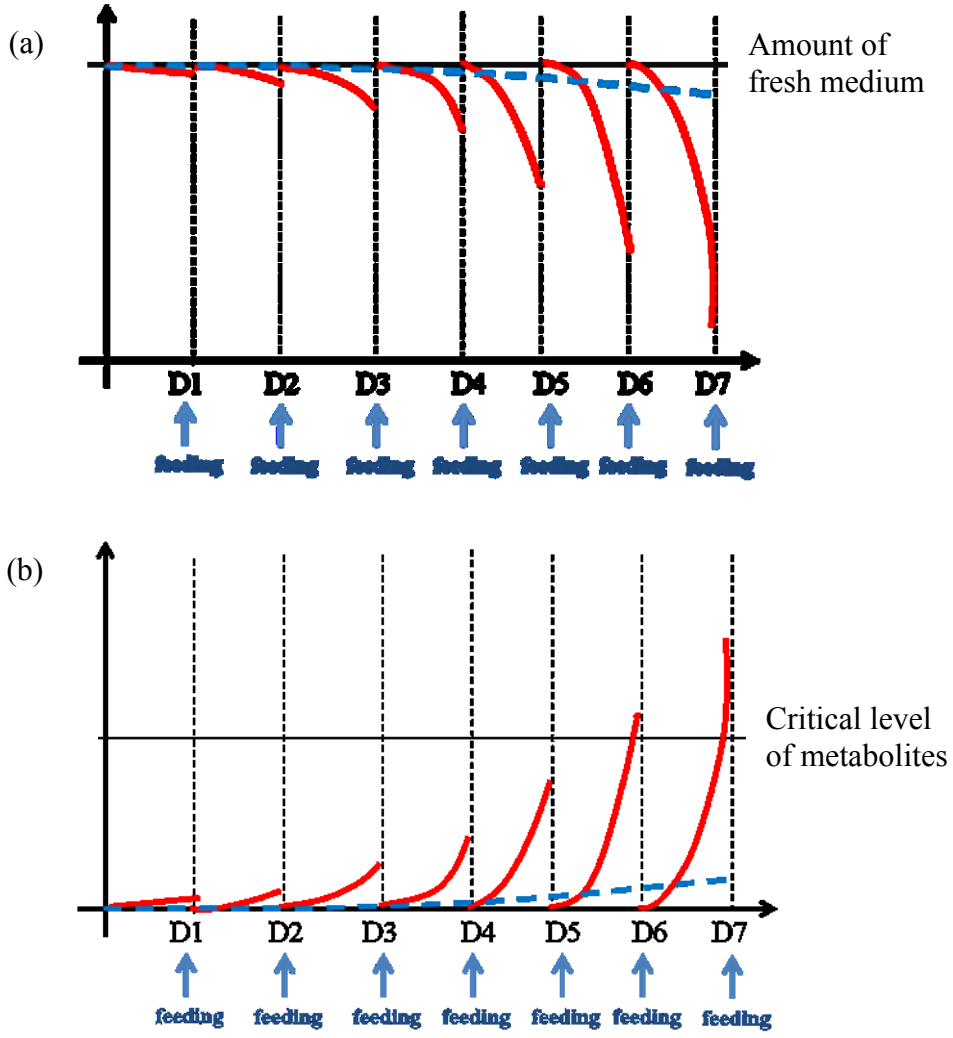

Figure 2-8 Exemplary illustration of (a) nutrients, and (b) metabolites levels in non-perfused (red solid line) and perfused (blue dotted lines) cultures

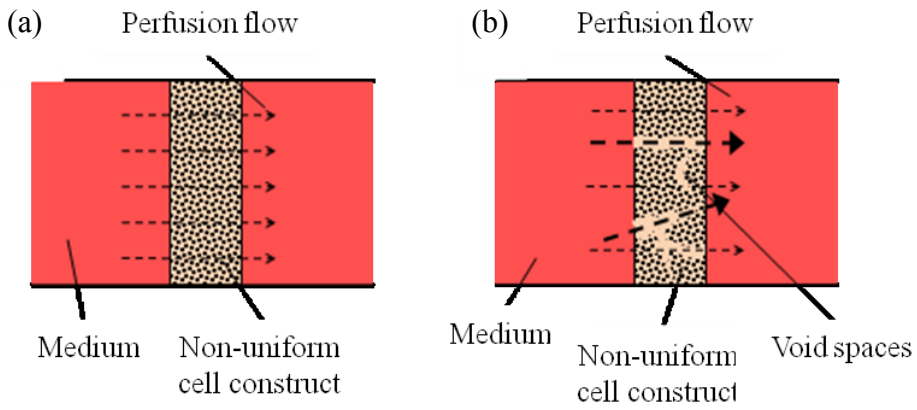

Figure 2-9 Illustration of (a) total perfusion with uniform flow through a homogeneous construct, and (b) partial perfusion where non-uniform flow results from a non-homogeneous construct [108]

In general, higher cell numbers were achieved in perfused cultures than conventional static cultures; and the expansion efficacy obtained in the perfused systems is similar to that achieved in spinner flasks [94]. Cell distribution within a construct was more homogeneous and the cell metabolism was more aerobic in perfused cultures than static and spinner flask cultures. This is because perfusion can modulate oxygen availability inside the bioreactor [94, 99, 109]. However, total and partial perfusion can give rise to drastically different transport profiles within the construct [107]. Under total perfusion, oxygen cannot be transported into regions further from construct periphery efficiently, resulting in lower cell density and viability than those along the peripheral surfaces. One solution to alleviate this problem is to increase the environmental oxygen level, thus providing enough oxygen to meet the minimum survival threshold in deeper regions of the construct. In partial perfusion, medium will flow through regions of lower resistance preferentially, resulting in significantly higher flow rates. Such regions of low resistance include channels and pores in constructs, regions with lower cell numbers and, for the case of suspended constructs, the outer regions around the suspended constructs. When the presence of low-resistance

regions is insignificant, the construct is akin to having uniform resistance and will result in a total perfusion system. Otherwise, cells will be more densely distributed along the peripheral surfaces that are exposed to low-resistant regions and transport beyond the peripheral surfaces will be predominantly diffusion and not convection. This scenario will be similar to that in non-perfused systems.

In several bioreactor designs, it has been shown that incorporating perfusion can improve cardiomyocyte differentiation and maturation, thus it is beneficial to producing cardiac constructs for clinical applications. Perfused bioreactor has enhanced cardiomyocyte differentiation of murine ESCs due to a more consistent control of environmental factors like pH, glucose and lactate concentrations [110]. Besides inducing more cardiac differentiation, perfused cultures can also improve cardiomyocyte maturation. For instance with perfused environment, cardiac constructs of neonatal rat cardiomyocytes showed more uniformed distribution [94] and better contractile properties like higher contraction frequencies and twitch forces than non-perfused cultures [111, 112].

Considering the different parameters involved in bioreactor designs, the advantages and disadvantages of the bioreactors, which are discussed, for large scale cell proliferation and cardiomyogenesis of embryonic stem cells is summarised in Table 2.2.

Table 2-2 Summary of the advantages and disadvantages of various bioreactor configurations

Config	*Advantages*	*Beneficial effects*	*Disadvantages*	*Detrimental effects*
Spinner flasks	- Well-mixed environment - Convective nutrient transport - Easy to scale up and incorporation of new configurations	- Higher cell proliferation and viability - Better uniformity in cell expansion and cardiomyogenesis	- High shear envrionment	- Cell damage and death
RCCS	- Well-mixed environment - Convective nutrient transport - Negligible or shear environment	- Higher cell proliferation and viability - Better uniformity in cell expansion and cardiomyogenesis	- Difficult to scale up incorporation of new configurations	- Limited clinical applications
Shaker flasks	- Well-mixed environment - Convective nutrient transport	- Higher cell proliferation and viability - Better uniformity in cell expansion and cardiomyogenesis	- Less efficient nutrient transport than spinner flasks and RCCS	- Inability to meet cell metabolism needs for cardiomyogenesis
Perfused bioreactor	- Consistent environment over time	- Better uniformity in cell expansion and cardiomyogenesis	-	-

2.4 Using 3D substrate

For easier handling of cells in scalable and dynamic bioreactors, the use of substrate for cardiac and progenitor cell attachment will be required. Moreover, higher cell densities can be achieved with 3D constructs than a 2D culture using the same vessel volume [113]. These constructs also provide a 3D environment, which better mimics the *in vivo* environment, enabling cell-cell and cell-matrix interactions in all directions. ESCs have been cultured as 3D cellular aggregates through suspended EB formation, cell seeding in a 3D scaffold and encapsulation in a hydrogel. When using substrates for cell culture, choice of the substrate material and scaffold design to be used for cardiomyogenesis must be considered.

To scale up cardiomyogenesis of human and murine ESCs in bioreactors, many studies formed and cultured EBs without attachment on any substrate material [6, 91, 114-118]. However, cellular products derived from this method are highly dependent on bioreactor operational parameters such as rotation and shear environment. The resulting variations in the cellular aggregate population will impose difficulties in controlling cardiomyocyte differentiation and maturation. Besides using the substrate-free EB formation method for cardiomyogenesis, biomaterial scaffolds and substrates that enable 3D culture in bioreactors can also be utilised. Under the dynamic/suspension bioreactor systems, control of the cell aggregates' properties and process scalability can be more readily achieved [5, 119]. Alternatively, ESCs, adult stem cells and cardiomyocytes can be encapsulated in hydrogels for differentiation in bioreactors [120-125]. Encapsulation in hydrogels, such as Ca-alginate, provides better control of the size of aggregates during proliferation and can maintain the culture over a longer

period [124-126]. The hydrogels also provide a protective barrier against any detrimental environment effects in the dynamic bioreactors like high shear stress.

An important consideration when selecting a suitable substrate for cell culture is the substrate material. The material should be biocompatible and can be sterilised prior to usage in cell culture. For cardiac constructs, mechanical properties of the selected material must also be similar to the myocardium as there should be no compromise in the contractile ability when transplanted. For instance, a post-mortem human ventricle has a passive bulk modulus of 0.25 GPa and shear modulus of 60 – 148 kPa. [127]. Therefore, the material would preferably have similar Young's modules, tensile strength and stiffness. The extent and rate of material degradation must also be suitable for the application. Upon degradation, the material should not exude any cytotoxic components.

The materials commonly used for synthesizing substrate are classified into two main types: (1) naturally derived polymers and (2) synthetic polymers. Naturally derived polymers include alginate and collagen, and can usually facilitate cell attachment and maintain cell differentiation [128-131]. However, compared to the substrates made from synthetic polymers, the mechanical properties of natural polymers are more difficult to control and less consistent due to high inter-batch variability based on the resources. Meanwhile, using synthetic polymers like poly(ethylene glycol), poly(lactic acid) (PLA) and phosphoester allows better control of mechanical properties through tuning parameters of the synthesis process. However, cell adhesion is not as efficient on synthetic substrates as on those from naturally derived polymers. To enable better adhesion and enhanced cardiomyogenesis, studies have incorporated extracellular matrix (ECM) derived proteins and peptides like laminin, gelatin and Arg-Gly-Asp (RGD), on both

naturally derived and synthetic polymer chains [132-135]. For instance, incorporating RGD peptides on substrates has improved cardiomyocyte viability and enhanced their contractile performance [123]. The physical anitropsy and mechanical properties of synthetic polymer substrates can also be tuned to desired configurations for directing cell attachment and alignment, which can be beneficial for improving the contractile properties of cardiac construct [133, 134]. This is demonstrated on grooved or channelled surfaces and anisotropic geometry of the scaffolds where alignment and contractile properties of cardiomyocytes were improved [136-138].

2.4.1 Alginate hydrogel encapsulation

As previously mentioned, hydrogel encapsulation is one method to enable 3D cell culture for cardiomyogenesis. Hydrogel is a class of highly hydrated scaffold which meets the desirable requirements of biomaterials for cardiac tissue engineering in terms of: (1) biocompatibility, (2) starting materials that can be sterilised, (3) controllable biodegradability, (4) soft and pliable nature, (5) modulation of mechanical properties, and (6) high permeability for efficient transport of nutrients and metabolites [139-141]. One form of hydrogel encapsulation is in the form of small spherical beads, where cells are uniformly distributed within these beads. Such configuration allows 3D culture with enhanced exchange of soluble factors between the environment and scaffold interior as spheres have the highest surface area to volume ratio. Moreover, spherical hydrogels have the potential to allow direct injection into a wound site.

Use of alginates for hydrogel synthesis has been well-established in the tissue engineering field. Alginate is a negatively charged polysaccharide derived from brown seaweed and comprises of alternating chains of α-L-guluronic and β-D-

mannuronic acid residues. Alginate solution initially exists in liquid state and upon the presence of divalent ions, usually Ca^{2+}, the polymer chains will crosslink, forming a 3D network and giving rise to a solid state with an oriented and regular structure. This 3D network can be roughly described by an "egg-box" model [142] as illustrated in Figure 2.10. The solid circles represent calcium ions which bind to chains of α-L-guluronic acid residues of alginate polymers, resulting in V-shaped structures. Meanwhile, β-D-mannuronic acid residues which are not bound to calcium ions will be free-hanging chains at the ends of this "egg-box" structure of guluronic acid residues and calcium ions.

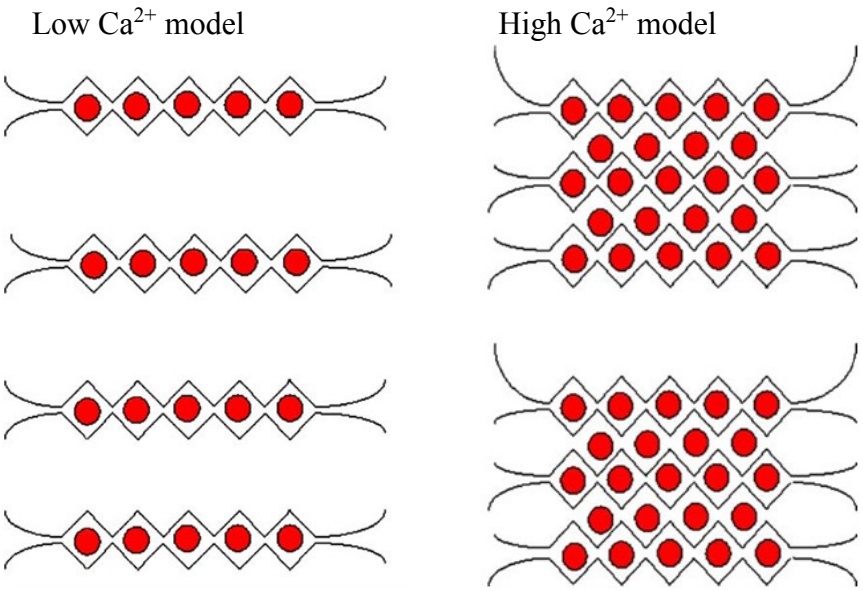

Figure 2-10 Schematic diagram of the ''egg-box'' models in low and high calcium ions concentration. Adapted from Simpson et al. [142].

Mechanical and transport properties of alginate hydrogel depend on the extent of inter-chain binding and porosity. These are controlled by several synthesis parameters like alginate solution concentration, multivalent cation concentration, duration of crosslinking, temperature and stirring [139]. The alginate hydrogel

properties are highly reproducible under the exact same conditions, making it a favourable candidate for usage in bioreactors and tissue engineering. However, multivalent ions may escape the 3D network and cause accelerated degradation under high shear stress environment or during prolonged culture. Thus, gelatin could be added during the encapsulation process to increase network integrity. Incorporation of gelatin will enable cell-mediated contraction and packing of the crosslinked alginate network [143], thus improving network integrity and allowing long term culture. Alginate hydrogel has been utilised for cardiomyocyte differentiation and maturation [130]. Novel composite hydrogels of alginate and materials alike can be used to improve contractile properties of the cardiac constructs. For instance culturing neonatal rat cardiomyocytes in composite hydrogels of alginates and hyaluronic acid, barium, RGD or nanowires enabled better structural maturation and contractile properties than in pure alginate hydrogels [131, 144-146]. Utility of alginate encapsulation for cardiomyogenesis has also been demonstrated in bioreactors of different configurations like spinner flasks, rotary vessels and perfused bioreactors [92, 126, 147, 148] .

2.5 Incorporation of mechanical and electrical stimuli in bioreactors for cardiomyogenesis

2.5.1 Mechanical stimulation for cardiomyogenesis

The pumping action of the myocardium is based on synchronised contractile motion of cardiac muscles cells. There are two main stages during cardiac pumping. First, the two atria will contract simultaneously during the diastole stage, resulting in delivery of blood and filling of the ventricles. During the next systole stage, the ventricles will produce strong, rhythmic contractions which will pump the blood through the aortic and pulmonary valves and deliver blood to other parts of the body. While the blood is being pumped from the ventricles, blood will start flowing into and fill the atria. After the blood has been pumped from the ventricle, the ventricular muscle will relax, bringing another onset of this cycle. These pumping actions require that the cardiomyocytes, which are to be used for clinical therapies, possess mechanical properties suitable for synchronised contraction of a normal myocardium which experiences pressure ranging from 10 to 130 mmHg.

Mechanical stimuli can affect cellular development such as differentiation and phenotype modulation. Such effects are even more significant in mechanically dynamic tissues like cardiac tissues. Mechanical stimuli can take on forms of cyclic strains, pressure or shear stress. Studies have demonstrated that incorporation of 1 Hz cyclic stretch at 1 – 20% of the cardiac construct's space length could provide cues that affected cellular expressions and functionalities such as a 40% increase in α-sacromeric actin gene expression, a 14 – 44% decrease in twitch duration and more organised cell elongations and alignment [149-152]. With the cyclic stretch, cardiomyocyte alignment was also more

organised with a general orientation that was transverse to the stretch [153]. Thus incorporation of mechanical stimuli could produce cardiac constructs with contractile properties that would better mimic the native cardiac muscle.

Bioreactors have made use of designs that allow cyclic stretching of the scaffolds on which the cells are seeded. This type of design uses either a pulsing flow of fluid to cause alternating expansion and contraction of scaffold volume or direct stretching of the scaffolds, as illustrated in Figure 2.11. Cyclic stretching of scaffolds will induce cyclic strains on the seeded cells, providing mechanical cues for cardiac differentiation. ESCs and BM-MSCs under these cyclic strains have been reported to give elevated cardiac gene expression [9, 10, 154, 155], showing that mechanical stimuli can enhance cardiomyogenesis from cell sources like stem cells. Meanwhile, this type of mechanical stimuli can also improve contractile properties of cardiomyocytes such as better cell alignment and higher contracting forces [156, 157].

(a) Expansion and contraction of scaffold volume

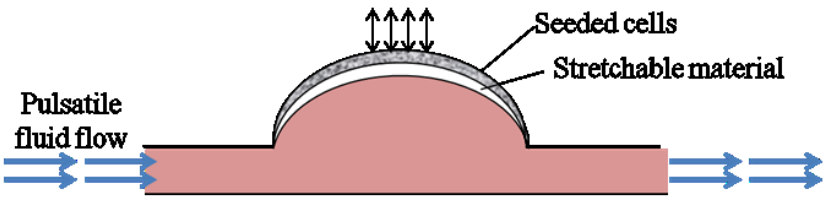

(b) Direct stretching of cardiac construct

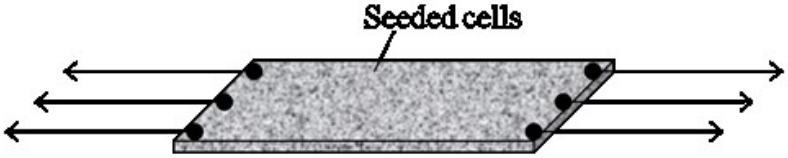

Figure 2-11 Examples of designs to cause cyclic stretching of cardiac constructs

The other method of providing mechanical cues is via pulsatile perfusion through the cardiac constructs [8, 147]. Brown et al. [8] has developed one such bioreactor where the cardiac construct was sandwiched in between two gaskets, and medium would flow perpendicularly through the seeded cells (Figure 2.7 (b) in Section 2.3.1). This flow would cause shear stress on the cells and thus, provide mechanical cues for differentiation and maturation. Neonatal rat cardiomyocytes, when cultured in this bioreactor, has observed better maturation, i.e. increased hypertrophy and elongations.

As seen from these designs, components producing mechanical stimulation can be incorporated into the bioreactor to enhance cardiomyogenesis and produce cardiac constructs with better contractile properties for clinical applications.

2.5.2 Electrical stimulation for cardiomyogenesis

During cardiac pumping, natural pacemaker cells in sinoatrial (S-A) node will produce a wave of electrical excitation. The electrical signal will then be transmitted to atrioventricular (A-V) node through a coordinated contraction of the atria. Thereafter, the A-V node will spread the electrical excitation (action potential) via ventricles' network of nerve fibres to obtain ventricular synchronised mechanical contraction. Therefore, for cardiomyocytes to be suitable for clinical transplantation, they must be able to conduct electrical signals that support normal myocardium activities. Furthermore, during embryonic development, there are endogenous electromagnetic fields which affect the development like placement of components [158, 159]. From this, it can be deduced that using electrical stimuli can improve cardiac differentiation and maturation.

Studies have demonstrated the benefits of electrical stimulation on both cardiac differentiation and maturation. When ESCs are subjected to electrical treatments ranging from 0.1 – 1 V/mm, they displayed a 5 – 10% increase in number of beating areas and a 6-fold increase in cardiac Troponin-T gene expressions [160-162]. Similarly, when cardiac constructs of neonatal rat cardiomyocytes are placed in platforms with ionic buffer or arrayed electrodes, the electrical cues improved their contractile properties lowering the excitation threshold, and produced better cardiomyocyte alignment and well-formed striations [163-167].

3 Using a novel rotary perfused bioreactor for ESC cardiomyogenesis

As presented in Teo et al (2014), Biotechnology Letters. 36 (5): 947-960

3.1 Background

As previously mentioned, cardiomyocytes have limited proliferative capacity, thus the human cardiac muscle is unable to regenerate itself on the onset of myocardial infarction. This presents a major challenge in finding treatment for patients to restore full cardiac functionality in the infarcted areas. A potential clinical treatment for myocardial infarction is cellular therapy and cardiac regeneration. However, utilising cellular therapy for cardiac regeneration is met with limitations such as the production of clinically relevant cell numbers, cardiac functionality and tissue integration. A therapeutic course for myocardial infarction requires a minimum of 10^8 – 10^9 functional cardiomyocytes in each treatment [3]. Such high numbers are required for efficient replacement of damaged or dead ventricular cardiomyocytes and substantial improvement in function of the infarcted heart. To achieve the production of cardiomyocytes in high cell numbers, the usage of highly proliferative cells as cell sources, such as ESCs, have to be considered.

In order to obtain clinically relevant numbers of cardiomyocytes, scale-up of cell culture bioprocesses is necessary. Conventional differentiation of ESCs requires multiple steps of ESC expansion, EB formation and finally replating of EBs for directed cardiomyocyte differentiation. As TCPs usually have size limitations, large-scale expansion of ESC cultures involves large quantities of vessels. Therefore, the multistep culture process and the large number of vessels will make this conventional differentiation process laborious and highly dependent on inter-batch variability.

Given these issues, 3D cultures and bioreactors have been utilised as more efficient platforms with enabled control of environmental conditions for scaling up production of cell products and to ensure better reproducibility. In developing such platforms, one must consider the hydrodynamic profiles and feeding strategy, as they will affect the cell's microenvironment and thus cellular activities. Studies have shown that homogeneous environments, as seen in spinner flasks [6, 7, 42, 89], or rotary vessels [90, 91] could circumvent potential problems faced by TCP static cultures such as spatial gradients of physiochemical concentrations [168, 169]. Improved homogeneity in bioreactors could result in better reproducibility of cardiomyocyte yield. In contrast, conventional cultures usually require manual medium exchange, known as a fed-batch method. Periodic medium changes will cause fluctuations in the cell microenvironment which make cause detrimental effects to the cells. Conventional culture practices also makes monitoring and control of culture parameters difficult for large scale culture and will affect the reproducibility between different batches. Perfusion, which can be incorporated into bioreactors, can provide a more consistent environment throughout the culture period [42].

Arising from these needs, our laboratory has previously designed a rotary wall bioreactor incorporated with perfusion [170, 171]. Such bioreactor design was hypothesised to provide a low shear stress and continual medium exchange that were preferred for inducing cardiomyogenesis and improving uniformity within 3D cardiac constructs. As briefly illustrated in Figure 3.1, medium was perfused from holes in a central perfusion inlet stick and undergo radial mixing. To allow efficient oxygen and carbon dioxide exchange between the culture medium and

the controlled incubator's environment, the culture vessel wall was made of an air-permeable membrane.

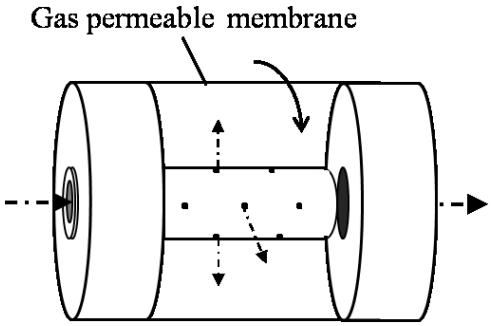

Figure 3-1 Brief illustration of culture vessel in novel rotary perfused bioreactor

In this chapter, this novel bioreactor was used for directing cardiomyogenesis in mESCs. To evaluate the impact of hydrodynamics in the perfusion system, the efficiency in driving cardiomyocyte differentiation of encapsulated mESCs in this platform was compared to those in conventional TCP and commercialised RCCS bioreactor cultures. These systems differed in their hydrodynamic profiles such as static and dynamic environments, and fed-batch and perfused feeding strategy. Through this study, I hope to investigate the feasibility of using this novel bioreactor to produce cardiomyocytes with clinical relevant numbers from cell sources such as embryonic stem cells. Murine ESCs were used as a model to study the overall impact of a novel design perfused bioreactor on cardiomyogenesis and these results would help to evaluate the feasibility and benefits of this novel bioreactor toward the bioprocess efforts in pluripotent stem cell cultures.

3.2 Materials and methods

3.2.1 Maintenance of murine ESCs

Murine ESCs (mESCs, cell line: E14TG2a, ATCC) were maintained in cultures seeded on 0.1% porcine-gelatin (Sigma) coated vessels with an ESC maintenance medium. The ESC maintenance medium was made up of high-glucose Dulbecco Modified Eagle's Medium (DMEM) (Gibco, Invitrogen), 10% heat-inactivated fetal bovine serum (FBS) (Gibco, Invitrogen), 0.1 mM 2-mercaptoethanol (Sigma), 2 mM L-glutamine (ATCC, LGC Standards), 1x penicillin-streptomycin (ATCC, LGC Standards) and 1000 U/mL leukemic inhibitory factor (LIF) (Chemicon, Millipore), which served to prevent spontaneous differentiation and thus maintain ESCs' pluripotency. To ensure enough nutrients for ESCs' rapid proliferation and pluripotency, medium was changed daily.

When mESCs reached 70 – 80% confluency, typically after 2–3 days of seeding, passaging was conducted. Cells were first washed with PBS twice prior to enzymatic digestion by 0.05% trypsin-EDTA. After enzymatic digestion, ESCs would detach from TCP surface. Trypsin was then inactivated by fresh maintenance medium and cells were separated from the solution via centrifugation at 200 g for 5 mins. The cell pellet was re-suspended and uniformly mixed by gentle pipetting to ensure uniform singular cell distribution. Finally the re-suspended cells were seeded onto a newly gelatin-coated TCP for further culturing. Uniformity was required to ensure that the newly seeded ESCs would proliferate into colonies with more uniformity, thus reducing the variability in cell phenotype due to events like undesired spontaneous differentiation of larger colonies.

3.2.2 Preparation of HepG2 conditioned medium (HepG2-CM)

HepG2-CM was shown to provide cues to direct mESCs towards mesodermal lineage [79, 80]. The conditioning to mesodermal lineage will then help to increase cardiomyocyte yield from mESCs. To obtain HepG2-CM for priming mESCs towards mesodermal lineage, medium was collected from HepG2 cultures and several reagents were added prior to usage. Before collection of media, human hepatoma cells (cell line: HepG2, ATCC) were first routinely cultured and passaged to ensure stable phenotype. Thereafter, HepG2 was seeded on uncoated TCP flasks at 5 x 10^4 cells/cm^2. Normal HepG2 maintenance medium was used for HepG2 culture and consisted of high-glucose DMEM, 10% heat-inactivated FBS and 1x penicillin-streptomycin. After 4 days of culture, the medium in HepG2 culture was collected and sterilised by passing through a 0.22 μm filter. This collected medium could then be used to make HepG2-CM or be stored at -80ºC.

To make HepG2-CM, several components must be added to the collected medium. First, there was supplementation of 0.1 mM of 2-mercaptoethanol, 2 mM of L-glutamine and 1000 U/mL of LIF were added. The supplemented medium was finally mixed with equal volume of ESC maintenance medium to make the final HepG2-CM.

3.2.3 Alginate encapsulation of mESCs

Encapsulation of mESCs in alginate hydrogels required two solutions: alginate polymer solution and Ca^{2+} cross-linking solution. Alginate polymer solution was made of 1.1% alginic acid sodium salt (Sigma) and 0.1% porcine gelatin (Sigma) in PBS solution, while the Ca^{2+} crosslinking solution consisted of 100 mM calcium chloride (Sigma), 10 mM N-(s-hydroxyethyl) piperazine-N-(2-ethane

sulfonic acid) (HEPES) (Sigma) and 1% tween (Bio-Rad) . The pH of both solutions were adjusted to pH 7.2 and sterilised by passing through 0.22 μm filter.

To prepare cells for encapsulation, mESCs were homogenised in alginate polymer solution at 2.5 x 10^6 cells/mL. The cell suspension was passed through a sterile tubing and 25-gauge needle, and slowly dripped by peristaltic pumping into the crosslinking solution (Figure 3.2 (a)). In brief, the dripping was done at a height of 50 mm from surface of the crosslinking solution. The height was required as alginate gelling would happen upon contact with the crosslinking solution. 50 mm height would give sufficient time for formation of spherical hydrogels (beads) where their diameters averaged around 2.5 mm. After alginate gelation, the encapsulated cells were washed thrice with PBS to remove residual Ca^{2+} prior to culture.

(a)

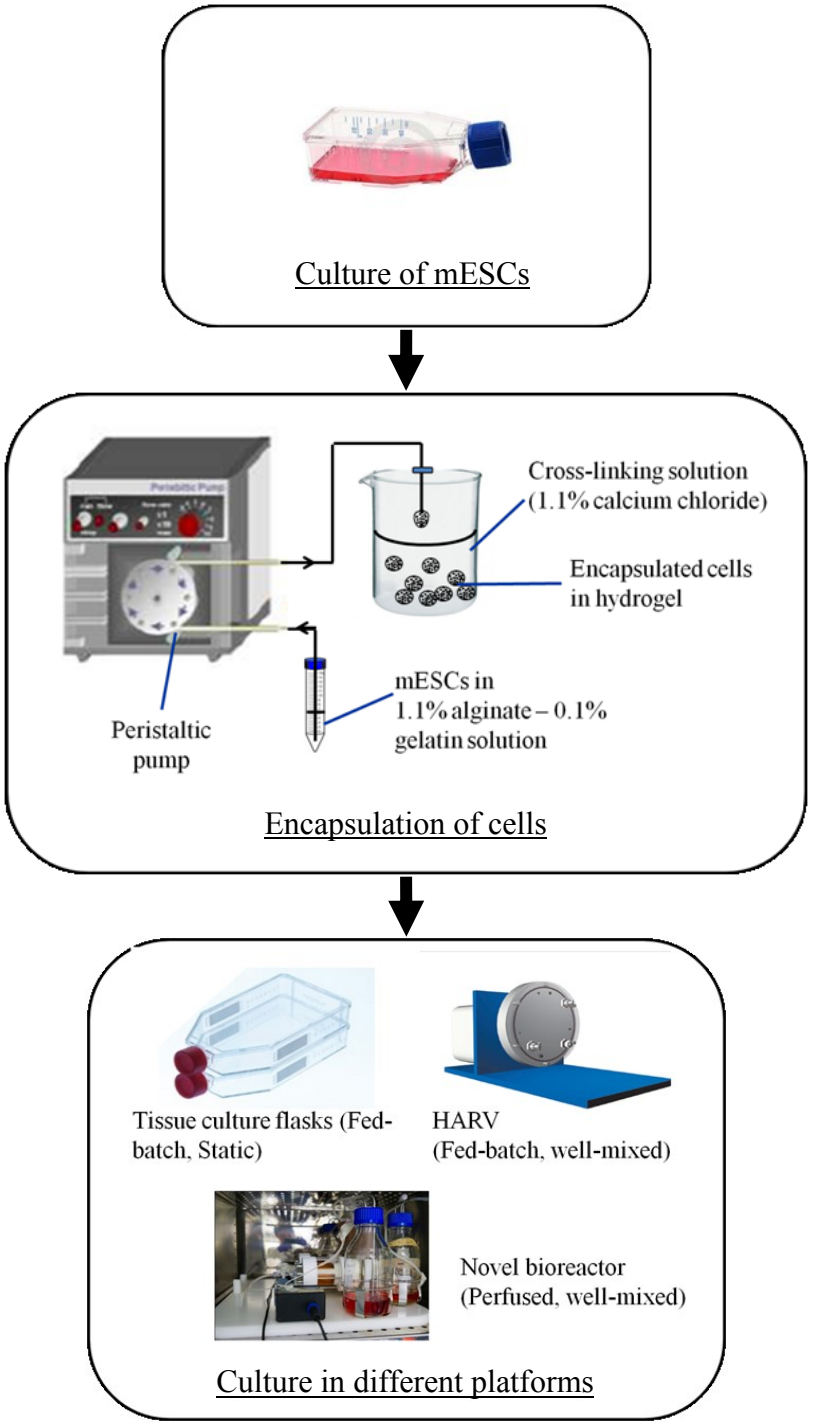

(b)

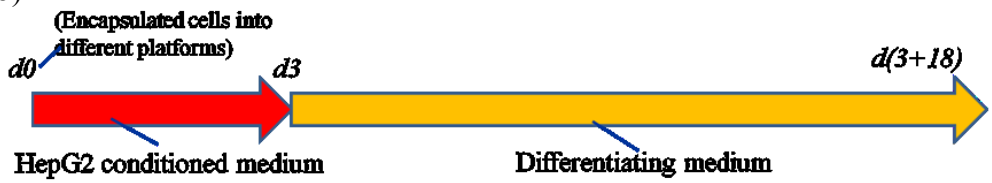

Figure 3-2 (a) Schematic diagram of procedure in encapsulation and culture of mESCs in different bioprocess platform. (b) Timeline of different stages of cardiomyogenesis in the platforms

3.2.4 Comparative study in various culture platforms

Encapsulated mESCs were cultured in three different culture platforms with different hydrodynamic profiles and feeding strategy. They were (1) T-175 flasks (static and fed-batch), (2) 50 mL HARV vessels (dynamic and fed-batch), and (3) our novel perfused bioreactor (dynamic and perfused), as illustrated in Figure 3.2 (a). As there was no mixing and minimal fluid flow in T-175 flask cultures, they were considered static cultures. Meanwhile, HARV and perfused bioreactor cultures are coined as dynamic cultures since they provided mixing and moving fluid inside the culture vessels. A total of 500 hydrogel beads were added and cultured in each platform, and two independent experimental runs were conducted for each setup.

For cardiomyocyte differentiation of mESCs, the cells were subjected to expansion and priming towards mesodermal lineage for the first three days by using HepG2-CM for culture. The priming towards the mesodermal lineage was then followed by the directed differentiation toward cardiomyocytes. In directed differentiation, Iscove's modified Dulbecco's medium (IMDM) basal medium was used over the conventional DMEM for its reported higher levels of cardiomyogenesis by Guan et al. [172]. Therefore, the differentiation medium consisted of high-glucose IMDM (Gibco, Lifetech), 20% heat-inactivated FBS, 2 mM L-glutamine, 1x penicillin-streptomycin, 450 μM 1-thioglycerol and 0.25 μM Cardiogenol C (Sigma). Cardiogenol C is a diaminopyrimidine used as cardiomyogenic-inducing agent through upregulation of Wnt11 expression [87]. As such, the final constituted medium was used for the remainder of differentiation period, typically 18 days. Throughout the 21 days of expansion/priming and differentiation, medium was replaced daily in both TCP

flasks and HARV cultures, while medium was perfused through the perfused bioreactor at 50 ml/day. The whole process is summarised in Figure 3.2 (b). Random beads were sampled on Day 21 and 25 for evaluating cell viability, aggregates' sizing and percentage of cells differentiated to cardiomyocytes. Cells were also extracted from the alginate hydrogel on Day 3, 6, 10, 16 and 21 for evaluation of cell proliferation and cardiac gene expressions.

3.2.5 Extraction of cells from encapsulation

To extract encapsulated cells from alginate beads, the alginate gel network was disrupted by a dissolution buffer. A dissolution buffer was made of 50 mM tri-sodium citrate dehydrate (Sigma), 77 mM sodium chloride (Sigma) and 10 mM HEPES (Sigma). Disrupting the alginate gel network produced a liquid solution with cell suspensions. The extracted cell suspension was then centrifuged at 200 g for 5 mins and washed twice with phosphate buffered saline (PBS) before further analysis.

3.2.6 Microscopic visualisation and sizing of encapsulated cell aggregates

Encapsulated cells were observed with an inverted optical microscope (Leica DMil) and their 10x magnification images were captured with accompanying camera (Olympus DP50). Encapsulated aggregates in the hydrogel were observed to take on a general shape of an ellipse. To size the encapsulated aggregates, the length (major diameter of the ellipse) and width (minor diameter of the ellipse) of each encapsulated cell aggregates were measured with the analysis^D software (Olympus). Thereafter these measurements for each aggregate were averaged and sorted into the respective size bins to obtain a size distribution in the different culture platforms. A total of 80 – 100 aggregates encapsulated in four randomly-sampled hydrogels were measured and binned for each culture platform.

3.2.7 Live/Dead Staining

Cell viability of encapsulated aggregates was analysed using LIVE/DEAD Mammalian Cells Viability/Cytotoxicity Kit (Invitrogen, UK) qualitatively. Five beads were collected from each run and were washed with PBS twice. They were next incubated with 2 μM calcein-AM and 4 μM EthD-1 for 30 mins at room temperature in the dark. Calcein-AM will stain for intracellular esterase activities in living cells while EthD-1 will stain for the nuclei of the dead cells. After incubation, the beads were washed with PBS twice to remove any residual dyes. They were then observed under an inverted fluorescence microscope (Olympus BX51, Olympus) in the dark for the viability staining. Finally images were captured using the accompanying imaging camera (F-view II, Soft imaging system) and analysis^D software.

3.2.8 DNA quantification

To determine the number of cells encapsulated in each bead, the amount of double stranded DNA content in a sampled population of beads was measured. DNA content was measured by using the Quant-IT PicoGreen dsDNA Reagent and Kit (Invitrogen). At different time points (Day 3, 6, 10, 16 and 21), 5–10 beads were used for sampling. The cells were extracted as described in Section 3.2.5. The cells were then incubated overnight at 37^{o}C in 50 μg/ml proteinase-K (Sigma) solution containing 100 mM dibasic potassium phosphate (Sigma, pH 8.0) for protein digestion. After incubation, Proteinase-K was heat-inactivated by incubating at 90^{o}C for 10 mins. The solution was next centrifuged to remove any cell debris as a pellet and to collect double-stranded DNA (dsDNA) in the supernatant. The PicoGreen reagent was diluted accordingly to the manufacturer's instruction. Thereafter an equal volume of diluted PicoGreen reagent in 1x TE buffer (pH 7.5) was added to the dsDNA. Last but not least,

fluorescence was produced by the binding of PicoGreen reagent to the dsDNA and measured with a fluorometer (MFX microplate fluorometer; Dynex technologies). A cell number-fluorescence standard curve was also prepared to interpolate the sampled cell numbers.

3.2.9 Quantitative PCR

Cardiac differentiation of mESCs was determined with gene expression levels measured by quantitative polymerase chain reaction (PCR). Total RNA was first isolated from extracted cells using RNeasy kit (Qiagen) and RNase-free DNase kit (Qiagen) according to the manufacturer's instructions. RNA collected was quantified with a UV spectrophotometer (Eppendorf). After RNA quantification, 1 μg of RNA was used for synthesis of first strand of complementary DNA (cDNA). cDNA was synthesized using a Reverse Transcription Kit (Promega).

To compare cardiomyogenesis in different culture platforms, quantitative PCR was carried out with SensiFAST^{TM} SYBR Hi-ROX Kit (Bioline). In brief, 100 ng cDNA was added to 10 μl of mastermix, 400 nM of primers. Nuclease-free water was also added to make up to a final volume. The mixture underwent PCR amplification process and measurement in StepOne^{TM} Plus (Applied Biosystems^{TM}). The PCR process involved initial denaturation at 95^{o}C for 2 mins and an amplification stage with 40 cycles of denaturation at 95^{o}C for 5 secs and annealing/extension at 60^{o}C for 30 secs. Different genes were analysed with the different primers (Invitrogen), as shown in Table 3.1. PCR end products were also analysed with electrophoresis in 2% agarose gel and ethidium bromide and melt curves were conducted after every PCR run to ensure the absence of any side products and formation of primer-dimers. After checking that all primers have similar amplification efficiencies under the parameters used, the gene

expressions among different culture platforms were normalised to the endogenous control gene, GAPDH, and then to the static controls on Day 3 (which corresponded to the start of directed cardiac differentiation) and finally compared using $2^{-\Delta\Delta CT}$ method. The $2^{-\Delta\Delta CT}$ method has been widely used in determining relative gene expressions in samples to that in the control groups and has been described in detail by Schmittgen et al. [173]. Briefly, the fold change of target gene expression in sample from that in control was calculated with Equations (3.1) and (3.2).

$$\Delta\Delta C_T = \left[C_{T,sample}(target\ gene) - C_{T,sample}(endogenous\ control\ gene)\right] - \left[C_{T,control}(target\ gene) - C_{T,control}(endogenous\ control\ gene)\right] \quad \text{…. Equation (3.1)}$$

$$Fold\ change\ of\ target\ gene = 2^{-\Delta\Delta C_T} \quad \text{…. Equation (3.2)}$$

, where C_T refers to the threshold cycle from quantitative PCR data.

Table 3-1 List of studied genes and their respective primers in studying effects of hydrodynamics on cardiomyogenesis

Gene	*Forward primer*	*Reverse primer*
Housekeeping gene		
GAPDH	AGGTCGGTGTGAACGGATTTG	GGGGTCGTTGATGGCAACA
Cardiac genes		
Brachrury T	AAGGAACCACCGGTCATCG	CGTGTGCGTCAGTGGTGTGTAATG
Nkx2.5	AGCAACTTCGTGAACTTTG	CCGGTCCTAGTGTGGA
cTNT	CTCCATCGGGGATCTTGGGT	CAGAGGAGGCCAACGTAGAAG
α-MHC	ACCGTGGACTACAACAT	CTTTCGCTCGTTGGGA
β-MHC	ACCCCTACGATTATGCG	GGTGACGTACTCGTTGCC
Pluripotent genes		
Nanog	CCTGATTCTTCTACCAGTCCCA	GGCCTGAGAGAACACAGTCC
Oct-4	TGTGGACCTCAGGTTGGACT	CTTCTGCAGGGCTTTCATGT

3.2.10 Flow cytometry

To quantify the percentage of mESCs differentiating to cardiomyocytes in the different culture set-ups, flow cytometry was used to determine the percentage of cells positive for expression of cardiac troponin-I.

First, the alginate network in hydrogel was depolymerised as described in Section 3.2.5. The extracted cells were then fixed in 4% paraformaldehyde (Sigma) for 15 mins and permeabilised in 0.1% Triton-X (Ultrapure grade, USB Corporation) for another 15 mins at room temperature. Thereafter, the cells were resuspended in PBS containing 5% goat serum, 0.1% Triton-X and 1% sodium azide to a concentration of 1 – 5 x 10^6 cells/ml. 100 µl of the resulting cell suspension was transferred to a new tube, and 2 µl of cardiac Troponin-I primary antibody (H-41, Santa Cruz Biotechnology) was added. It was then incubated for 2 hours at 4ºC. After incubation, the cells were washed twice with cold PBS and incubated with 100 µl of FITC-conjugated secondary antibody (Santa Cruz Biotechnology) diluted in 3% bovine serum albumin in PBS for 1-hour at room temperature in the dark. Next, the cells were washed twice with cold PBS. To store the cells prior to flow cytometry, the cells were re-suspended in PBS consisting of 2% paraformaldehyde, 3% bovine serum albumin and 1% sodium azide and kept in 4ºC. Finally, stained cells were analysed on the flow cytometer (FACSCalibur, BD Biosciences) and the percentage of positively stained cells were quantified in in a flow cytometry analysis software FlowJo (Tree Star).

3.2.11 Immunocytochemistry of sacromeric α-actinin and connexin-43 networks

Encapsulated cells from different culture platform were fixed with 4% paraformaldehyde (Sigma) in PBS for 1 hour at room temperature. Next, they underwent a serial dehydration with increasing concentrations of 50%, 70%,

90%, 95% and 100% ethanol and finally pure xylene. They were then immersed in paraffin-saturated xylene overnight at room temperature to condition for paraffin embedding. On the following day, these dehydrated samples were paraffin-embedded with Paraplast (Sigma) and sectioned to 5 μm slices. Before immunostaining was conducted, the sectioned sample underwent a serial rehydration, starting immersion in pure xylene and then decreasing concentrations of ethanol (100%, 95%, 90%, 70% and 50%). Finally they were incubated in an antigen-retrieval buffer (10mM tri-sodium citrate dihydrate, pH 6.0, Sigma) at 96^{o}C for 30 mins.

After antigen retrieval, immunostaining was carried out. The samples were first incubated with 10% goat serum for 45 mins at room temperature to block out all unspecified binding. They were then incubated overnight with primary antibodies of sacromeric α-actinin (EA-53, Santa Cruz Biotechnology, 100x dilution in primary diluents of 0.1% sodium azide and 1% bovine serum albumin in PBS) or connexin-43 (CXN-6, Santa Cruz Biotechnologies, 400x dilution in primary diluents) at 4^{o}C. Thereafter, the slides were washed with PBS thrice prior to 1 hour-incubation with FITC-conjugated or TRITC-conjugated secondary antibodies respectively (100x dilution in 1% bovine serum albumin in PBS) at room temperature. The slides were then washed with PBS on a shaker for 10 mins. This washing step was repeated thrice to ensure that the stained samples were free of residual antibodies. Last but not least, the samples were incubated with DAPI dye for 5 – 10 mins to stain for nuclei. The immunostaining results were finally imaged with fluorescence microscope (Olympus) and AxioVision 4.0 (Olympus).

3.2.12 Statistical analysis

All statistical analysis was conducted by using Microsoft Office Excel analysis tool package (Excel 2013, Microsoft). To check for significant differences in cell numbers (through dsDNA quantification), quantitative PCR data, and flow cytometry data between experimental groups, equal variances were first checked using F-test with 95% significance level. The results showed that there were unequal variances in most comparison pairs. Thus student t-test with unequal variances were thus used to test for inter-group differences of 95% significance. Error bars on the charts represent standard deviations of each group. The sample populations (N) represented total number of biological replicates from 2 independent experimental runs and are indicated in the legends of each respective figures.

3.3 Results

3.3.1 Denser and more uniform aggregates in dynamic cultures

mESCs were initially encapsulated as a single-cell suspension, which resulted in uniform distribution of individual cells within an alginate bead. Each bead has an average diameter of 2.5 mm and a cell number of 2 x 10^4 cells. Over the culture period, these encapsulated ESCs proliferated and started to form clusters of cells called aggregates. In this study, the growth of these aggregates (sizes and densities) was monitored.

After 3 days of cell expansion and priming towards mesodermal lineage in HepG2-CM, microscopic observations revealed that cells in the dynamic culture platforms, namely HARV and the novel perfused bioreactor, formed more aggregates than those in the static culture (TCP flasks) (Figure 3.3 (a – c)). Moreover, it was also observed on Day 21 that there was presence of cells in the static culture which failed to form cell aggregates (as indicated by red arrows in Figure 3.3 (d)). On the other hand, such observations were insignificant in the dynamic cultures (Figure 3.3 (e – f)).

While a visual inspection may not clearly distinguish differences in cell aggregates amongst the different cultures, a more quantitative method is sought after. The sizes of 80–100 aggregates from each culture were evaluated by measuring their dimensions and binning them, as described in Section 3.2.6. Binning of aggregates by size helped in the evaluation of aggregates' size distribution in various culture platforms and thus provided an insight into the uniformity of aggregate cell growth. Each bead had numerous encapsulated cell aggregates and each aggregate were of different sizes, despite being in the same bead. The distribution was as depicted as in Figure 3.3 (g). Cells in static culture

gave rise to a distribution where two aggregate sizes were more common (modes). They were the bins of 40 – 60 μm and > 220 μm. These two modes represented two extreme aggregate sizes that were more common in static cultures. Two modal aggregate sizes of 100 – 120 μm and 160 – 180 μm were observed in the novel bioreactor. These two values were not as drastically different as those observed in static cultures. Meanwhile, HARV cultures produced the best size distribution with only one modal size at 140 – 160 μm. The two extreme modal aggregate sizes in static cultures showed the larger variation in cell growth due to absence of mixing and hydrodynamic flows. In comparison, HARV and the novel bioreactor produced higher numbers of aggregates with higher uniformity.

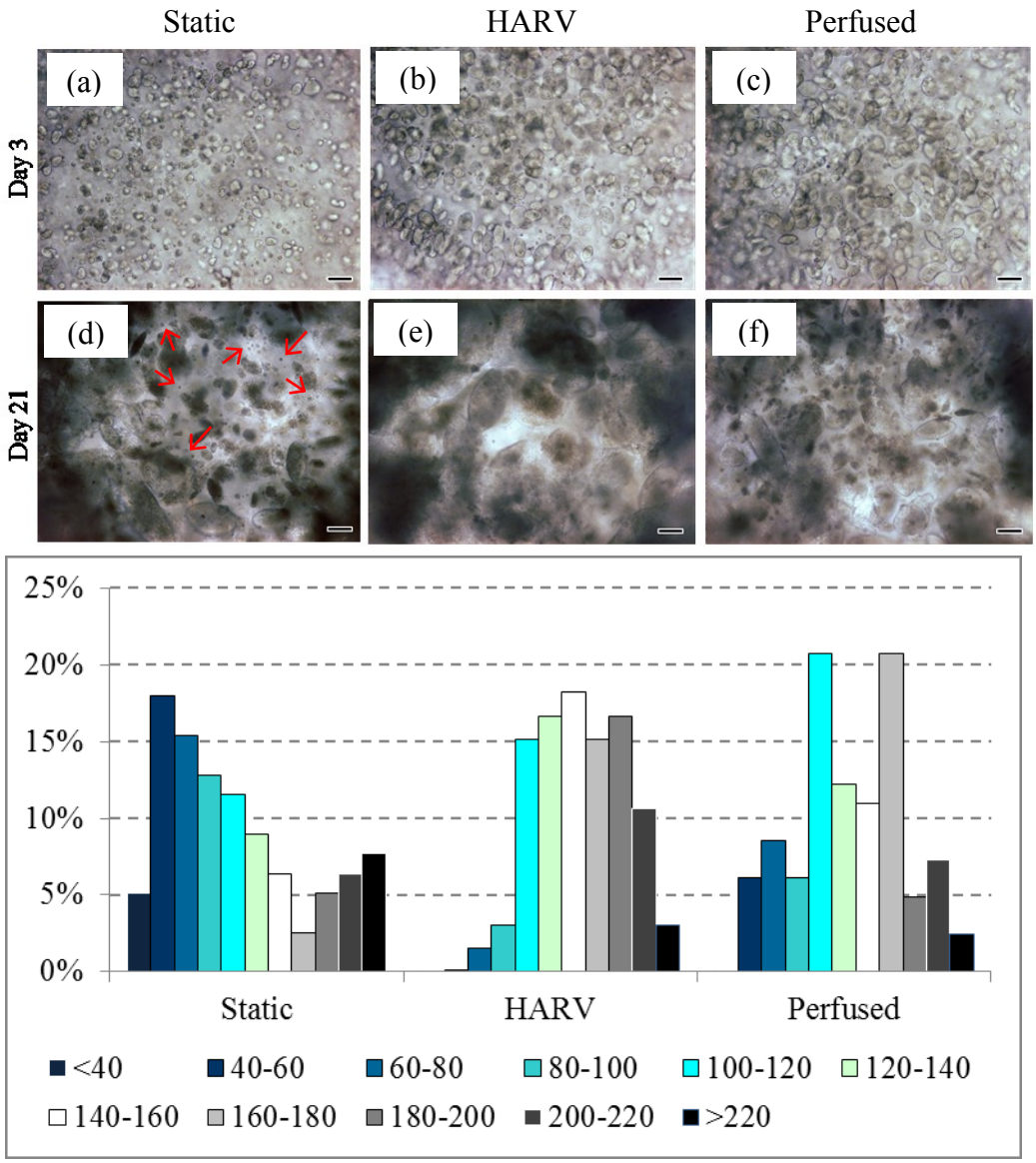

Figure 3-3 (a – f) Micrographs of encapsulated aggregates in alginate hydrogel on Day 3 days and 21. The red arrows in (d) indicate the cells which failed to proliferate into cellular aggregates. Scale bar represents 100 µm. (g) Population distribution of aggregate sizes after 21 days of culture. Size was calculated as an average of the aggregate's length and width and binned into the respective size range. Binning of 80 aggregates from 4 beads cultured in the respective systems.

3.3.2 Higher viability and cell numbers in dynamic cultures

From the observed cell numbers via dsDNA quantification, it was observed that there were better cell growths in HARV and the novel bioreactor than in static cultures (Figure 3.4). After 3 days in culture, there was minimal cell growth in the static cultures, producing an average cell density of 1.5 x 10^5 cells/bead for

the whole culture period consistently. In contrast, significantly higher cell numbers were obtained from HARV and the novel bioreactor at the end of 21-day culture period. HARV gave rise to the highest and fastest cell proliferation, where it produced an estimated 4 x 10^5 cells/bead by Day 10. This high cell density population was then maintained till the end of culture. Meanwhile, the cell growth was slower but more consistent in novel bioreactor. After 21 days, encapsulated cells in the novel bioreactor amounted to 3.8 x 10^5 cells/bead, a density which was similar to HARV cultures. The improved cell proliferation in dynamic cultures coincided with the improved uniformity and denser cell aggregates as described in Section 3.3.1.

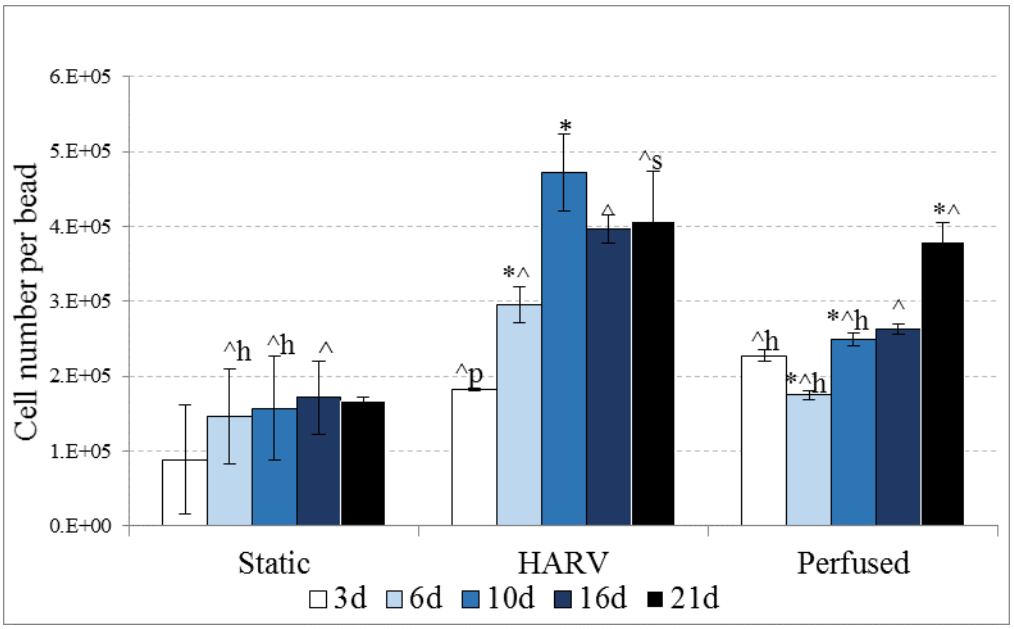

Figure 3-4 Cell numbers in different culture platforms. * represents significant difference from previous time point in the same platform. ^ represents significant difference from other platforms (or indicated platform) at the same time point. $p < 0.05$, N = 4 from 2 independent runs.

From the live/dead fluorescence micrographs (Figure 3.5), cell viabilities in both dynamic cultures were significantly better than those in static cultures. In the HARV and novel bioreactor cultures, all encapsulated cell aggregates from

HARV and novel bioreactor cultures were highly viable, where the presence of dead cells was negligible. On the other hand, presence of dead cells was evident in the static cultures; some aggregates consisted a significant portion of dead cells. Comparing the cell numbers and viabilities obtained from these three culture platforms, lack of hydrodynamics in static environment clearly posed significant transport limitations in culturing 3D cardiac construct. Such impact of hydrodynamics could be due to the lack of nutrient transport to the encapsulated cell aggregates in static cultures, thus compromising cell growth and viability.

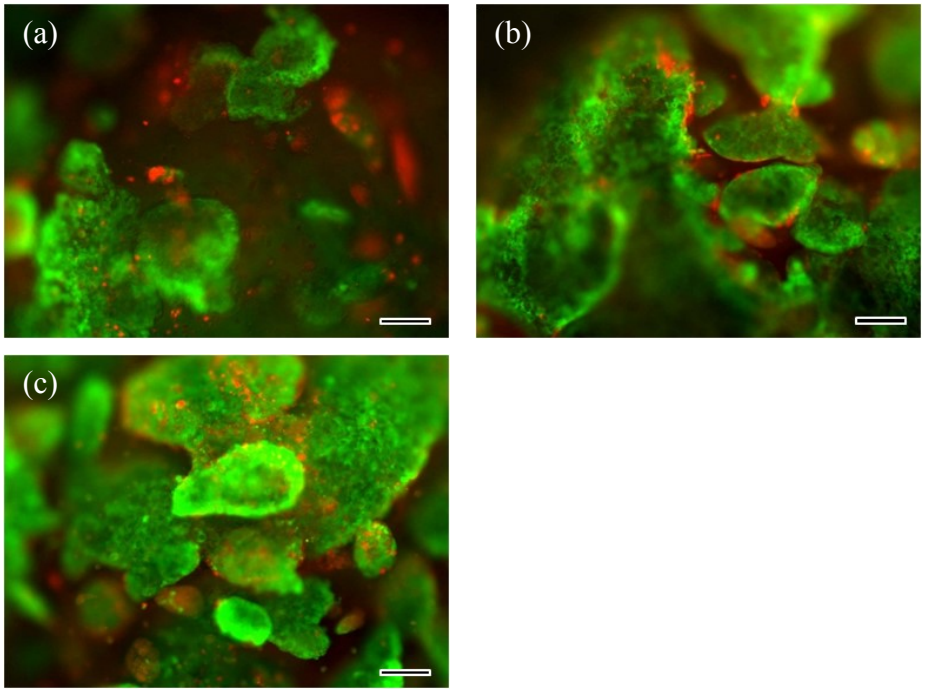

Figure 3-5 Live/dead fluorescence images at of encapsulated aggregates at day 21 in (a) static platform, (b) HARV reactor, and (c) perfused bioreactor. Green and red fluorescence represent live and dead cells respectively. Scale bar represents 100 µm.

3.3.3 Earlier and higher cardiac marker expressions in perfused platform

To determine extent of cardiomyogenesis in different culture platforms, various gene expressions, indicating the different stages of ESC differentiation towards cardiomyocytes, were tested. These included Brachyury-T and Nkx2.5 which

represented early mesodermal lineage commitment of ESCs and specificity towards cardiac progenitors respectively. At each respective time point during the 21-day culture, no significant differences in the Brachyury-T and Nkx2.5 gene expressions between different culture platforms were observed (Figure 3.6). Although all platforms gave rise to similar levels of early cardiac markers, there were significant differences in the expressions of late cardiac genes such as cardiac troponin-T (cTNT), α- and β- myosin heavy chains (MHC).

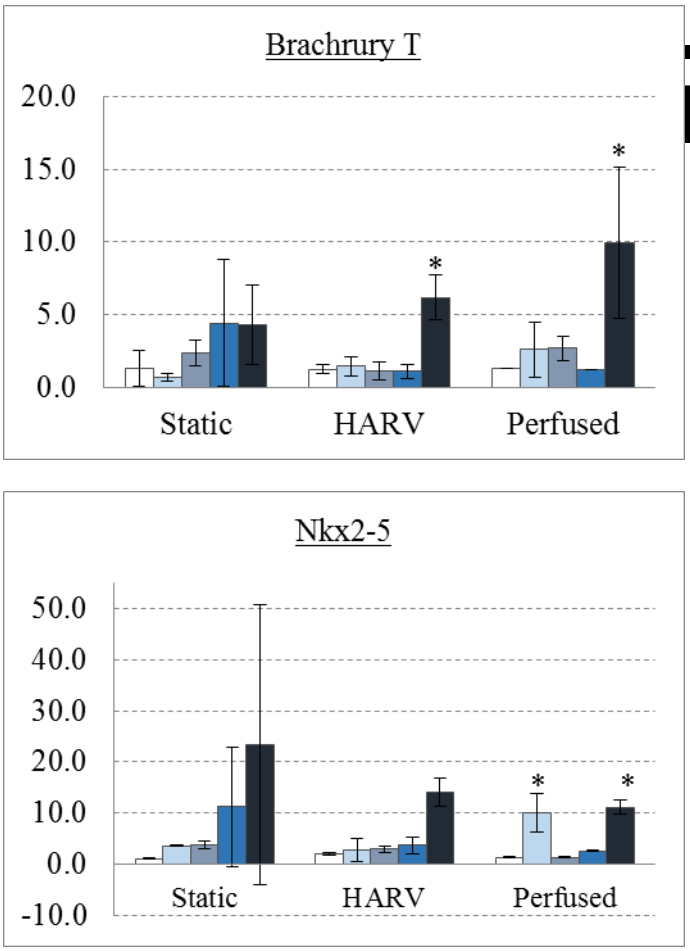

Figure 3-6 Fold changes in expression of (a) mesodermal marker Brachyury T, and (b) early cardiac progenitor Nkx-2.5 culture period. * represents significant difference from previous time point sample from the same platform. ^ represent significant difference from other platforms (or indicated platform) at the respective time point. 's': static, 'h': harv, 'p': perfused bioreactor. p<0.05, N=2

Cardiac troponin is a regulatory protein complex involved in cardiac calcium signalling. When it is bound to calcium signalling ion, it allows interaction between cardiac actin filaments and myosin to achieve muscle contraction. It consists of three subunits: troponin T, troponin I and troponin C. In this study, an

upregulation of cardiac troponin T (cTNT) on Day 6 was observed in novel bioreactor but not in the static and HARV cultures (Figure 3.6 (a)). This upregulation was transient and was absent thereafter. It was only till 21 days of culture where it was again upregulated in novel bioreactor. By this day, cTNT was also upregulated in the other platforms. However, its expression was significantly the highest in novel bioreactor culture. The phenomenon of an early transient upregulation, which was followed by a later stage upregulation was similar to observations made by Antin et al. [174]. cTNT was first up-regulated temporarily during mesodermal commitment and a late upregulation happened again at more localised regions in maturing cardiomyocytes during differentiation.

Another type of markers for late cardiac differentiation is the contractile structural protein, myosin heavy chain. Cardiac myosin is a motor protein that moves along cardiac actin filament for generation of muscle contraction. It consisted of four light chains and two heavy chains, forming a dimeric structure. The heavy chains exist in two isoforms, α-MHC and β-MHC. These two isoforms differ in their ATPase activity levels and their amount of force generated in the muscles. On Day 16, the novel bioreactor produced an earlier upregulation of both MHC isoforms, which was absent in the HARV and static (Figure 3.7 (b – c)). On Day 21, α-MHC upregulation was also significantly higher in perfused culture than the other two platforms. MHC markers are an indication of mESC differentiation towards cardiomyocytes, and such earlier and higher expressions implied the benefits of a perfused and well-mixed environment in enhancing cardiomyogenesis of 3D encapsulated mESCs.

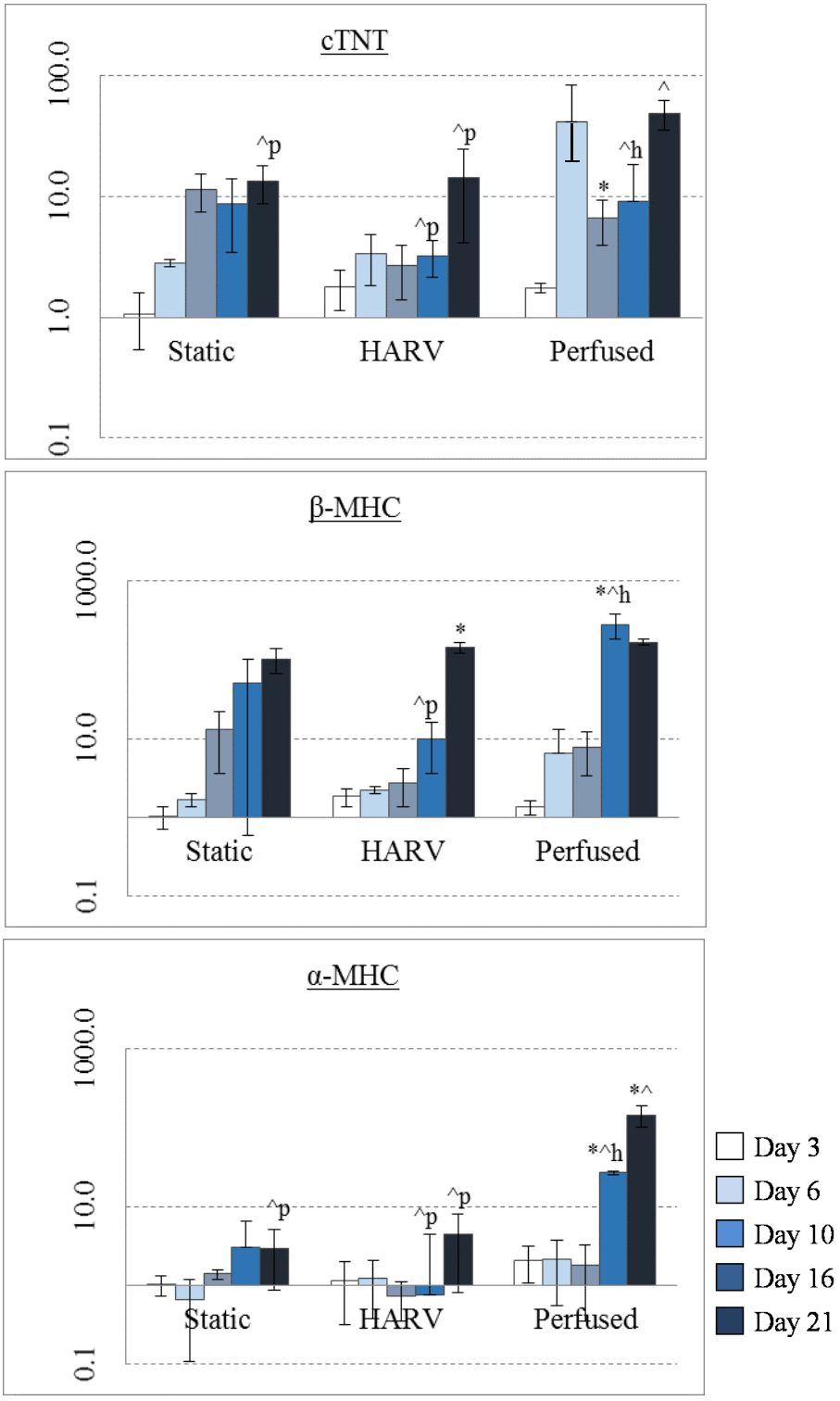

Figure 3-7 Fold changes in expression of cardiac markers (a) cTnT, (b) β-MHC, and (c) α-MHC during culture period. * represent significant difference from previous time point in the same platform. ^ represent significant difference from other platforms (or indicated platform) at the same time point. 's': static, 'h': harv, 'p': perfused novel bioreactor. $p < 0.05$, N = 2

3.3.4 Higher percentage of cardiac Troponin-I-positive cells in novel bioreactor

The percentages of cardiomyocytes obtained from different culture setups were determined by positive expression of cardiac Troponin-I (cTNI) in flow cytometry analysis. Similar to cTNT which is used in Section 3.3.3, cTNI is involved in calcium signalling central to cardiomyocytes' contractile motion. Figure 3.8 shows that a population with the highest percentage of cardiomyocytes is produced in the novel bioreactor on both Day 21 and 25. HARV cultures, on the other hand, produced the lowest percentage of differentiated cardiomyocytes. Together with the results from cardiac gene expressions, this flow cytometry data shows that a continuously perfused environment in the novel bioreactor is beneficial for cardiomyogenesis of mESCs.

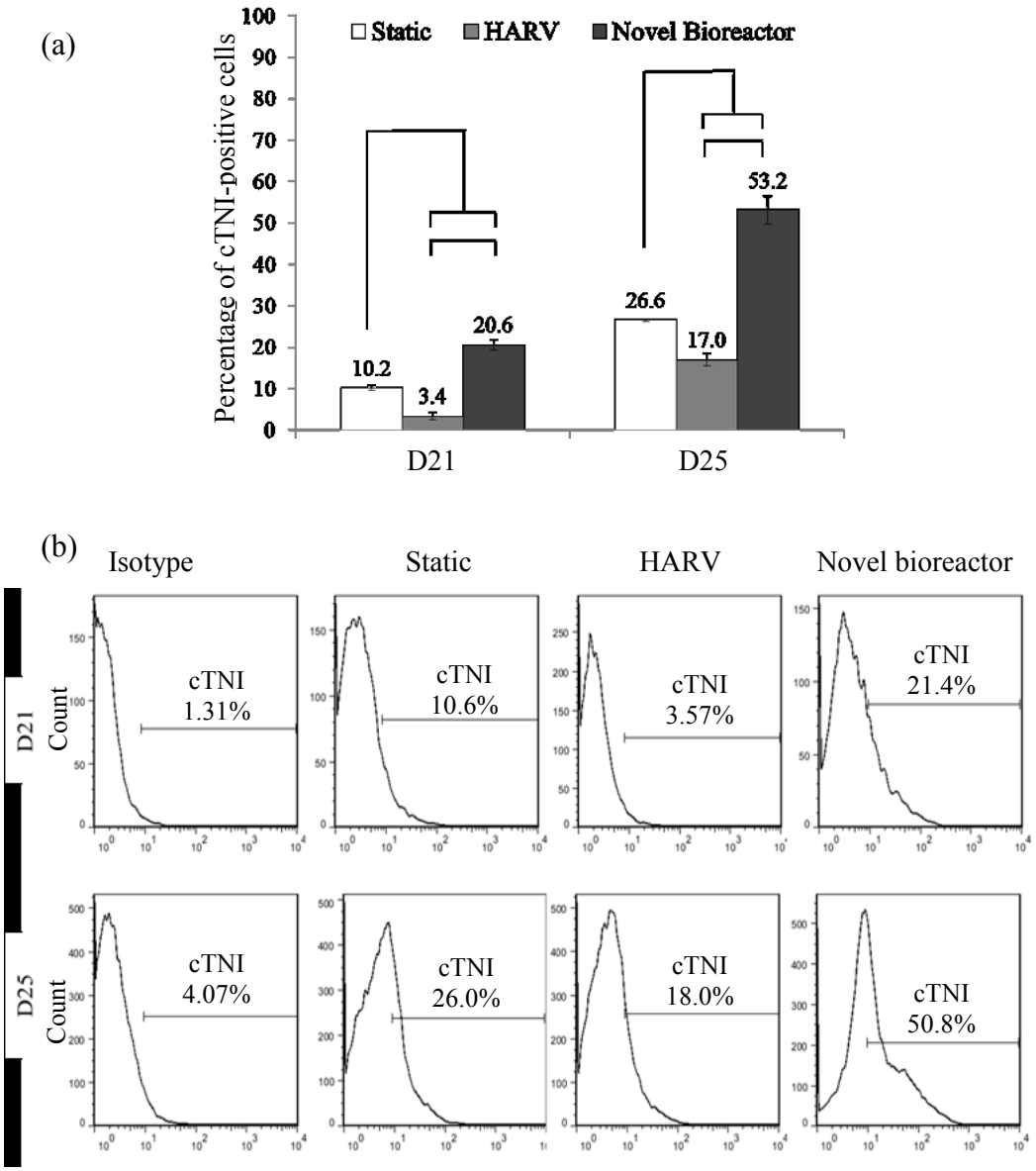

Figure 3-8 (a) Percentage of cTNI-positive cells as obtained from different culture platforms. Bar represents significant difference of indicated sample from the non-treated control. $p < 0.05$, N = 2. (b) Representative flow cytometry histograms of fluorescence conjugate-isotype control, and of cTNI-positive cells from static, HARV and novel bioreactor cultures after 21 and 25 days.

3.3.5 Levels of pluripotency in different platforms

The level of pluripotency in ESCs was monitored with two stem cell markers: Nanog and Oct-4 (Figure 3.9). In static culture, Nanog was downregulated (< 1.0 fold after normalisation to Day 3 static culture) after 16 days while Oct-4 was downregulated as early as after 3 days. However, high levels of Nanog and Oct-4 were consistently expressed in HARV and these expressions were downregulated only after 16 days. This downregulation coincided with the upregulation of cardiac markers, signifying the loss of pluripotency due to differentiation. Meanwhile, in the novel bioreactor, expression profiles of Nanog and Oct-4 did not correspond to each other. For instance Nanog expression was significantly downregulated at Day 6 while Oct-4 expression increased instead. The increase in Oct-4 expression could be explained by some reported results showing that the commitment towards cardiac lineage was also accompanied by transient Oct-4 increase. Oct3/4 binds to and targets genes which participate in mesodermal and cardiac lineage specificity and a 2–8 fold increase in Oct3/4 is required for ESCs' cardiac differentiation [175]. Furthermore, it was also reported that a large percentage of ESCs expressed Oct-4, coupled with Mixl1 after 4 days of differentiation [176]. Mixl1 is indicative of primitive streak formation and commitment towards mesodermal and endodermal lineages. Thus it can be inferred that the Oct-4 upregulation is associated to mesodermal lineage commitment instead of pluripotent indication, as observed in the novel bioreactor.

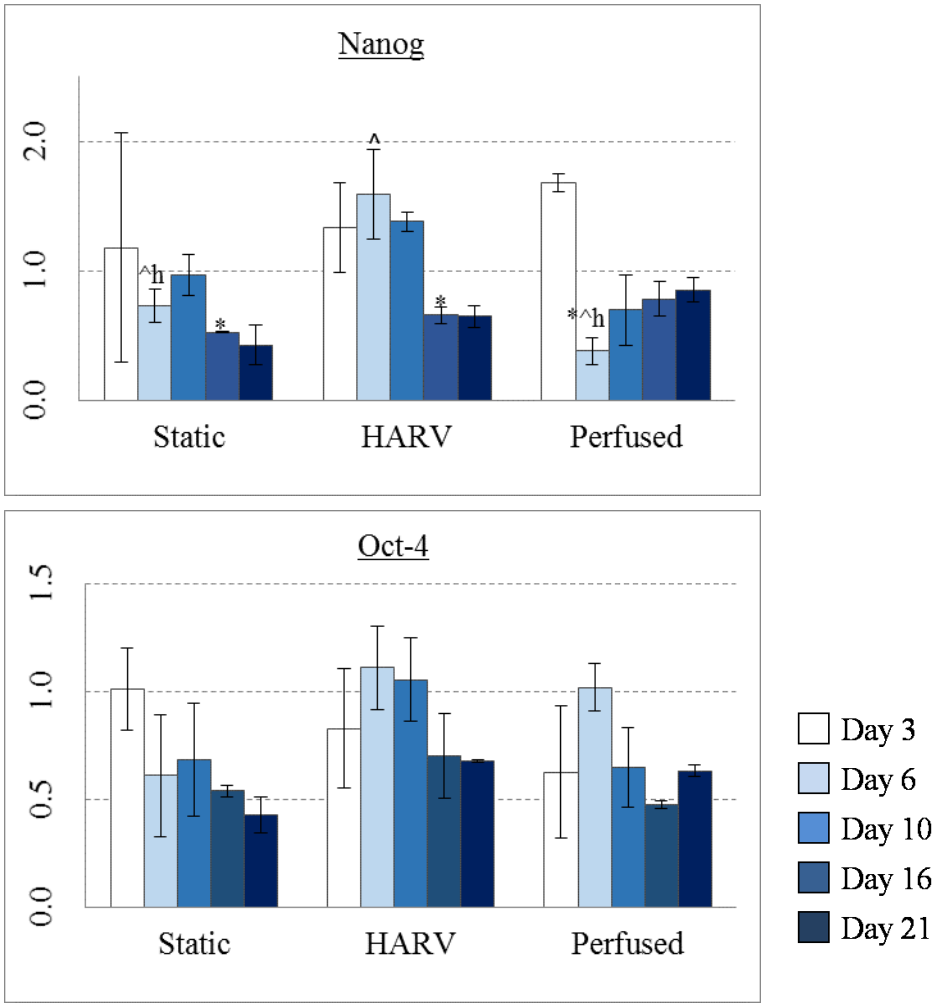

Figure 3-9 Fold changes in expression of pluripotent markers (a) Nanog, and (b) Oct-4 during culture period. * represents significant difference from previous time point in the same platform. ^ represents significant difference from other platforms (or indicated platform) at the same time point. 's': static, 'h': harv, 'p': perfused bioreactor. $p < 0.05$, N = 2

3.3.6 Higher uniformity of intra-aggregate scaromeric α-actinin expression and signalling network in novel bioreactor

In creating 3D cardiac constructs, the nutrient availability beyond the construct peripheral surface is an important consideration; this can be significantly affected by hydrodynamic profile and feeding strategy. In this thesis, the impact of hydrodynamics on cells in the aggregates' core was evaluated via staining for both sacromeric α-actinin and connexin-43 proteins.

Scaromeric α-actinin (ATN) is a binding protein that attaches actin filament to dense striations in cardiomyocytes. When evaluated against their respective nuclei staining, expressions of ATN in static and HARV cultures were localised only to the peripheral regions after 21 days (Figure 3.10 (a – b)). In contrast, the intra-aggregate expression of ATN in the novel bioreactor culture was more uniformly distributed throughout the construct and corresponded to the nucleic staining (Figure 3.10 (c)). Uneven distribution of ATN could be due to inferior transport of nutrients and oxygen to the aggregates' cores, limiting differentiation ability towards cardiomyocytes.

Connexins are gap junction proteins that are responsible for intercellular signalling through involvement in exchange of small molecules across cell-cell interfaces. Thus, they are essential for coordination of cardiomyocyte depolarisation. In the atrial and ventricular tissue, connexin-43 is the most abundant type of gap junction proteins [177]. Therefore, its network was visually analysed through immunostaining of aggregates. Samples from novel bioreactor showed uniform fluorescence intensity throughout the cell aggregate, indicating a uniform intra-aggregate development of connexin-43 (Figure 3.11). In contrast, connexin-43 networks within the aggregates from static and HARV cultures showed regions of lower intensity as indicated in Figure 3.11 (a) and (b). These regions are beyond the aggregates' peripheral surface. The uneven distribution and inferior formation of intra-aggregate connexion-43 networks in static cultures could be due to transport limitations into these inner regions. Such transport limitations happened as they were primarily driven by diffusion due to absence of hydrodynamic profile. Meanwhile, in HARV cultures, sizes of aggregates might

have too large, which inhibited efficient transport of nutrients and oxygen into the aggregates' cores.

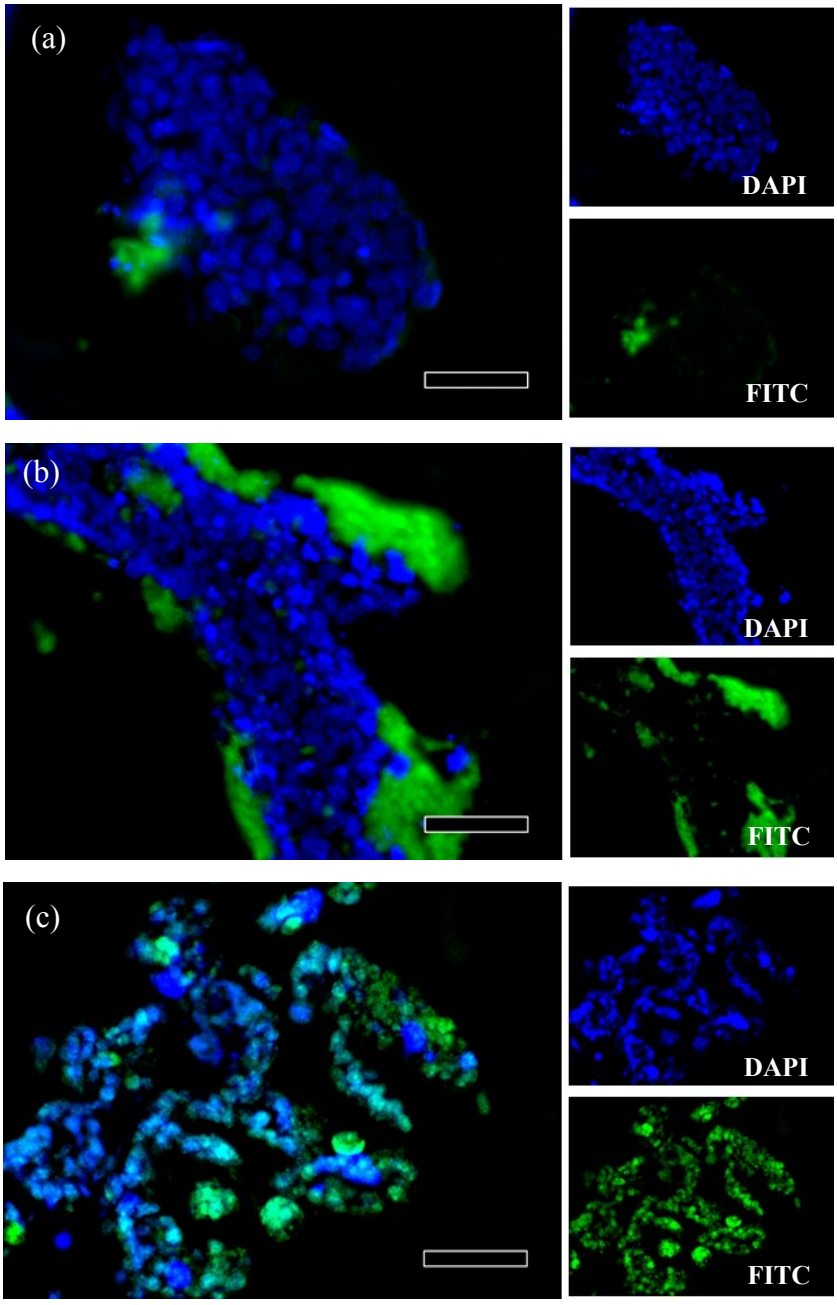

Figure 3-10 Fluorescence micrographs of ATN protein expression (green) and nuclei (DAPI-blue) in encapsulated aggregates from (a) static, (b) HARV, and (c) perfused bioreactor cultures. Scale bar represent 50 µm.

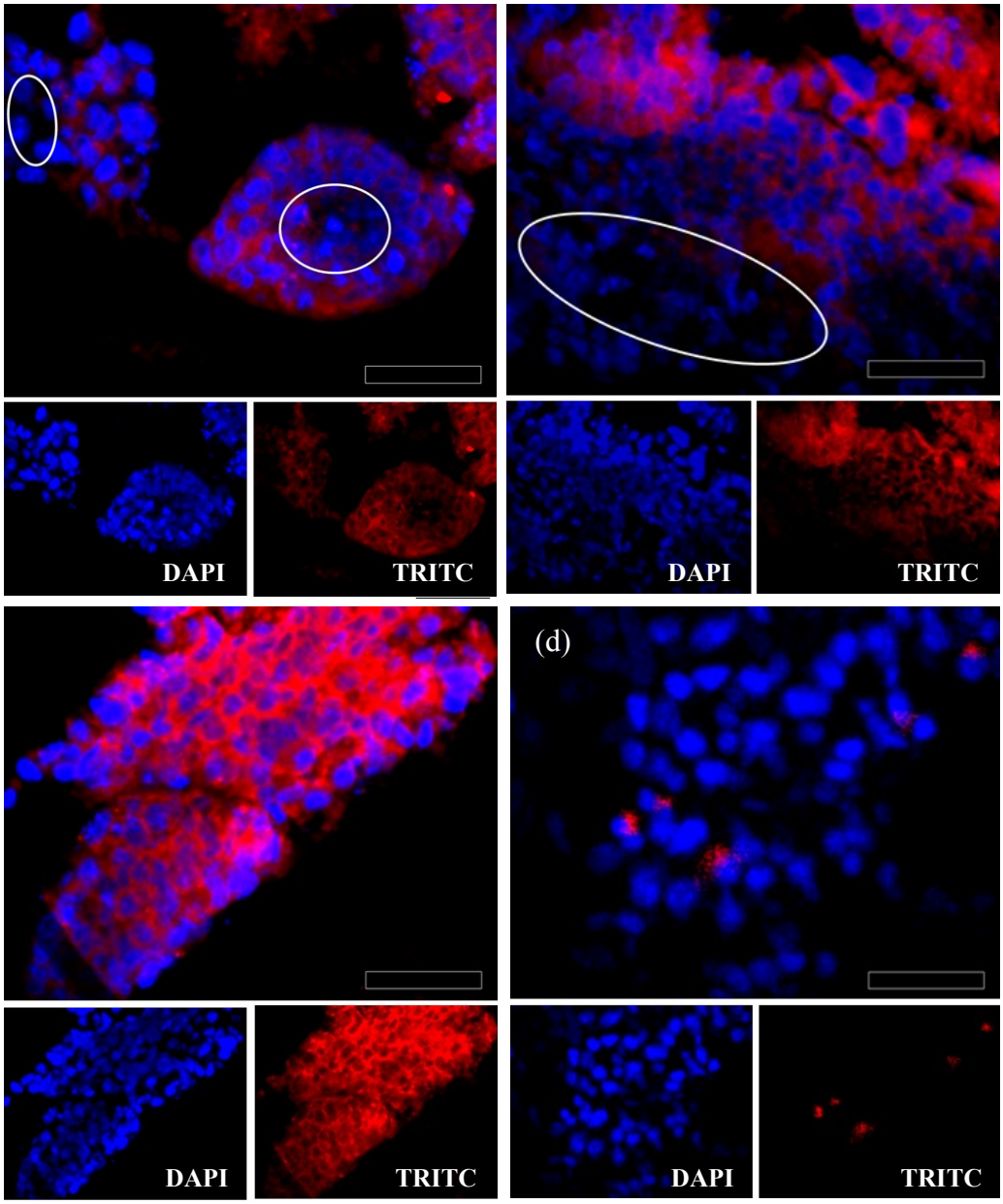

Figure 3-11 Fluorescence micrographs of Connexin-43 networks (Rhodamine - red) and nuclei (DAPI - blue) in encapsulated aggregates from (a) static, (b) HARV, (c) perfused bioreactor cultures, and (d) negative control. Scale bar represent 50 µm.

3.3.7 Optimisation of aggregates' size distribution via the novel bioreactor's rotational speed

As previously described in section 3.3.1, a bimodal aggregate size distribution was initially obtained in the novel bioreactor (Figure 3.3 (g)), and such distribution was usually not preferred for directed differentiation of ESCs. Aggregate distribution with a single and distinct modal size is typically more ideal for directed differentiation as it provides better uniformity and control in directing ESCs towards the desired lineage. It was hypothesized that improved hydrodynamics in the novel bioreactor could improve mESC growth. One operational parameter, which could be tuned to alter culture hydrodynamics and possibly address the bimodal issue, is the rotary speed of the novel bioreactor. When the bioreactor was operated at 10 rpm, it was noticed that the hydrogel beads tend to settle at bottom of the rotating vessel. At a faster rotation, a longer period of uplifting was achieved and this would enable better mixing of medium surrounding the encapsulated cell beads. With improved mixing, supply of nutrients among the numerous encapsulated aggregates would be more equally distributed. Therefore, when the rotary speed was increased from the initial 10 rpm to 12.5 rpm, improved cell aggregate profile distribution was achieved. After 21 days of culture at a rotation speed of 12.5 rpm, size distribution of the mESC aggregates improved significantly, giving one distinct modal size (120 – 140 μm) and a much smaller size range, as depicted in Figure 3.12.

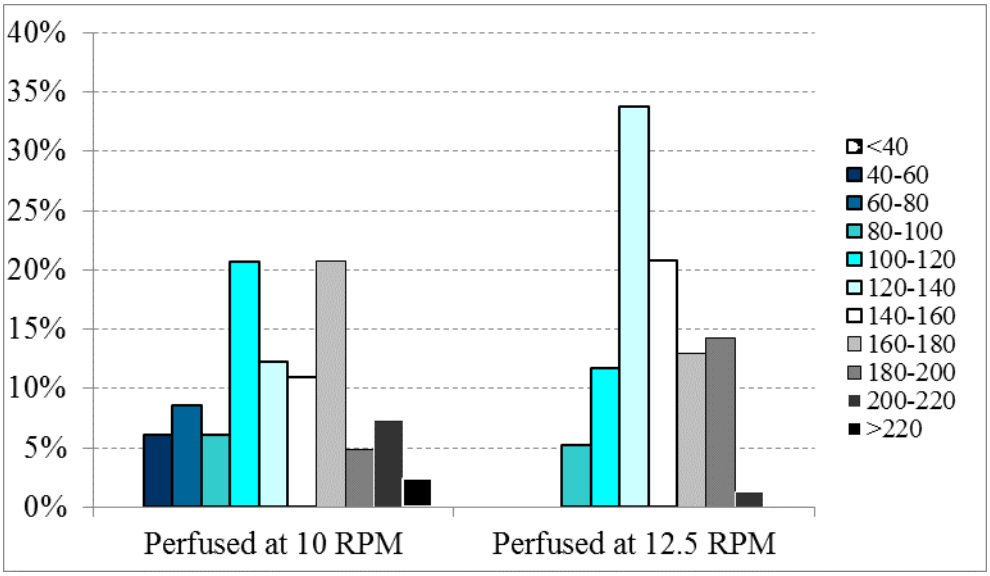

Figure 3-12 Population distribution of aggregates' sizes after 21 days of culture in perfused bioreactor rotating at 10 rpm and 12.5 rpm. Legend represents sizes in µm. Binning of 80 – 100 aggregates from 4 randomly-sampled beads in each rotation speed.

3.4 Discussion

Conventional method of cardiac differentiation of ESCs involves a multi-step procedure which makes it laborious for scaling up production of cardiomyocytes. This impedes further development of efficient regenerative clinical therapies for myocardial infarctions. In this study, encapsulation of mESCs was used to enable an integrative single-step cell proliferation and differentiation process in mESC culture. Initiating various stages of mESC differentiation was achieved simply by changing the medium feed. This minimises the need for the lab operator to handle ESCs and conduct EB selection. Eventually, it will reduce contamination risks, human errors and improve product reproducibility.

In numerous studies involving bioreactor cultures, freely suspended aggregates or encapsulation in micron-sized hydrogel was used to differentiate mESCs towards cardiomyocytes [7, 42, 116, 117, 126]. However, encapsulated mESCs in spherical hydrogels were significantly larger. The hydrogel beads used in this study were of 2.5 mm in diameter while most studies used microencapsulated technologies that produced substrates with sizes ranging from 200–500 μm. Larger-sized cardiac constructs are more relevant to tissue engineering and clinical therapeutic applications. However, cell culture in such large-sized scaffolds can face limitations in nutrient and oxygen transport. Thus utility of dynamic and well-mixed culture environment becomes increasingly beneficial over static conditions. This comparative study showed the benefits of dynamic culture platforms and perfusion for culturing large-sized cardiac constructs.

Clinically-relevant cell numbers would demand a cell culture platform that enables efficient large-scale production, and this is more readily achievable in

bioreactors. It was demonstrated that dynamic cultures, i.e. HARV and the novel perfused bioreactor, produced an average of 4 x 10^5 cells per hydrogel bead. Considering the number of beads that were used for each platform, this translated nearly 2 x 10^8 cells i.e. a 20-fold increase from initial number of cells seeded. This meant that 2 x 10^8 cells were produced in a vessel volume of 50 mL. In contrast, the same volume of static culture produced only 7.5 x 10^7 cells, which translated to a 7.5 fold increase. Besides rotary bioreactors, cultures in stirred bioreactor also produced higher cell expansion [7]. These studies clearly demonstrated the benefits of dynamic cultures to obtain clinically relevant cell numbers.

Another feature of the novel bioreactor was incorporation of perfusion. In this study, cardiomyogenesis in the novel bioreactor was compared to fed-batch platforms. Perfusion can ensure a constant supply of soluble factors and removal of metabolic by-products, thus achieving environmental consistency during cell culture period. The results of this study showed that perfusion was beneficial to cardiac differentiation of mESCs. First, the novel bioreactor culture produced high cell density with high cell viability and homogeneity. What was more distinct to perfusion was the enhanced cardiomyogenesis in the novel bioreactor. Though the onset of enhanced cell proliferation was faster in HARV, cardiomyogenesis was faster and enhanced in novel bioreactor. Late cardiac markers were significantly upregulated in novel bioreactor since Day 16 while such upregulation was only later present in HARV and static cultures on Day 21. The novel bioreactor also yielded higher percentage of cardiomyocytes than both HARV and static cultures. Such improved cardiomyogenesis in perfused platforms could also be due to diluting effect of inhibitory factors. Besides this

novel bioreactor, which is based on rotary mixing, perfusion could also enhance cardiomyogenesis in non-rotary bioreactors, as demonstrated by Niebruegge et al. [7]. Perfused stirred bioreactors produced more cardiomyocytes from ESCs than their non-perfused counterparts. Another advantage of the perfused feeding strategy is improved 3D organisation and uniformity within a 3D cardiac construct. In this study, sacromeric α-actinin expression and connexin-43 network was found to be more uniform within the encapsulated cellular aggregates. Perfusion culture onto cardiac construct has been reported coherently that they produced cell distribution and contractile properties of higher uniformity [94, 111, 112]. These advantages of incorporating a perfused feeding strategy could be attributed to (1) a consistent supply of cardiogenic factors balanced with a continual removal of inhibitory factors, and (2) the improved delivery of soluble factors and oxygen to aggregates' cores via convective-diffusive transport.

One concern was that aggregate size distribution in this novel bioreactor was not as uniform as HARV despite its better effects on cardiomyogenesis. It was initially hypothesized that a consistent and uniform environment throughout cell culture period will enable a more uniform size distribution of the encapsulated aggregates. On the contrary, the novel bioreactor gave rise to a bimodal size distribution while fed-batch HARV cultures produced the more ideal distribution. This implied that operation of this novel bioreactor might require further optimisation. Besides the feeding strategy, another distinct difference between these two dynamic platforms was the rotary speed. HARV and the novel bioreactor were operating at 18–20 rpm and 10 rpm respectively. HARV's higher rotary speed enabled the encapsulated cells to be suspended in the vessel's mid

region while the encapsulated cells in the novel bioreactor could not achieve this state. Rungarunlert et al. found out that the optimal rotary speed for culturing embryoid bodies in slow turning lateral vessel (a similar rotary designed vessel) was 10 rpm [117]. However, hydrogel beads used in this study might require a higher rotating speed. After changing the novel bioreactor's rotary speed to 12.5 rpm, a better size distribution with one modal size was produced, thereby resolving the issue of inferior aggregates' uniformity.

3.5 Conclusion

Choosing the correct cell culture platform is important in 3D cardiac tissue engineering and producing cardiomyocytes for clinical therapies. Its hydrodynamic profile and feeding strategy will affect availability of nutrients and delivery of biochemical cues to the cells. In this study, the feasibility of using the novel bioreactor, as previously designed by our laboratory, was demonstrated for accelerated cardiomyogenesis of mESCs, so as to produce cardiomyocytes with clinically relevant numbers. The dynamic and well-mixed environment in this bioreactor could ensure good transport efficacies, which is particularly important for larger constructs to maintain cell viability and continued cell growth. Improved consistency of environmental parameters due to perfusion also made an impact on cardiomyogenesis of mESCs. After establishing such benefits of the dynamic and well-mixed environment could have on mESCs, the feasibility of using such a system for human pluripotent stem cells could serve a step towards translation towards producing cardiomyocytes with clinically relevant numbers.

4 Sensitivity of ESC cardiomyogenesis on extracellular pH in 3D bioprocess

As presented in Teo et al (2014), Biochemical Engineering Journal. 90: 8-15

4.1 Background

Utilising cardiomyocytes for clinical therapies require the culture process to be defined and cellular products to be well-characterised. In efficient scaled-up cultures, ability to control and monitor process variables will be essential to achieve reproducible products that can meet the clinical requirements. Perfused rotary bioreactors have the benefit of doing so. They are able to allow a well-mixed environment and a consistent exchange of soluble factors. This feature enables culture conditions to be defined and controlled, as compared to fed-batch platforms (bioreactors and conventional cultures) where cells will experience uncontrolled biochemical and physiological environmental fluctuations, such as extracellular pH.

Amount of hydronium ions in the cellular microenvironment determines its pH. These ions participate in numerous biochemical reactions and proteins' structural conformation and activities. Hence cellular pathways and cell fates will be affected by extracellular pH. Moreover, myocardium is highly sensitive to its localised pH variations. For instance pH changes are associated with myocardial infarction. In a canine model, the usual myocardial cell pH is 6.94 [178]. However, its pH decreases to 6.83 at the onset of infarction and eventually is reduced to 6.59. Though this pH change is only 0.35 units, cardiac functionality is already compromised, showing the high sensitivity of cardiomyocytes to pH changes. Thus creating a controlled environment with monitored levels of hydronium ions will be useful in optimising and controlling scaled-up cardiomyocytes production.

Such high sensitivity of cardiac cells to pH indicates that pH can affect their contractile properties. Besides the observation on the *in vivo* myocardial infarction, several studies have also demonstrated that extracellular pH changes had an impact on contractile properties *in vitro*. For instance, cardiomyocytes displayed lower contractile forces at pH 6.4 but an increase of pH to higher values (between 7.4 and 8.4) would do otherwise [179, 180]. Maintaining cultures between pH 7.4 and 7.8 can also increase protein synthesis and prevent protein degradation [181, 182]. This may limit myocardial infarction and thus benefit clinical therapies. Changes in extracellular pH are observed to affect ion exchange channels such as Cl- channels [183, 184]. Human ether-a-go-go related gene (hERG) voltage-gated K+ channel is a voltage-insensitive channel and is rather difficult to control with conventional ionic gradient. However, Zhou et al. has shown its sensitivity to pH changes [185]. With pH's effects on these channels, extracellular pH can be a physiological parameter that influences cardiomyocytes' contractile properties such as cellular volume and action potential.

Modulation of pH has also been shown to affect the proliferation and differentiation activities of stem cells and progenitors [186-189]. One direct mechanism is via intracellular pH changes [187, 190, 191]. For instance, as extracellular pH varied from 6.7 to 7.3, the intracellular pH in Syrian hamster embryo cells changed correspondingly [191]. This intracellular pH change then affected cellular mitogen-transduction activities such as tyrosine phosphorylation and epidermal-growth-factor induced signalling. Another mechanism of pH modulation is through the changes in ion signalling activities [187, 192] caused by different levels of H^+ ions. One instance was observed in HCO^{3-} channels in

mouse macrophages [192]. Regardless of mechanism, changes in extracellular pH were demonstrated to affect signalling pathways and endogenous production of soluble factors that play important roles in cardiomyogenesis of stem cells. Two such factors are hypoxia induced factor – 2α (HIF-2α), which affects stem cell proliferation and pluripotency [193], and p38 mitogen activated pathway kinase (p38 MAPK), a sensitive control for mitogen-activated pathways which regulates cardiomyogenesis [194].

Studies investigating the effects of extracellular pH on stem cells and progenitors are limited. To date, pH ranging around 7.6 was found to be generally more beneficial for cell differentiation and maturation than pH 7.1 to 7.4 [188, 189, 195]. In comparison, optimal pH for cell expansion is not straightforward and is more dependent on the cell type. Colonic cells such as HeLa and Chang liver cell lines experienced maximum proliferation at pH 8.0 and lower pH levels than 8.0 would affect their growth adversely. On the other hand, expansion of hemapoetic progenitors and embryo cells was preferred in lower pH ranges such as 6.8 to 7.1 instead [188, 189, 196].

Despite the number of studies evaluating pH effects on possible cardiomyogenesis has been limited, it is understood that culture pH variation can significantly impact differentiation of these cells. Besides determining the optimal pH, the cells' sensitivity towards any pH changes must also be considered. Inconsistent culture conditions, not uncommon in conventional ESCs differentiation protocols, will lead to inter-batch variations of the differentiated products [197], undermining efficient production of cardiomyocytes for clinical applications. Furthermore, embryo cells are highly sensitive to pH changes. Pagano et al. demonstrated an intracellular pH shift of 0.2 units would cause

irreversible changes on embryogenesis [198]. Therefore, this section studied effects of different pH levels, which were commonly used in ESC cardiomyogenesis, to evaluate the pH sensitivity of pluripotent cells during cardiac differentiation.

Manual feeding strategy often produces fluctuations in physiological environment and pH values due to the sudden removal of spent medium and additional of fresh medium. To achieve conclusive results to determine pH sensitivity, extracellular pH conditions should be maintained at the required value consistently throughout the culture period. Perfusion enables consistent supply of nutrients and removal of metabolites, thus eliminating the need for manual medium changes and minimizing physiological fluctuations. With regular monitoring, perfusion rate could also be adjusted to address any pH changes due to cellular requirements (such as increased respiration and acidosis with higher cell numbers). Thus utility of a perfusion system is highly beneficial for conducting pH investigation in this study to ensure better homogeneity and control of the culture environment. In the previous chapter, the ability of a novel rotary, perfused bioreactor to enhance cardiomyogenesis of mESCs was demonstrated. This bioreactor can provide a homogeneous and consistent culture environment throughout the culture period through its rotary mixing and perfusion. Therefore, this bioreactor was used to determine the pH effects on cardiomyocytes differentiation of mESCs.

4.2 Materials and methods

4.2.1 mESC maintenance and encapsulation in 3D hydrogel

mESCs were maintained as described in Section 3.2.1 in mESC maintenance medium comprising of high glucose DMEM (Gibco, Lifetech), 10% FBS (gold standard, PAA Laboratories), 0.1 mM 2-mercaptoethanol (Sigma), 2 mM L-glutamine (Gibco, Lifetech), 1x penicillin-streptomycin (PAA Laboratories) and 1000 U/ml LIF (Millipore, Merck). To initiate cardiomyogenesis in 3D culture environment, mESCs were encapsulated using materials and methods as described in Section 3.2.3.

4.2.2 Collection of HepG2-CM

HepG2-CM was used to condition mESCs towards mesodermal lineage during the 3-day expansion stage as illustrated in Figure 4.1. In brief, HepG2 cells were routinely cultured in high glucose DMEM (Gibco, Lifetech), 10% FBS (gold standard, PAA Laboratories) and 1x penicillin-streptomycin (PAA Laboratories). To make the complete HepG2-CM, the medium was collected after 4 days of HepG2 culture and prepared as described in Section 3.2.2.

4.2.3 Cardiomyogenesis of murine ESCs under different pH levels in rotary perfused bioreactor

Murine ESCs were encapsulated in alginate hydrogels at a cell density of 2 x 10^6 cells/ml and cultured in the novel rotary perfused bioreactor for investigation of their response and sensitivity to different pH levels that were commonly used in cell cultures. Differentiation protocol was adopted from previous section (Section 3.2.4) and illustrated in Figure 4.1. After 3 days of using HepG2-CM medium feed for mESC expansion and mesodermal-conditioning, the feed was changed to differentiating medium of the various pH values (pH 6.8, 7.1 and 7.4). Differentiating medium consisted of high glucose IMDM, 20% FBS (gold

standard, PAA Laboratories), 450 μM 1-thioglycerol (Sigma-Aldrich), 2 mM L-glutamine (Gibco, Lifetech), 1x penicillin-streptomycin (PAA Laboratories) and 0.25 μM Cardiogenol C (Sigma-Aldrich). The basal IMDM medium used was reconstituted from powder (Gibco, Lifetech) and did not contain any sodium bicarbonate. Different amounts of sodium bicarbonate were added to achieve the required pH values in final differentiating medium. 1.0 g/L, 3.0 g/L and 4.8 g/L of sodium bicarbonate (Sigma) were first added to the reconstituted IMDM basal medium. After supplementing with other components, the final medium had sodium bicarbonate concentrations of 0.8 g/L, 2.4 g/L and 3.84 g/L. When equilibrated with 5% carbon dioxide in humidifier incubator, they produced environments with pH 6.8, 7.1 and 7.4 respectively. During differentiation, 50 mL medium was perfused daily to achieve a continuous exchange of nutrients and metabolites.

(a)

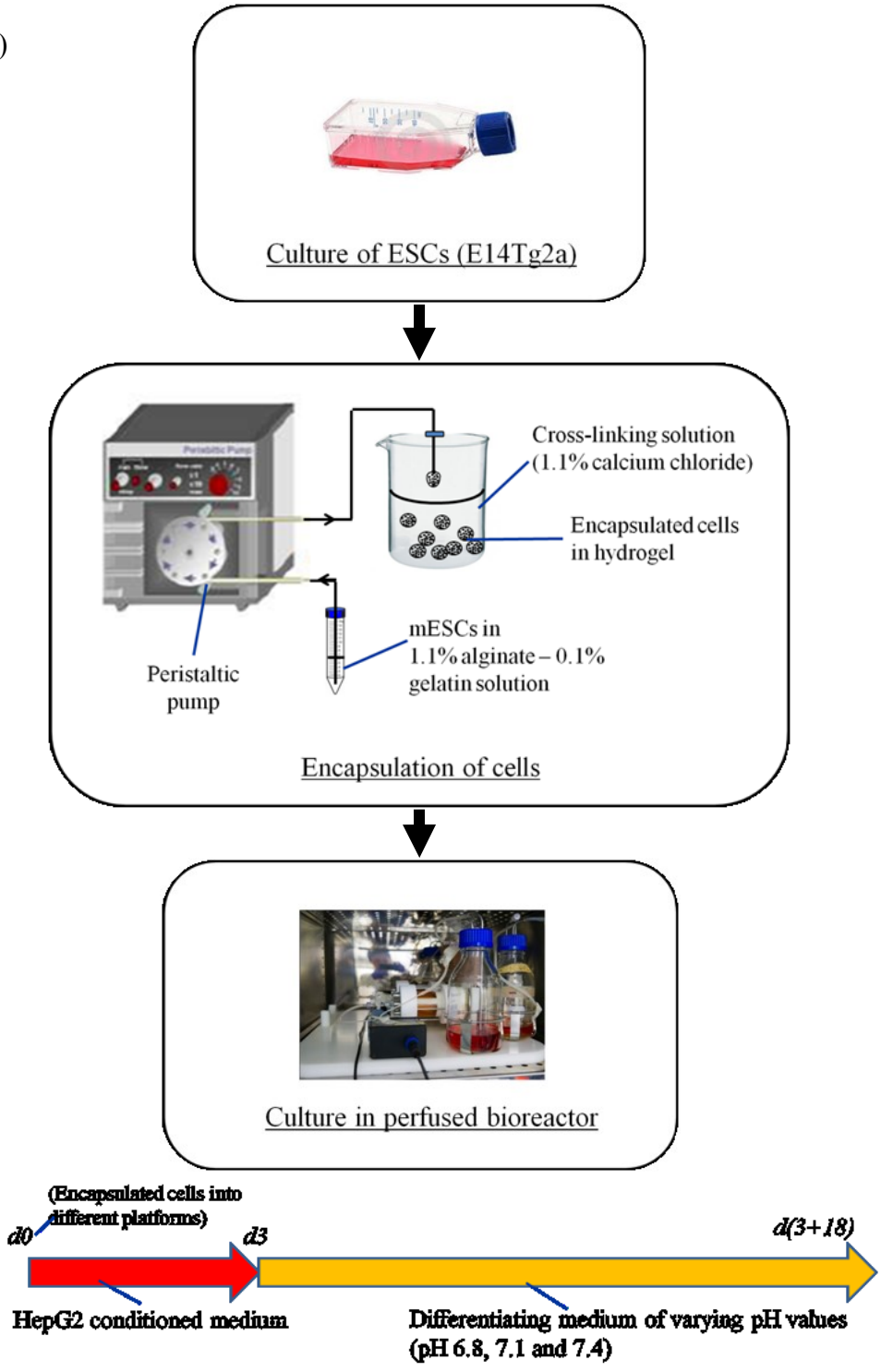

Figure 4-1 (a) Schematic diagram of procedure in encapsulation and culture of mESCs in perfused bioreactor for studying pH effects on cardiomyogenesis. (b) Timeline of medium introduction into perfused bioreactor. HepG2-CM was used for initial three days of cell expansion and conditioning towards mesodermal lineage. Thereafter differentiating medium of various pH values was used.

4.2.4 Maintenance of culture pH in bioreactor setup

Continuous rotation of the novel bioreactor enables a dynamic culture environment that ensured homogeneous distribution of nutrients. It was demonstrated that more rapid and efficient transport of nutrients was achieved throughout the culture vessel and in alginate beads for perfused bioreactor compared to that in conventional static cultures [170, 199]. As there was negligible diffusion limitations in alginate hydrogel in the perfused bioreactor [199], a uniform pH environment was assumed to be maintained through the bulk medium and in the encapsulated cells.

The extracellular pH was then monitored throughout the differentiation process via sampling every two days by sampling the spent medium collected in waste bottle and also by sampling medium in culture vessel during every sample collection point (i.e. Day 6, 10, 16 and 21 of culture). During each time point, two samples were withdrawn from each set up and measurements were taken with a pH meter (Ezdo PL600, Gondo Electronic Co. Ltd.). With a daily perfusion rate of one bioreactor vessel volume (50 ml/day), the culture pH values (from Day 3 to end of culture) were maintained at 6.80 ± 0.02, 7.11 ± 0.03 and 7.38 ± 0.03 respectively. Therefore, the perfused bioreactor was able to ensure a tight control of pH over a long-term culture, which made it possible to study the effects of pH on cardiac differentiation of mESCs.

4.2.5 Microscopic visualisation and live/dead staining

Cell proliferation was observed with an inverted optical microscope (Axiovert 200M, Zeiss) and images were captured with its accompanying camera (AxioCam MRc, Zeiss). Cell viability of encapsulated cell aggregates were assessed by incubation with 2 μM of calcein-AM (Sigma) and 4 μM of

propidium iodide (Sigma-Aldrich) for 30 mins at 37°C in the dark. Thereafter, the encapsulated cells were washed with PBS twice to remove any residual dye. Their overall viability was evaluated qualitatively with fluorescence images that were captured by inverted fluorescence microscope (Axiovert 200M, Zeiss) and camera (AxioCam MRc, Zeiss).

4.2.6 Cell proliferation assay

Cell proliferation under different pH environment was also compared quantitatively with tetrazolium salt, WST-8* (Cell Counting Kit 8, Dojindo). WST-8* will be reduced to yellow formazon by cellular dehydrogenase activities. Measurement of the yellow absorbance will be indicative of cellular dehydrogenase activities and thus cell numbers and proliferation.

To measure for cell proliferation activities, five beads were sampled for every experimental setup. Each bead was first placed into an individual 96-well and washed twice with PBS. Thereafter, they were each incubated with 100 µl of fresh medium and 10 µl of WST-8* reagent in 37°C, 5% CO_2 incubator for two hours. Meanwhile, 100 µl fresh medium was also incubated with 10 µl WST-8* to serve as blank samples. After incubation, 100 µl of reacted solution from the blank controls and samples were transferred to a new 96-well. They were finally measured for the yellow absorbance of formazon at 450 nm in microplate spectrophotometer (Bio-rad).

4.2.7 Quantitative PCR

Total RNA was extracted from collected cell pellets using RNeasy kit (Qiagen) according to manufacturer's instructions. Extracted RNA was then quantified with a UV spectrophotometer (Evolution 500, Thermo). To synthesize the first strand of cDNA from 1 µg RNA, M-MLV reverse transcriptase, oligo-dT

primers, dNTP mix and RNasin were used according to manufacturer's instructions (all reagents from Promega). The final volume was made up to 25 µl with nuclease-free water (Microbiology grade, Hyclone).

For comparison of cardiomyogenesis and differentiation under different pH environments, various gene expressions (as seen in Table 4.1) were quantified via quantitative PCR after ensuring that all primers have similar amplification efficiencies. Target genes were amplified and quantified with SensiFAST^{TM} SYBR Green Fluorescein kit (Bioline). 100 ng cDNA was mixed with 10 µl mastermix and 400 mM primers (1st Base Asia, Table 4.1), and nuclease-free water was added to make a final volume of 20 µl. The samples then underwent PCR amplification and measurement in iQ5 (Bio-rad). A typical PCR amplification protocol involved an initial step of 2 mins denaturation at 95^{o}C and amplification stage of 40 cycles of 10 secs denaturation at 95^{o}C and 30 secs annealing/extension at 60^{o}C. PCR end products were analysed with electrophoresis in 2% agarose gel and ethidium bromide to ensure the absence of any side products and formation of primer-dimers. A melt curve were also conducted after every PCR run to ensure the specificity of amplification to the target gene. PCR data was normalised to the pH 7.1 samples on Day 3, which corresponded to the introduction of different pH environments, and fold changes were calculated with $2^{-\Delta\Delta CT}$ method, as described in Section 3.2.9.

4.2.8 Flow cytometry

To investigate the effects of pH on the amount of mESCs differentiating to cardiomyocytes, flow cytometry was used to determine the percentage of cells positive for expression of two cardiac proteins, namely cardiac troponin-I and sacromeric α-actinin.

First, cells were extracted from the alginate hydrogel as described in Section 3.2.5 and the extracted cells were treated in preparation for antibody incubation as described in Section 3.2.10. The cells were then incubated with 2 µl of each primary antibody shown in Table 4.2 for two hours at 4ºC. Next, the cells were washed twice with cold PBS and incubated with 100 µl of secondary antibodies (Table 4.2) for another one hour at room temperature in the dark. To remove any residual antibodies, the cells were washed twice with cold PBS. Finally, the cells were re-suspended in PBS consisting of 2% paraformaldehyde, 3% bovine serum albumin and 1% sodium azide, and were kept in 4ºC for storage up to one week. Finally, these stained cells were processed in flow cytometer (FACSCalibur, BD Biosciences) and analysed in flow cytometry software FlowJo (Tree Star).

Table 4-1 List of studied genes and their respective primers in studying effects of pH environments on cardiomyogenesis

Gene	*Forward primer*	*Reverse primer*
Housekeeping gene		
GAPDH	AGGTCGGTGTGAACGGATTTG	GGGGTCGTTGATGGCAACA
Cardiac genes		
Brachrury T	AAGGAACCACCGGTCATCG	CGTGTGCGTCAGTGGTGTGTAATG
Nkx2.5	AGCAACTTCGTGAACTTTG	CCGGTCCTAGTGTGGA
cTNT	CTCCATCGGGGATCTTGGGT	CAGAGGAGGCCAACGTAGAAG
α-MHC	ACCGTGGACTACAACAT	CTTTCGCTCGTTGGGA
β-MHC	ACCCCTACGATTATGCG	GGTGACGTACTCGTTGCC
Pluripotent genes		
Nanog	CCTGATTCTTCTACCAGTCCCA	GGCCTGAGAGAACACAGTCC
Oct -4	TGTGGACCTCAGGTTGGACT	CTTCTGCAGGGCTTTCATGT
Pathway markers		
HIF-2α	GGGAACACTACACCCAGTGC	TCTTCAAGGGATTCTCCAAGG
MAP14	CCCCAGAGATCATGCTGAAT	ACAACGTTCTTCCGGTCAAC

Table 4-2 List of antibodies used in flow cytometry

Primary antibody	*Corresponding secondary antibody*
Cardiac Troponin I (H-41, Santa Cruz Biotechnology)	Goat anti-rabbit IgG-FITC (400x dilution, Abcam)
Sacromeric α-actinin (EA-53, Santa Cruz Biotechnology)	Goat anti-mouse IgG1-PerCP (100x dilution, Santa Cruz Biotechnology)

4.2.9 Immunocytochemistry

Encapsulated cells cultured under different pH environments were fixed and processed for immunostaining as described in Section 3.2.10. For immunostaining, the sectioned samples were first incubated with 10% goat serum for 30 mins at room temperature to block out non-specific binding. They were then incubated with sacromeric α-actinin (EA-53, Santa Cruz Biotechnologies, 100x dilution in primary diluents of 0.1% sodium azide and 1% bovine serum albumin in PBS) and SSEA-1 (MC-480, Santa Cruz Biotechnologies, 100x dilution) primary antibodies at 4ºC for two hours. Thereafter, the slides were washed with PBS thrice and incubated with FITC-conjugated and TRITC-conjugated secondary antibodies respectively (100x dilution in 1% bovine serum albumin in PBS) at room temperature in the dark. After incubation the slides were washed on a shaker for 10 mins thrice to remove any residual unbound antibodies. Finally, the samples were incubated with DAPI dye for 5 – 10 mins for nuclei-staining and imaged under a fluorescence microscope (Axiovert 200M, Zeiss) and camera (AxioCam MRc, Zeiss).

4.2.10 Statistical analysis

All statistical analysis was conducted by using Microsoft Office Excel analysis tool package (Excel 2013, Microsoft). After verifying with F-test that there were unequal variances in the different data sets, student t-test with unequal variances were used. This was used to test for inter-group differences of 95% significance in cell proliferation data, quantitative PCR data, and flow cytometry data. Error bars on the charts were representative of the standard deviations. The sample populations (N) are indicated in the legends of the respective figures and represent the total number of biological replicates from two independent experimental runs.

4.3 Results

4.3.1 ESCs' proliferation and viability under different pH environments

Cell growth of the encapsulated mESCs in different pH environments were monitored under the microscope. Figures 4.2 showed aggregate densities under various pH values at Day 10 and 21. At Day 10 (Figure 4.2 (a – c)), the aggregates at pH 6.8 were slightly more sparsely packed and smaller than those at pH 7.1 and 7.4. By Day 21 (Figure 4.2 (d – f)), these differences were more attenuated. Similar observations throughout the whole differentiation period suggested that aggregates cultured at pH 6.8 were not as dense as those at pH 7.1 and 7.4 and indicated that a slight increase in acidity could cause lower cell number and proliferation.

Proliferation assay also showed similar trends as indicated by these microscopic observations (Figure 4.3). Throughout the entire differentiation period, cell expansion was the lowest at pH 6.8, giving 2.8-fold increase after 21 days. Meanwhile, cell culture at pH 7.4 produced the highest expansion fold of 3.4 folds after 21 days, which was 10% and 21% more than that at pH 7.1 and 6.8 respectively. Different pH environments also affected the onset of exponential growth during proliferation. For instance at pH 7.1 and 7.4, the exponential growth started before Day 3. However, this was only observed at pH 6.8 on Day 6, indicating a longer lag phase induced by acidic environment.

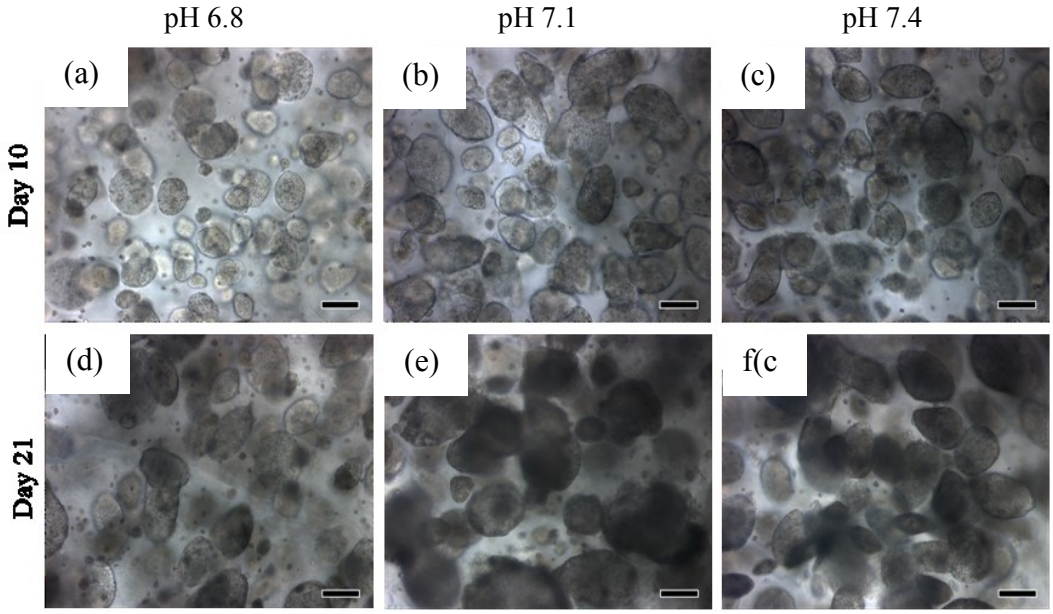

Figure 4-2 Photomicrographs of encapsulated aggregates in alginate hydrogel after (a-c) 10 days, and (d-f) 21 days of culture. Scale bar represents 100 µm.

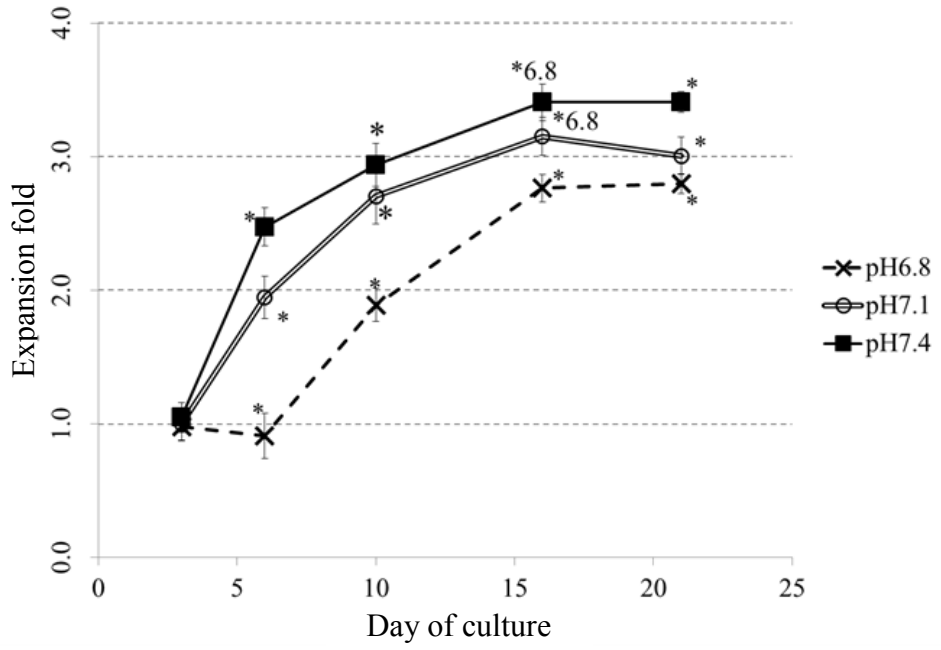

Figure 4-3 Cell proliferation profiles under different pH environments. Expansion fold of respective point is obtained by normalising its assay absorbance to that on Day 3. Unless indicated, * represents significant differences from the other two pH environments at each respective time point. p < 0.01., N = 10 from two independent runs

Another effect of pH on cellular expansion is cell viability. From the fluorescence micrographs of live/dead staining after 21 days of culture (Figure 4.4), the highest percentage of dead cells was observed at pH 6.8. These dead cells were most probably caused by exposure to unfavourable extracellular conditions such as higher amount of hydronium ions at lower pH. The nutrients transport limitations as a probable cause was ruled out because cell viabilities were not compromised in cultures at pH 7.1 and 7.4 and these regions of dead cells were mostly concentrated along the periphery of cell aggregates, which did not face limited nutrient supply.

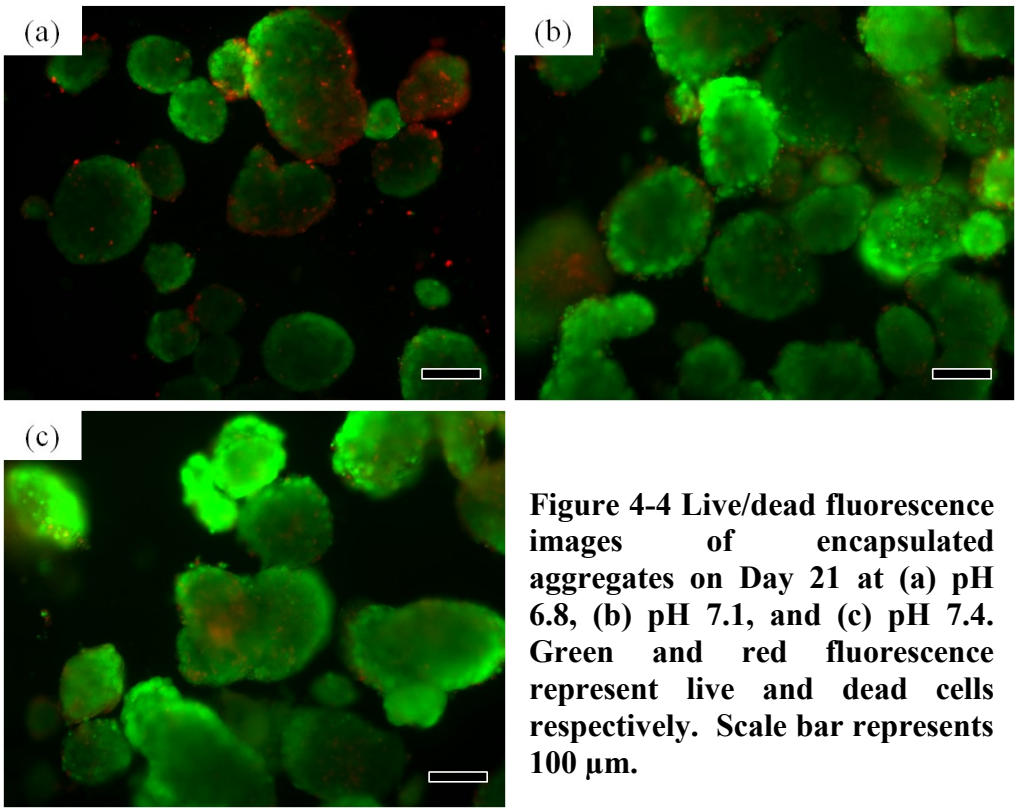

Figure 4-4 Live/dead fluorescence images of encapsulated aggregates on Day 21 at (a) pH 6.8, (b) pH 7.1, and (c) pH 7.4. Green and red fluorescence represent live and dead cells respectively. Scale bar represents 100 µm.

4.3.2 Cardiomyocyte differentiation and sensitivity towards pH environment

Effects of pH on directed differentiation of mESCs towards cardiomyocytes was evaluated by comparing cardiac gene expressions of cells cultured at different pH

levels. Gene expressions of all samples were normalised to those expressed at Day 3 of culture, which corresponded to the start of directed differentiation. Upon comparing various cardiac gene levels expressed at different pH values, it showed that the genes were more upregulated at pH 7.1 and 7.4 than at pH 6.8 by Day 21. For instance on Day 21, mesodermal marker Brachyury T and cardiac progenitor marker Nkx-2.5 had the lowest expression levels at pH 6.8 while no significant difference was observed for cultures at pH 7.1 and 7.4 (Figure 4.5).

Late cardiac markers also showed similar trends as those for Brachyury T and Nkx-2.5. Gene expressions for structural motor proteins α- and β-MHC and regulatory calcium-signalling protein cTNT were higher at pH 7.1 and 7.4 than at pH 6.8. On Day 21, expression of α-MHC in cells cultured at pH 6.8 gave around 20 fold increase while that at pH 7.1 and 7.4 ranged around 1000 – 1500 fold (Figure 4.6 (a)). This showed that the slight decrease in pH could cause a significant reduction in α-MHC expression. Expression of β-MHC was also lower at pH 6.8 (Figure 4.6 (b)). On Day 16, expression of β-MHC was upregulated by 11 folds at pH 6.8 while cells experienced an 100-fold upregulation at pH 7.1 and 7.4. The difference of such extent persisted till Day 21, where cells produced about 40 and 400 folds upregulation of β-MHC at pH 6.8 and the other two higher pH environments respectively. Meanwhile, in Figure 4.6 (c), cTNT expression was initially highest at pH 6.8 on Day 16. However, this upregulation stagnated at around 50-fold increase for the last 5 days of differentiation. In contrast, cells at pH 7.1 and 7.4 produced an exponentially increase in cTNT expression of about 1000 – 1500 folds, which corresponded to the increase in α- and β-MHC expression. Observations from these various

cardiac markers showed the significant reduction of mESCs' cardiomyogenesis that a slight pH decrease could cause.

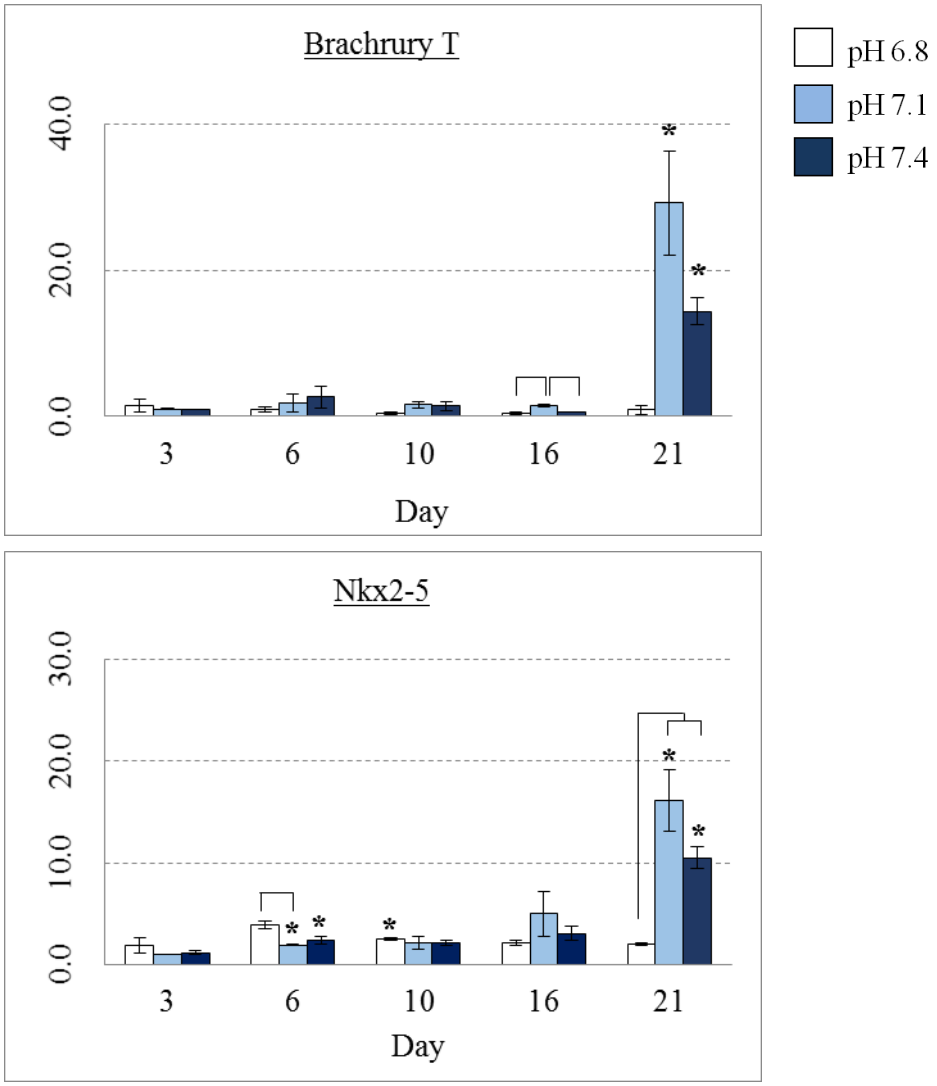

Figure 4-5 Fold changes in gene expression of (a) mesodermal marker Brachyury T, and (b) early cardiac progenitor marker Nkx2.-5 on respective days of differentiation process. * represent significant difference from the previous time point under same pH condition. Indicated bars represent significant differences from other pH conditions at the same time point. $p < 0.05$, N = 2

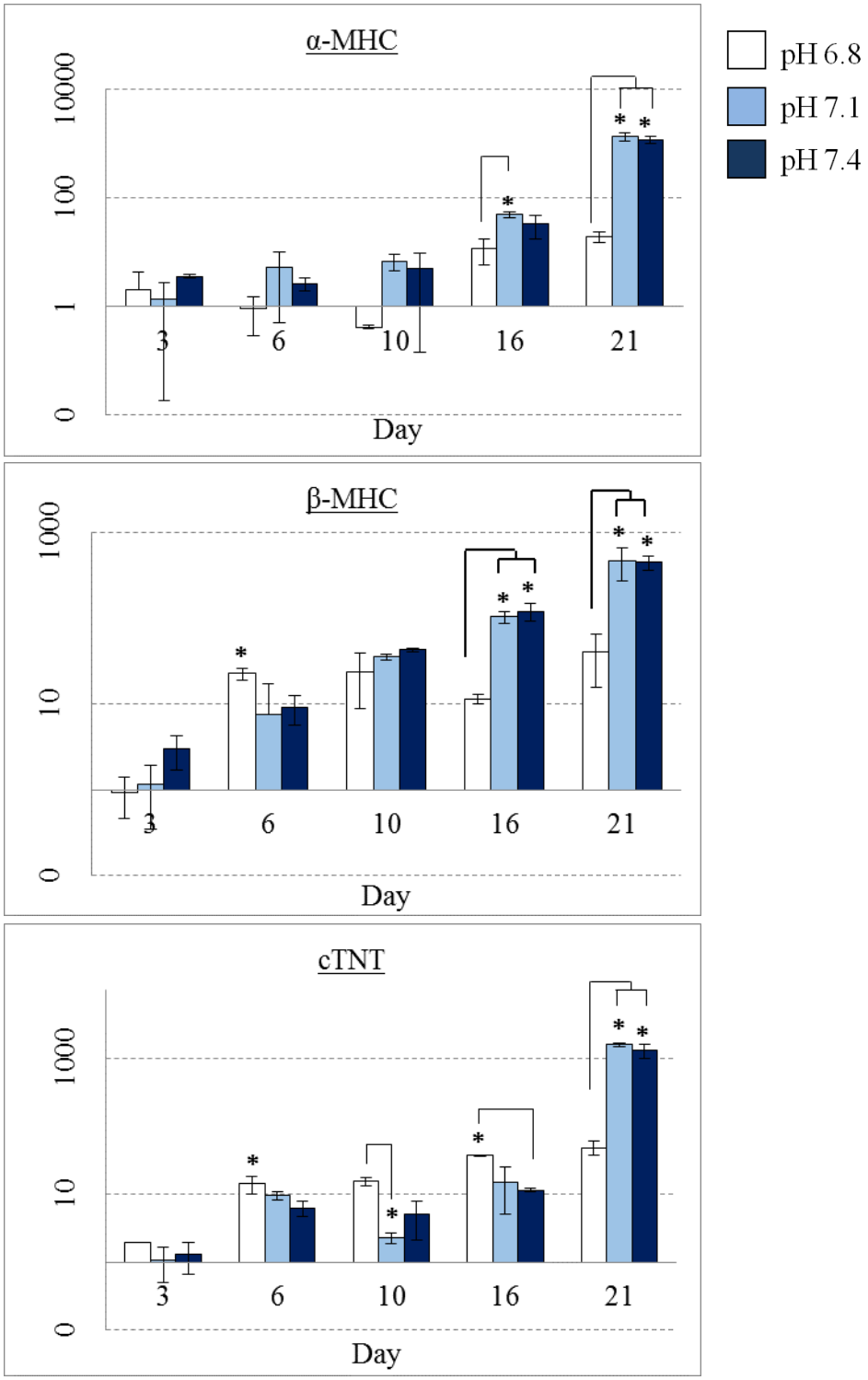

Figure 4-6 Fold changes in gene expression of late cardiac markers (a) α-MHC, (b) β-MHC, and (c) cTNT on respective days of differentiation process. * represent significant difference from the previous time point under same pH condition. Indicated bars represent significant differences from other pH conditions at the same time point. $p < 0.05$, $N = 2$

Percentages of cells differentiating to cardiomyocytes under different pH environments were also evaluated by flow cytometry for sacromeric α-actinin (ATN) and cardiac troponin I (cTNI). α-actinin is a cytoskeleton protein and includes α- and β-spectrins and dystrophins. Sacromeric α-actinin (ATN) is found in the Z-disc and dense striations in cardiomyocytes, anchoring the actin filament and taking part in the contractile motion of cardiomyocytes. Meanwhile, cTNI is a sub-unit of cardiac troponin, which participates in calcium signalling for cardiomyocytes' contractile motion. From gene expression data, the significant observation is the reduced cardiac gene expressions at pH 6.8 as compared to pH 7.1 and 7.4. Since there was no significant difference between the cardiac genes at pH 7.1 and 7.4, only samples from pH 6.8 and 7.1 were used to investigate the effects of reduced pH on the cardiomyocyte yield.

From the flow cytometry analysis (Table 4.3 and Figure 7.4), a slight pH decrease to pH 6.8 lowered the percentage of cells positive for cTNI and ATN expressions, indicating reduced cell yields in differentiated cardiomyocytes. At Day 21, there were 20.6% of cTNI-positive cells under pH 7.1 while only 10.3% of cells were positive for cTNI under pH 6.8 conditions. The expressions of these cardiac proteins correlate to the cardiac gene expressions and indicate an inhibition effect in cardiomyogenesis by slight pH decrease.

Table 4-3 Comparison of cTNI-positive and ATN-positive cells evaluated by flow cytometry for pH 6.8 and 7.1 at Day 21 and Day 25. * represents significant difference of respective samples on the same day. p<0.05, N=2

	cTNI		ATN	
	D21	D25	D21	D25
pH 6.8	10.3 ± 1.4 (*)	23.6 ± 0.8 (*)	10.4 ± 0.8	16.4 ± 0.8 (*)
pH 7.1	20.6 ± 1.2 (*)	53.2 ± 3.3 (*)	9.4 ± 2.1	37.9 ± 0.8 (*)

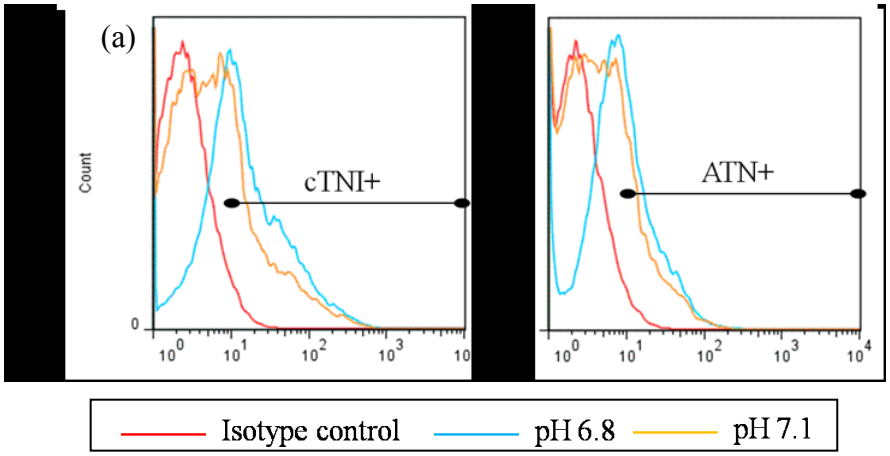

Figure 4-7 Representative flow cytometry histograms of cTNI- and ATN-positive cells in isotype control and cells differentiatied at pH 6.8 and 7.1 on Day 25.

4.3.3 Sacromeric α-actinin network under different pH environments

Sacromeric α-actinin (ATN) networks within encapsulated cell aggregates were visualised via immunocytochemistry to compare the extent and uniformity of sacromeric networks formed in differentiated cardiomyocytes. At pH 6.8, the aggregates produced non-uniform distribution of cardiomyocyte differentiation; areas which displayed strong ATN expression were along the cellular aggregates' peripheral regions while the inner cores were absent of ATN (Figure 4.8 (a)). On the other hand, Figures 4.8 (b) and (c) showed a more uniform expression for areas that were positive for ATN in aggregates from pH 7.1 and 7.4.

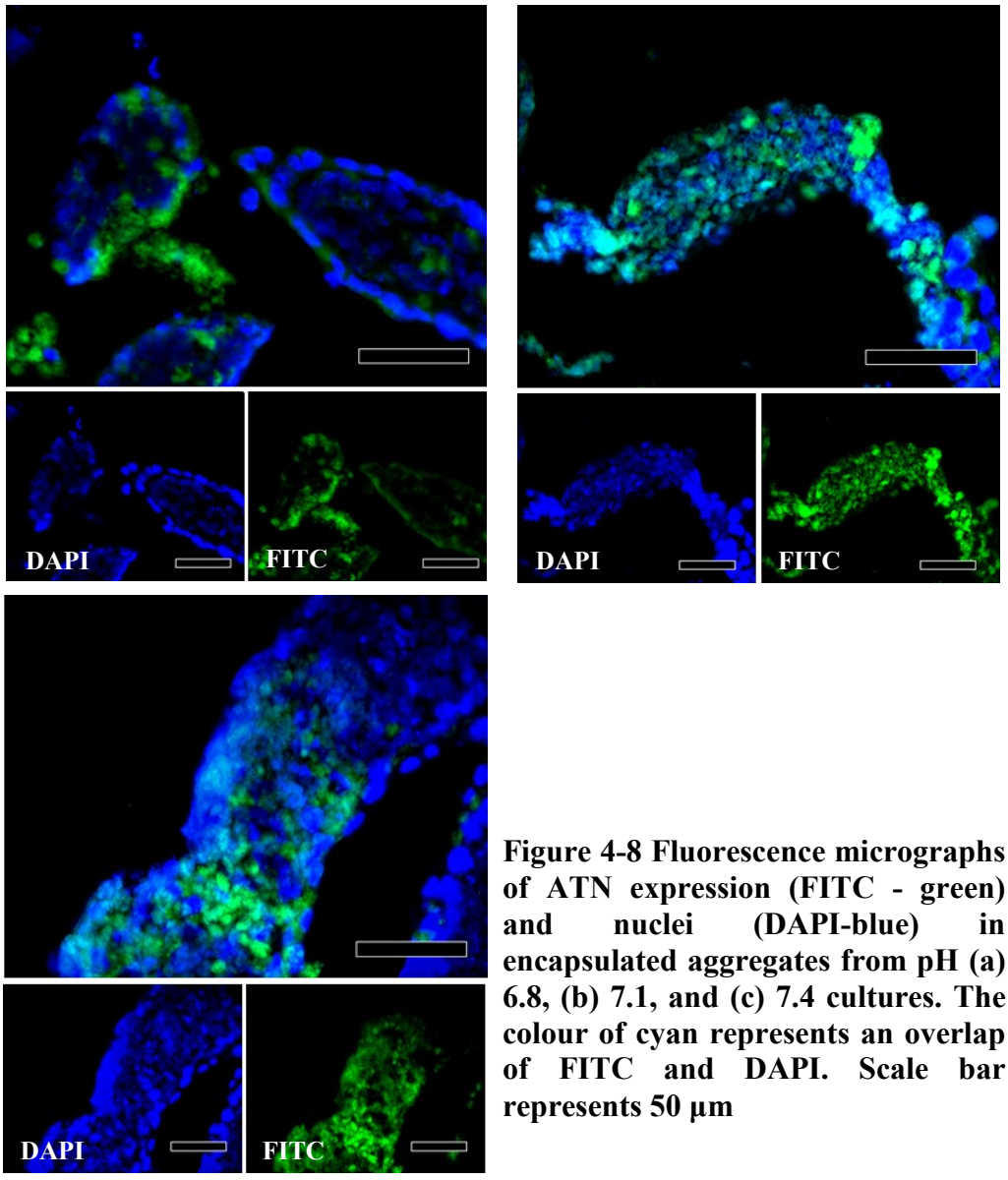

Figure 4-8 Fluorescence micrographs of ATN expression (FITC - green) and nuclei (DAPI-blue) in encapsulated aggregates from pH (a) 6.8, (b) 7.1, and (c) 7.4 cultures. The colour of cyan represents an overlap of FITC and DAPI. Scale bar represents 50 µm

4.3.4 Effects of pH on residual ESC pluripotency

Besides investigating expressions of cardiac genes, pluripotency and differentiation towards endodermal and ectodermal lineages was also briefly monitored. Residual pluripotency of ESCs was a major issue in its utility for clinical application. Undifferentiated ESCs can cause tetratomas when transplanted, causing highly detrimental effects to the patient. Thus, pluripotency levels of mESCs differentiated at these different pH environments was investigated by studying the gene expression of pluripotency markers, Nanog and Oct-4.

Expression of Nanog (Figure 4.9 (a)) was significantly higher at pH 6.8 than at pH 7.1 and 7.4 since Day 16. During the last five days of differentiation at pH 7.1 and 7.4, its expression decreased to levels lower than 0.5-fold, indicating a downregulation and loss of pluripotency. This is a strong correlation to the significant increases in cardiac gene expressions, showing directed differentiation of ESCs towards cardiomyocytes. However, cells at pH 6.8 experienced an upregulation of Nanog, giving a 3.4-fold increase. Such contrast between cells at pH 6.8 and at the other two pH environments was also observed for Oct-4 expression (Figure 4.9 (b)). At Day 21, Oct-4 was down-regulated at pH 7.1 and 7.4 while it showed an upregulation at pH 6.8.

Stage-specific embryonic antigen 1 (SSEA-1) protein expressions were also evaluated via immunostaining to determine the extent of residual pluripotency in the different pH environments. SSEA-1 plays an important part in adhesion and migration of the cells in the preimplantation embryo and is a marker of undifferentiated mESCs. Similar to the Nanog and Oct-4 gene expressions, SSEA-1 protein expressions on Day 21 were much higher at pH 6.8 than pH 7.1

and 7.4 (Figure 4.10). At pH 6.8, aggregates showed a high presence of SSEA-1 proteins while those at pH 7.1 and 7.4 showed lower levels and scattered regions of SSEA-1 expressions. Results of the pluripotent gene expressions and protein expression showed that ESC maintained a higher level of residual pluripotency at lower pH.

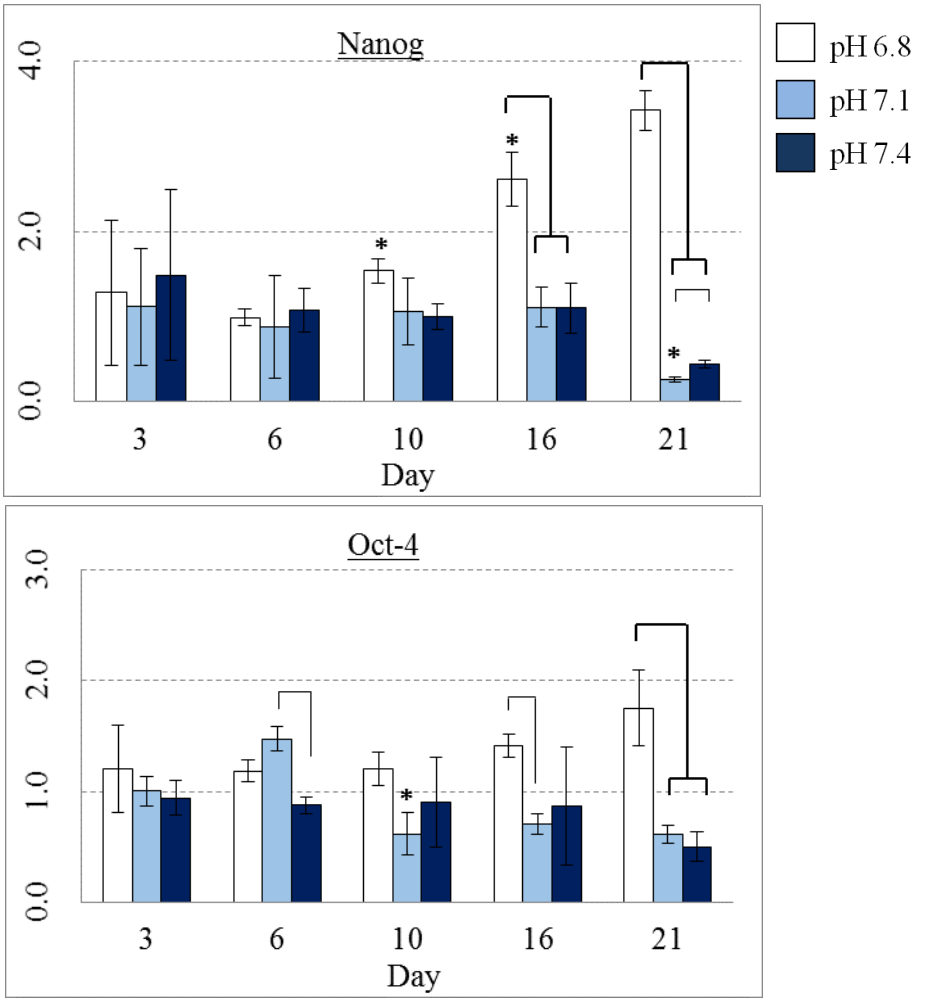

Figure 4-9 Fold changes in gene expression of pluripotent markers (a) Nanog and (b) Oct-4 on respective days of differentiation process. * represent significant difference from the previous time point under same pH condition. Indicated bars represent significant differences from other pH conditions at the same time point. $p < 0.05$, N = 2

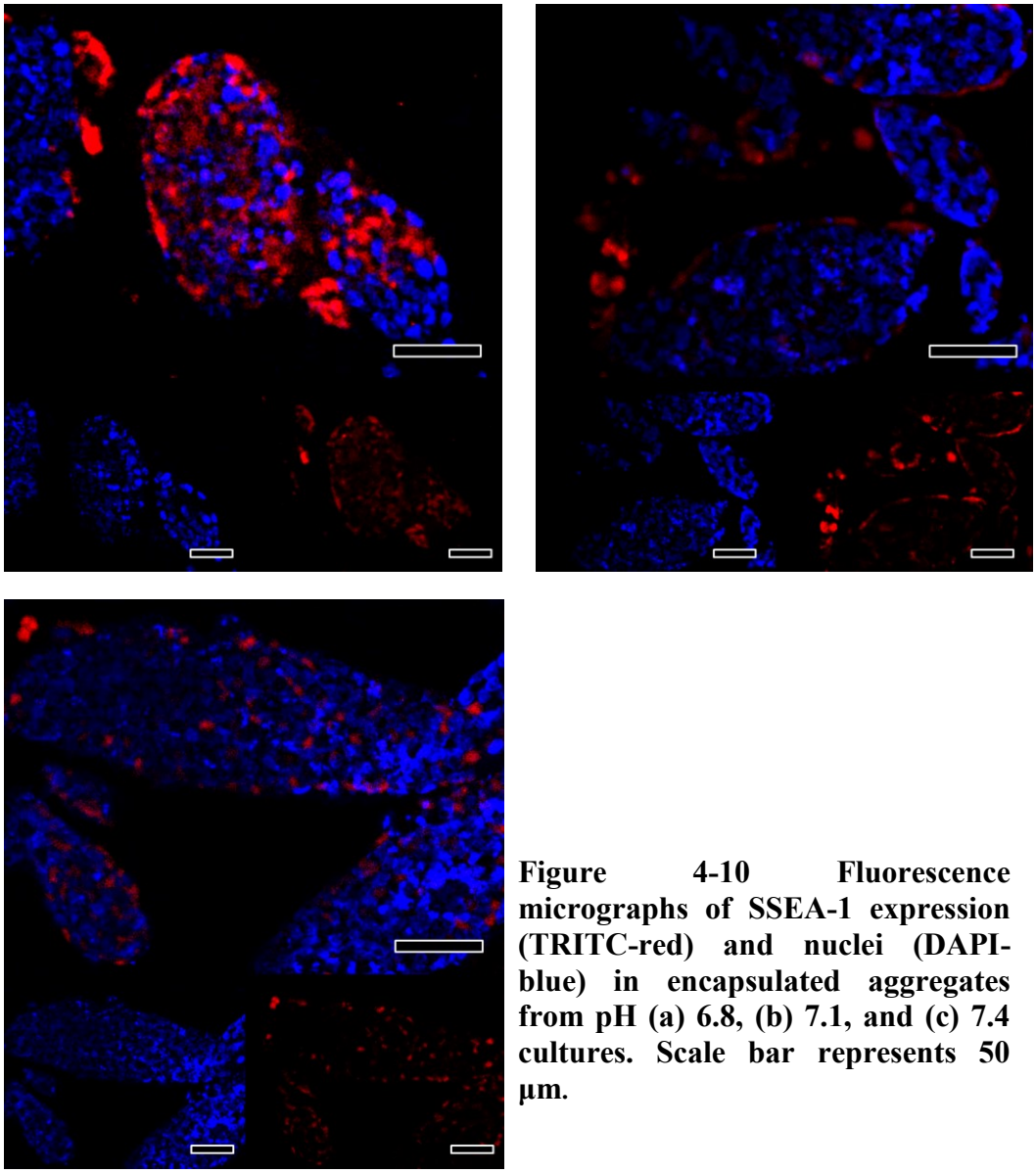

Figure 4-10 Fluorescence micrographs of SSEA-1 expression (TRITC-red) and nuclei (DAPI-blue) in encapsulated aggregates from pH (a) 6.8, (b) 7.1, and (c) 7.4 cultures. Scale bar represents 50 µm.

4.3.5 Effects of pH on spontaneous endodermal and ectodermal differentiation of ESCs

Undesired ESC differentiation towards endodermal and ectodermal lineages was briefly evaluated with α-fetoprotein (AFP) and nestin markers respectively. For AFP, no significant difference between the different pH environments was observed (Figure 4.11 (a)). This implies that endodermal differentiation was not as sensitive as cardiomyogenesis of mESCs at this tested pH range. Meanwhile, nestin expression levels showed otherwise, as seen in Figure 4.11 (b). At Day 21, it showed a higher gene expression at pH 7.1 than pH 6.8 and 7.4. Expressions of

all cardiac and pluripotent markers had produced similar levels at pH 7.1 and 7.4 but nestin was the only exception. This indicates that within the tested pH range of 6.8 to 7.4, ectodermal differentiation of mESCs will be quite sensitive to any slight pH changes, thus affecting the efficacy of producing cardiomyocytes for clinical therapies.

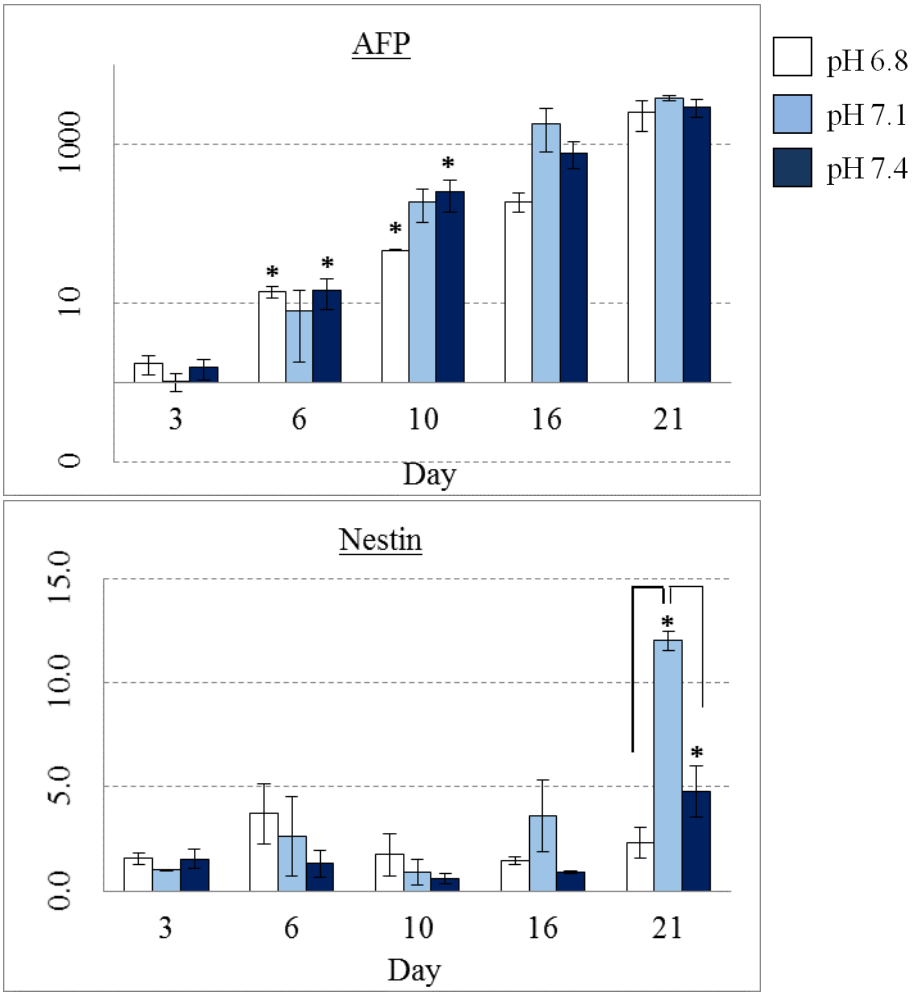

Figure 4-11 Fold changes in gene expression of (a) early endodermal marker AFP, and (b) early ectodermal marker Nestin on respective days of differentiation process. * represent significant difference from the previous time point under same pH condition. Indicated bars represent significant differences from other pH conditions at the same time point. $p < 0.05$, N = 2

4.3.6 Expression of signalling proteins, HIF-2α and MAPK14

Two important signalling pathways that could link to the differences observed in mESC pluripotency and cardiomyogenesis were studied. HIF-2α expression was found to be significantly higher at pH 6.8 than at pH 7.1 and 7.4 (Figure 4.12 (a)). Meanwhile, expression of p38 MAPK was studied via its isoform MAPK14 (Figure 4.12 (b)). It was also shown that expression of MAPK14 was highest at pH 6.8 and the lowest at pH 7.4. Significant differences in expression levels of HIF-2α and MAPK14 were found among all three pH values.

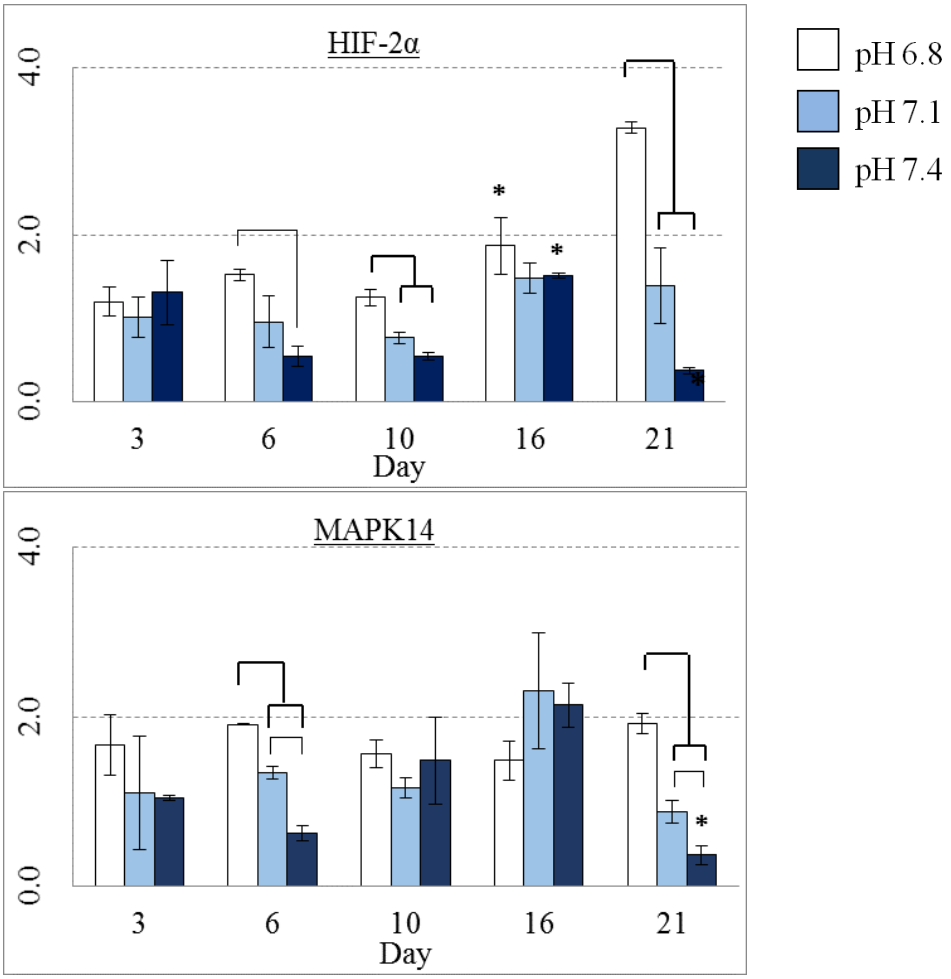

Figure 4-12 Fold changes in gene expressions of (a) HIF-2α, and (b) MAPK14 on respective days of differentiation process. * represent significant difference from the previous time point under same pH condition. Indicated bars represent significant differences from other pH conditions at the same time point. $p < 0.05$, N = 2

4.4 Discussion

Physiological environment is an important consideration in maximising cardiomyocyte yields. One such physiological parameter that could affect cell fate is the pH environment of cell culture. However, maintaining pH at a consistent value is often difficult in conventional flask cultures due to localised and perhaps rapid accumulation of metabolites, especially in high cell density cultures. Hence, investigation of pH effects on cardiomyogenesis in flask cultures will face challenges to obtain conclusive results. The rotary perfused bioreactor, on the other hand, is able to maintain an environment at a consistent pH value throughout cardiomyogenesis and therefore a suitable culture platform to study pH sensitivity. Furthermore, an optimal pH condition was believed to be necessary to maximise yields and homogeneity of cell output in the 3D cell culture bioprocess for pluripotent cells.

This chapter compared cardiomyogenesis under three pH environments which were commonly found in ex vivo studies: pH 6.8, 7.1 and 7.4. The tight pH range was chosen to simulate a study of the dependence and sensitivity of ESCs toward cardiomyogenesis under small variable changes in pH conditions. Under manual feeding such as in standard flask cultures, cells may suffer from an accumulation of metabolites which often gives rise to slightly acidic environment dropping to around pH 6.8. Such pH condition has also been observed commonly in damaged tissues as those found at the onset of myocardial infarction. Environments with pH 7.1 and 7.4 were chosen as they are common in the preparation of fresh cell culture medium. Moreover, pH 7.4 is found in peripheral blood of human body, thus it is also the usual standard pH recommended for cell culture. By studying

these three pH conditions and using mESCs as the pluripotent cell model, this study demonstrated the importance of pH control in 3D bioprocess.

Under conditions similar to damaged tissues, such as a slightly acidic environment of pH 6.8, stem cells like mesenchymal stem cells experienced growth inhibition and lower viabilities [200]. The pH value during fetus development ranges 7.0 to 7.5 due to the amniotic fluid environment. Therefore, a shift in pH from this range may affect both embryonic development and ex vivo cultures of ESCs. It was demonstrated in this chapter that a slight drop in pH to 6.8 resulted in compromised mESC proliferation and viability during cardiomyogenesis while pH 7.4 produced the highest number of cells. Using cardiomyocytes for tissue engineering and regenerative therapies faces a challenge of obtaining clinically relevant numbers efficiently. From these comparisons of cell numbers and viabilities at different pH environments, it was shown that pH plays a significant role in determining the bioprocess efficiency in producing required cell numbers.

The extent of cardiomyocyte differentiation and residual pluripotency of mESCs were also affected by slight variations in pH environments. A slight change to an acidic environment of pH 6.8 resulted in decreased cardiomyogenesis, as indicated by both lower cardiac gene expressions and percentage of ATN-positive and cTNI-positive cells. This could be attributed to changes in signalling pathway. Hydronium ions can influence protein conformation, thus affecting protein binding and signalling. Through studying the pH effects on signalling proteins, one could not only gain insight on impact on cardiomyogenesis but also on other possible cell fates where the studied signalling protein participated in.

MAPK signalling is one major pathway involved in cardiomyogenesis, and was studied to determine any possible effects due to the different pH environments.

MAPK signalling plays an important role in ESC differentiation and it depends on interplay of three major pathways: (1) c-Jun NH2-terminal kinases, (2) extracellular signal-regulated kinases, and (3) p38 MAPK. The first two pathways were shown to be required for cardiomyogenesis, where their inhibition would result in any upregulation of cardiac markers to cease [201]. Meanwhile, studies showed the complexity of p38 MAPK's effect on cardiomyogenesis, indicating that different stages of cardiomyogenesis might be more sensitive to p38 MAPK signalling. For instance, p38 MAPK was found to be essential for ESC commitment towards mesodermal lineage and cardiomyocyte differentiation [202]. However, inhibiting p38 MAPK signalling could enhance cardiomyocyte differentiation of ESCs [203, 204]. It was demonstrated that after 21 days, lower levels of p38 MAPK gene were expressed in cells cultured at pH 7.1 and 7.4, which corresponded to the increased cardiac markers. This implied that changes in hydronium ions concentration might have affected extent of mESC cardiomyogenesis via p38 MAPK signalling. p38 MAPK signalling is also involved in regulating mESC commitment towards neuronal cells, thus acting as a control between cardiomyogenesis and neural commitment [205]. Herein, different p38 MAPK expression levels were observed at pH 7.1 and 7.4, which may be an explanation for the higher level of spontaneous ectodermal differentiation at pH 7.1. These results showed that p38 MAPK signalling pathway involved in cardiomyogenesis is very sensitive to pH changes. Furthermore, there are other pathways partaking roles in differentiation towards other lineages which may be sensitive to pH changes and were not studied in this

chapter. Thus controlling pH in bioprocess can help to increase cardiomyocyte yield and purity from pluripotent sources.

Besides considering the level of cardiomyocyte differentiation, residual pluripotency of ESCs must also be considered in lieu of risk in forming teratomas. A slight decrease of pH to 6.8 caused higher residual pluripotency, even after 21 days of differentiation. A pH study on glioma stem cells [193] also showed that their stemness increased in environments with low pH. Such effect was attributed to induction of hypoxia-induced factor (HIF-2α). ESCs will experience upregulation of HIF-2α when subjected to stressful environment, and this will then enhance their pluripotent phenotype [206]. As demonstrated here, the higher pluripotency levels of cells at pH 6.8 was accompanied with higher expression of HIF-2α. This agreed with Hjelmeland et al. and Das et al. [193, 206], illustrating the effects of pH on residual pluripotency via HIF-2α signalling.

4.5 Conclusion

There was a significant impact on cell proliferation, viabilities and differentiation of ESCs even within the narrow range of the pH environments studied here. In general, a slight drop of pH to acidic environment of pH 6.8 resulted in compromised proliferation, viability and lower cardiomyocytes yield of mESCs. Furthermore, this slight pH change also resulted in higher residual pluripotency. Such differences were attributed to the changes in signalling pathways, such as level of p38 MAPK and HIF-2α expressions. From this study, cardiomyogeneis of mESCs were proven to be highly sensitive to the pH environment. Similarly, human pluripotent cells may also display sensitivities to pH environment during cardiac differentiation. Therefore, in the utility of human pluripotent cells for producing for clinical applications, pH environment should also be studied with great importance. The sensitivity of pluripotent cells towards pH demonstrates that a stringent pH control is important in 3D bioprocess to ensure a more efficient production of cardiomyocytes for tissue engineering and regenerative clinical applications.

5 Ultrasound as mechanical stimulation for cardiomyogenesis of ESCs

As presented in a manuscript for Plos ONE

5.1 Background

Mechanical stimulation has been used extensively to enhance cardiomyocyte differentiation and maturation for tissue engineering applications, as mentioned in Section 2.5.1. Ultrasound is a possible form of stimulation which can be incorporated into stem cell bioprocessing to produce cardiomyocytes for clinical purposes.

Ultrasound is a longitudinal wave, i.e. particles are displaced along the direction of wave propagation. Ultrasound source will produce a vibratory motion and result in compression and rarefaction of particles displacement. Therefore, subjecting cells to ultrasound will expose these cells to repeated and rapid vibratory particulate movements. This can have possible influence on cell fate through mechanotransduction and mechanical cues, as demonstrated in mechanical stimulation studies introducing shear stress or physical stretching on cardiac constructs [8, 10, 147, 156]. Intensity of ultrasound in diagnostic and therapeutic applications can be as high as 300 W/cm^2. However, using ultrasound of such high intensity will face problems of generating heat that causes detrimental effects to the treated cells, especially in ex vivo cultures where cells are highly exposed to any physiological stimuli. To alleviate this problem, low intensity ultrasound (LIUS) has been developed. LIUS has an intensity of lower than 1 W/cm^2, and is already utilised in biomedical applications like diagnostic imaging and bone fracture healing. The heat generated from LIUS is minimal and will not have any thermal nor destructive effects. Therefore, LIUS can be safely used as a mechanical stimulus and has great potential as a tool in producing cells for regenerative and clinical therapies.

LIUS has been shown to affect growth and differentiation of stem cells and progenitors for the production of various mature cells in tissue engineering and regenerative therapies. For instance, human MSCs exhibited higher proliferation and viabilities when subjected to LIUS [207, 208]. Effects of LIUS on osteogenesis and chondrogenesis of different cell sources have been extensively studied *in vivo* and *in vitro*. In a study by Cheung et al. [209], MSCs were first transplanted into bone fracture regions in rat models and these regions were treated with LIUS. The treated rats then experienced enhanced bone healing. Such benefits of LIUS ability to enhance directed differentiation towards osteogenic lineages were also demonstrated in ex vivo cell cultures. Studies showed LIUS treatments to increase osteoblastic gene expressions in differentiating adipose stem cells, myoblasts and hematoma progenitor cells [210-212]. Similarly, chondrogenesis was also enhanced by LIUS for cartilage tissue engineering and regeneration. LIUS treatments gave rise to higher chondrogenic gene expression, higher amounts of collagen and glycosaminoglycan, and better mechanical properties (i.e. higher similarity to *in vivo* cartilage) in differentiating MSCs [213-216]. LIUS can benefit both osteogenesis and chondrogenesis, thus allowing competition for lineage commitment of multipotent/pluripotent sources, hence reducing efficient production of required cells. To prevent this and enable efficient directed differentiation, chemical cues can be added to direct differentiation towards the intended lineage while using LIUS as a complementary and synergistic mechanical stimulus [217, 218].

Studies investigating effects of LIUS on cell differentiation were mostly in bone and cartilage regeneration. In contrast, such works on cardiac regeneration has

been very limited. A study related to this field was conducted by Park et al. [219]. In their study, they showed LIUS's ability to enhance myoblast differentiation towards matured myosin lineage. They subjected myoblasts to 10 mins of 30 mW/cm^2 LIUS daily. After six days, tropomyosin was present in the treated myoblasts and not in the untreated controls. This signifies that LIUS can provide mechanical cues which can enhance differentiation towards a myocyte lineage. Another evidence that suggested LIUS candidacy as a mechanical stimuli for cardiac regeneration is expression of angiotensin II Type 1 (AT1) receptors in osteoblasts. When osteoblasts underwent LIUS treatments, they produced an unregulated AT1 receptor expression [220]. AT1 receptor is a mechanoreceptor commonly found in cardiomyocytes, thus this enhancement displayed in osteoblasts may be also be possible in cell sources for cardiac regeneration.

These studies of LIUS effects on tissue engineering and regenerative therapies show the great potential of using LIUS to enhance cardiomyocytes differentiation and maturation. It was hypothesised that LIUS can serve to enhance cardiac differentiation of pluripotent cell sources in a cardiogenic environment via its mechanical cues. In this chapter, effects of LIUS on cardiomyocyte differentiation of mESCs were investigated in both 2D and 3D culture platforms. The primary motivation here is to show the feasibility of using ultrasound to enhance the cardiomyogenic environment of pluripotent stem cells by first demonstrating it on murine embryonic stem cells. The cells were subjected to daily treatment of LIUS for 10 mins at different intensities (30 and 300 mW/cm^2) and wave generation mode (continuous and pulsed wave). After 3 weeks of differentiation, cells were then evaluated for their viability and the various cardiac markers.

5.2 Materials and methods

5.2.1 Murine ESCs maintenance and HepG2-CM collection

mESCs (E14Tg2a, ATCC) were cultured and maintained as described in Section 3.2.1 prior to differentiation. Meanwhile, HepG2 cells were also cultured and HepG2-CM was prepared as described in Section 3.2.2.

5.2.2 Cardiac differentiation and ultrasound stimulation of mESCs in 2D culture

Prior to directed cardiac differentiation, mESCs were cultured in HepG2-CM and on TCP coated with 0.1% porcine gelatin (Sigma) for 3 days for conditioning towards mesodermal commitment. To initiate cardiac differentiation, EBs were formed in bacteriological grade Petri dishes. In brief, mESCs was enzymatically detached from TCP surface after 3-day culture in HepG2-CM. They were then gently re-suspended to small clumps and cultured in Petri dishes containing EB formation medium. The EB formation medium consisted of high-glucose IMDM (Gibco, Lifetech), 20% FBS (gold standard, PAA Laboratories), 2 mM L-glutamine (Gibco, Lifetech), 1x penicillin-streptomycin (PAA Laboratories) and 450 μM 1-thioglycerol (Sjgma). As the petri dishes used were of bacteriological grade and did not allow for cell attachment, the ESC clumps did not adhere and grew as an expanding cell aggregate while undergoing spontaneous differentiation. These cell clumps was left to grow in the EB formation medium for 5 days to form EBs and medium was changed every two days.

To direct differentiation towards cardiomyocytes, 0.25 μM Cardiogenol C (Sigma) was added into EB formation medium as an inducing agent and this final medium composition was known as differentiating medium. Suspended EBs was then plated onto gelatin-coated 6nwell plates and cultured in differentiating

medium for the remaining days of differentiation. Medium was changed every two days.

Ultrasound treatment was applied to cells 3 days after differentiation of mESCs was initiated in 2D culture (Figure 5.1). LIUS treatment on mESCs was conducted for 10 mins daily until Day 21. The cell-seeded plates were placed on top of LIUS probe (Model X Ultrasound, Rich-Mar) with an ultrasound transmission gel (Aquasonic 100, Parker Labs), which acts as a coupler between the two surfaces and prevent any presence of interfacial air bubbles that will affect the transmission of ultrasound.

This whole differentiation process is briefly illustrated in different stages as shown in Figure 5.1 and 4 independent sets of experimental runs were conducted.

(a)

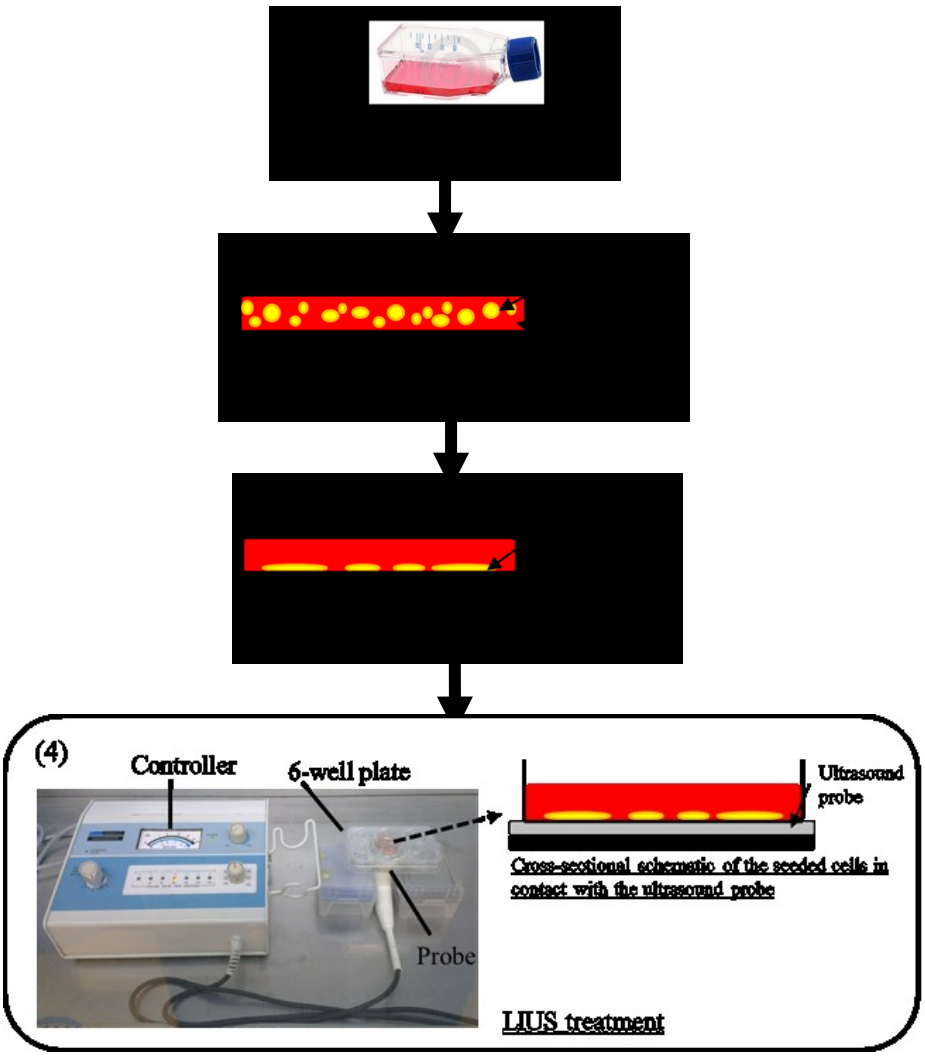

(b)

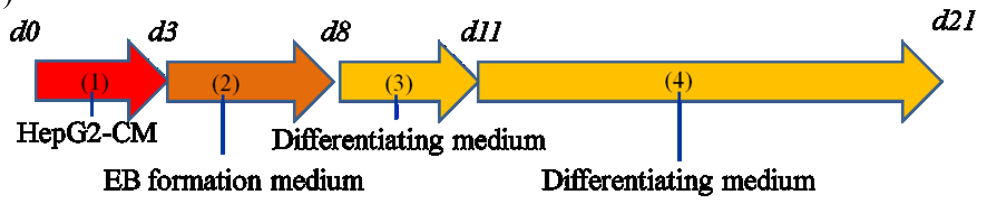

Figure 5-1 (a) Schematic diagram of procedure of 2D conventional differentiation of mESCs as seen in steps 1 to 3, followed by LIUS treatment in step 4. (b) Timeline of addition of different media in different steps of differentiation and LIUS treatment.

5.2.3 Ultrasound treatments

To compare the effects of ultrasound on cardiomyogenesis, mESCs were subjected to simulation by LIUS. Ultrasound used in this study has a working frequency of 1 MHz and an active area of 10 cm^2. Two parameters that were varied are the ultrasound generation mode, which could apply a continuous ultrasound wave or a pulsed ultrasound wave (Figure 5.2), and the intensity, which were selected to be 30 mW/cm^2 and 300 mW/cm^2. The generation mode (mode of application) determines if the ultrasound waveform would be transmitted continuously or with repetitive breaks (pulsed) while the intensity refers to the amplitude of ultrasound wave. The pulsed ultrasound waveform in this experiment has a pulsed repetition frequency of 1 Hz and a 20% duty cycle. This is illustrated in Figure 5.2, showing the contrast to the continuous ultrasound.

With these two operating parameter variations, four LIUS treatment conditions were obtained. They were:

(1) LIUS with pulsed waveform and 30 mW/cm^2 intensity (30pul),

(2) 30 mW/cm^2 continuous LIUS (30cont),

(3) LIUS with pulsed waveform and 300 mW/cm^2 intensity (300pul), and

(4) 300 mW/cm^2 continuous LIUS (300cont).

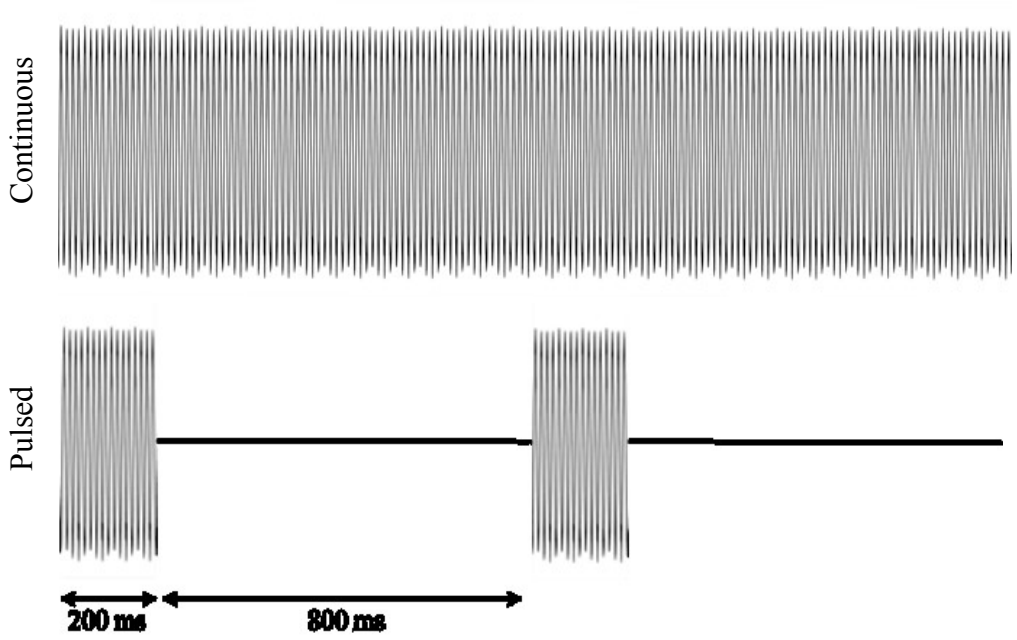

Figure 5-2 Illustration of LIUS waves in continuous and pulsed (1Hz pulsed repetition frequency and 20% duty cycle) generation mode.

5.2.4 Ultrasound stimulation in 3D encapsulated cultures of mESC

As 3D cultures provide more accurate insights of *in vivo* cell behaviour and higher cell expansion fold, the impact of ultrasound on 3D cultures of mESCs was also studied. To enable 3D culture, mESCs were encapsulated in Ca-alginate hydrogel at a seeding density of 2.5 x 10^6 cells per ml of sterile alginate solution at 1.1% alginic acid sodium salt (Sigma) and 0.1% gelatin in PBS, as described in Section 3.2.3. 3D encapsulated ESCs were cultured under HepG2-CM for 3 days in 6-well plates to undergo mesodermal lineage conditioning. As the 3D cultures of mESCs do not require an EB formation step, unlike the 2D cultures, the medium was changed to the differentiating medium on Day 3.

Eight days after changing to differentiating medium for directed cardiac differentiation in 3D cultures, ultrasound treatment was applied to the 3D cultures. At this stage, effects of LIUS on cardiac differentiation of mESCs had

been demonstrated in 2D cultures. Therefore, to investigate the effects of LIUS on 3D cultures, only two selected LIUS conditions (30pul and 300cont) were used. From Day 11 to Day 21, the encapsulated cells were treated with LIUS for 10 mins daily. The overall process is illustrated Figure 5.3 and three independent sets of experimental runs were conducted.

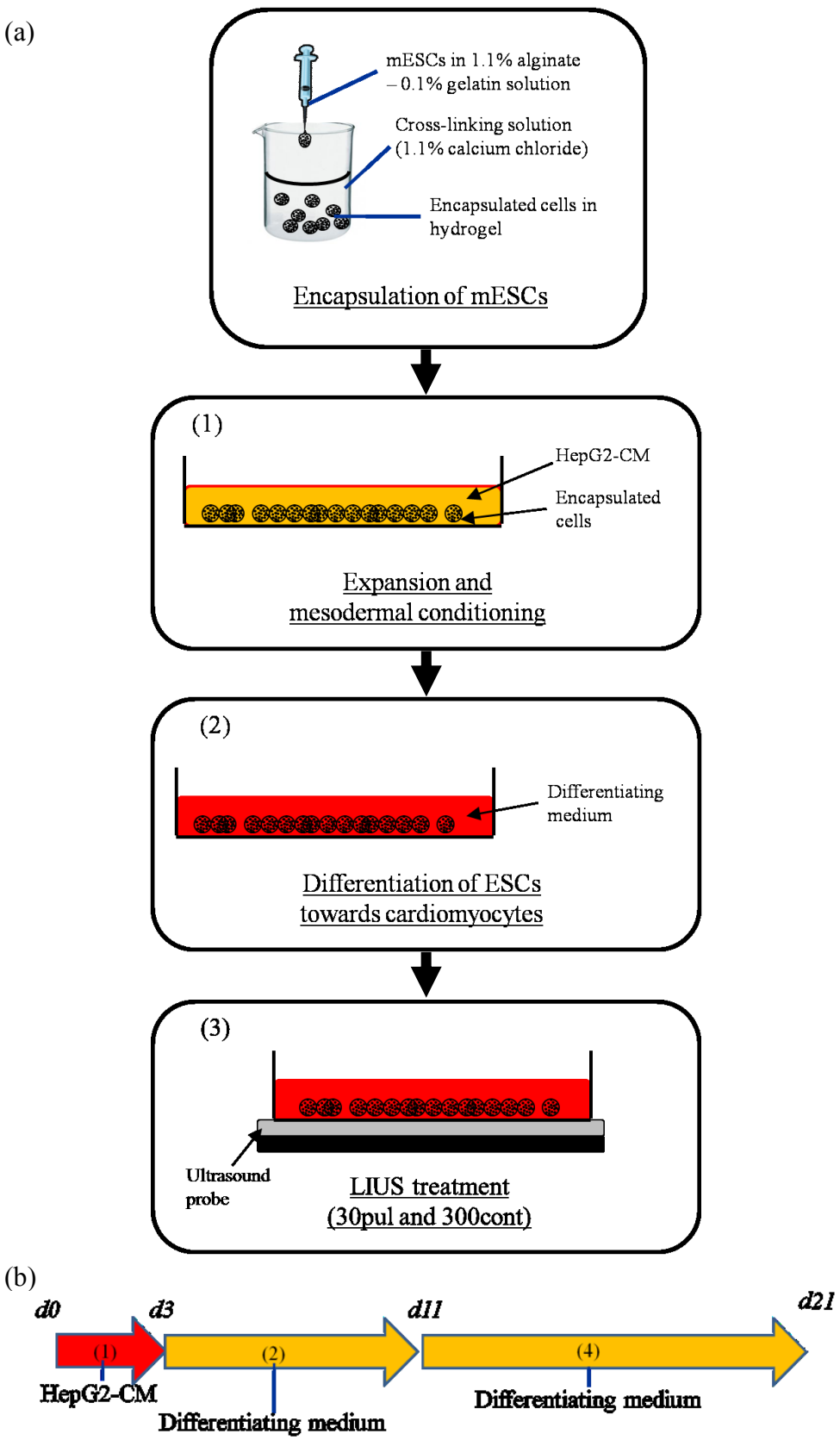

Figure 5-3 (a) Schematic diagram of procedure in differentiating and LIUS treatment of 3D encapsulated mESCs. (b) Timeline of addition of different mediums in different steps of differentiation and LIUS treatment.

5.2.5 Pressure measurement of LIUS

The pressure profiles caused by LIUS were measured and documented with a needle hydrophone ((HNA-0400, Onda Corporation) and digital oscilloscope (WaveSurfer 44MXs-B, Teledyne LeCroy). To make sure that the measured profiles were representative of mechanical strain and stress environments that the mESCs were subjected to, the hydrophone probe was positioned to a close proximity from the bottom well surface. The hydrophone probe was then immersed in degassed water. Thereafter, the LIUS transducer was placed beneath the whole set-up, simulating a similar set-up as the LIUS treatments on cells. LIUS was then transmitted according to the different conditions and the pressure was measured. Various points along the transducer's output plane were measured to verify spatial uniformity of LIUS on the 6-well plate.

5.2.6 Measurement of beating rates in contractile areas

Beating colonies of the differentiating mESCs were observed with an inverted optical microscope (Axiovert 200M, Zeiss). The number of beatings that occurred in 30 secs for each contractile area was recorded and the beating rate was calculated. Such measurements were taken for a total of 8 – 10 contractile areas and 12 – 16 contractile areas for each experimental condition on Day 18 and Day 21 respectively.

5.2.7 Quantitative PCR

Total RNA was isolated from cell samples with RNeasy kit (Qiagen) accordingly to manufacturer's instructions. The total RNA was then quantified with UV spectrometer (500 Evolution, Thermo) and calculations as described in Section 3.2.9. Using the same method in Section 3.2.9, the first strand of complementary DNA was synthesized from isolated RNA and used for quantitative PCR. Quantitative PCR was carried out with SensiFAST^{TM} SYBR Fluorescein Kit

(Bioline) in iQ5 PCR Machine (Bio-rad). A typical PCR protocol involved an initial denaturation step of 2 mins at 95°C, followed by 40 cycles of denaturation at 95°C for 5 secs and annealing/extension at 60°C for 30 secs. Different genes were targeted by amplification with the following primers as seen in Table 5.1.

After verifying that that all primers have similar amplification efficiencies and that there were no amplifications of non-targeted genes and primers-dimers, fold changes in the various genes expression were calculated with $2^{-\Delta\Delta CT}$ method. In the calculation of fold changes, the data were normalised to non-treated controls on Day 14, which corresponded to the start of ultrasound treatments.

Table 5-1 List of studied genes and their respective primers in studying effects of LIUS on cardiomyogenesis

Gene	*Forward primer*	*Reverse primer*
Housekeeping gene		
GAPDH	AGGTCGGTGTGAACGGATTTG	GGGGTCGTTGATGGCAACA
Cardiac genes		
Brachrury T	AAGGAACCACCGGTCATCG	CGTGTGCGTCAGTGGTGTGTAATG
Nkx2.5	AGCAACTTCGTGAACTTTG	CCGGTCCTAGTGTGGA
cTNT	CTCCATCGGGGATCTTGGGT	CAGAGGAGGCCAACGTAGAAG
α-MHC	ACCGTGGACTACAACAT	CTTTCGCTCGTTGGGA
β-MHC	ACCCCTACGATTATGCG	GGTGACGTACTCGTTGCC
Pluripotent genes		
Nanog	CCTGATTCTTCTACCAGTCCCA	GGCCTGAGAGAACACAGTCC
Oct -4	TGTGGACCTCAGGTTGGACT	CTTCTGCAGGGCTTTCATGT
Endodermal gene		
AFP	GAAGCAAGCCCTGTGAACTC	CCGAGAAATCTGCAGTGACA
Ectodermal gene		
Nestin	AGGACCAGGTGCTTGAGAGA	TCCTCTGCGTCTTCAAACCT

5.2.8 Flow cytometry

To access the LIUS effects on percentage of ESCs differentiating to cardiomyocytes, flow cytometry was used to determine the percentage of cells positive for sacromeric α-actinin expression.

The differentiated cells were first obtained as cell pellets after enzymatic detachment from 6-wells and washed with PBS. They were then fixed in 4% paraformaldehyde (Sigma) for 15 mins and permeabilised in 0.1% Triton-X for another 15 mins at room temperature. Thereafter they were re-suspended in PBS containing 5% goat serum, 0.1% Triton-X (Ultrapure grade, USB Corporation) and 1% sodium azide to a concentration of 1 – 5 x 10^6 cells/ml. 2 µl of sacromeric α-actinin primary antibody (EA-53, Santa Cruz Biotechnology) was added to 100 µl of the re-suspended cell solution and incubated for two hours at 4ºC. After incubation, the cells were washed twice with cold PBS and re-suspended in 100 µl of PerCP-conjugated secondary antibody (Santa Cruz Biotechnology, diluted 100x in 3% bovine serum albumin in PBS) for 1 hour at room temperature in the dark. The cells were next washed twice with cold PBS and stored in PBS with 2% paraformaldehyde, 3% bovine serum albumin and 1% sodium azide at 4ºC. To analyse the stained cells, flow cytometer (FACSCalibur, BD Biosciences) and the results were assessed in flow cytometry analysis software FlowJo (Tree Star).

5.2.9 Immunocytochemistry

Expressions of cardiac proteins in differentiated cells under different LIUS treatments were analysed with immunocytochemistry. On Day 21, cells were fixed with 4% paraformaldehyde in PBS for 1 hour at room temperature. The fixated cell samples were then treated with 0.1% Triton-X for 45 mins to enhance cells' permeability to antibodies. These samples were next incubated in primary antibody sacromeric α-actinin (EA-53, Santa Cruz Biotechnologies, 100x dilution in 0.1% sodium azide and 1% bovine serum albumin in PBS) overnight at 4ºC. After incubation with primary antibody, they were washed thrice with PBS before addition of FITC-conjugated secondary antibody (Santa Cruz Biotechnologies, 100x dilution in 1% bovine serum albumin in PBS). Residual traces of antibodies were removed by three extensive washes with PBS and shaking for 10 mins. This whole process was then repeated for the second cardiac protein, cardiac Troponin I (Santa Cruz Biotechnologies, 100x dilution) and its TRITC-conjugated secondary antibody (Santa Cruz Biotechnologies, 100x dilution). After incubations with antibodies, 300 nM DAPI was added to the samples and incubated for 5 – 10 mins at room temperature for nuclei staining. The fluorescence stains were finally visualised with inverted fluorescence microscope (Axiovert 200M, Zeiss) and camera (AxioCam MRC, Zeiss).

5.2.10 Quantification of cell viability

On Day 21, cell viability were assessed by trypan blue (Gibco, Lifetech) exclusion and enumerated with the usage of a hemocytometer and an optical microscope. Both live and dead cells were counted to obtain the viabilities of the different samples.

5.2.11 Live/Dead staining

On Day 21, cell viabilities in both 2D and 3D cultures were evaluated with calcein-AM (Sigma) and propidium iodide (Sigma-Aldrich). The cells or hydrogel beads were washed with PBS twice and incubated with 4 μM propidium iodide and 2 μM calcein-AM for 30 mins at room temperature in the dark. The samples were next washed with PBS twice. Samples were visualized and captured with an inverted fluorescence microscope (Axiovert 200M, Zeiss).

5.2.12 Cell proliferation assay

Cell proliferation of 3D encapsulated cells under different LIUS treatments and control conditions was also evaluated quantitatively with tetrazolium salt, WST-8* (Cell Counting Kit 8, Dojindo), as described in Section 4.2.5. Briefly, 5 sampled beads were washed twice with PBS and each incubated with 100 μl of fresh medium and 10 μl of WST-8* reagent in 37^{o}C, 5% CO_2 incubator for 2 hours. Blank samples consisted of 100 μl fresh medium and 10 μl WST-8*. Thereafter, 100 μl of reacted solution from blank controls and samples were transferred to a new 96-well and measured for absorbance values at 450 mm in microplate spectrophotometer (Bio-rad).

5.2.13 Statistical analysis

Statistical differences between different experimental groups were carried out with Microsoft Office Excel analysis tool package (Excel 2007, Microsoft). F-test was first used to determine for equal variances in the different data sets. Upon determining that there were unequal variances in some experimental groups, student t-test with unequal variances were used. Data in beating rates, quantitative PCR, flow cytometry, viability test, and cell metabolism assay were analysed with the student t-test with unequal variances for differences of 95% significance level. Error bars on the charts were representative of the standard deviations. The sample populations (N) are indicated in the legends of the respective figures and represent the number of independent experimental runs, unless as indicated in the legend. The error bars represent the standard deviation of different experimental groups and were calculated by the Microsoft Office Excel.

5.3 Results

5.3.1 Pressure levels exerted on cells under different intensities of LIUS

In this chapter, there were different conditions used in LIUS treatments on the cells, as described in Section 5.2.3. The combinations of intensity and ultrasound generation mode resulted in four LIUS treatment conditions as seen in Table 5.2.

Table 5-2 Operating conditions and naming convention of LIUS treatments

	Pulsed ultrasound	**Continuous ultrasound**
30 mW/cm2	*30pul*	*30cont*
300 mW/cm2	*300pul*	*300cont*

30 mW/cm^2 is commonly found in chondrogenesis and osteogenesis of stem cells and progenitors for cartilage and bone regeneration. Meanwhile, cardiomyogenesis under ultrasound stimulation with an intensity of a magnitude higher such as 300 mW/cm^2 was also investigated. 300 mW/cm^2 is chosen as it is still within the Federal and Drug Administration limit of 430 mW/cm^2 [221].

As seen in Figure 5.4, hydrophone measurements showed that 30 and 300 mW/cm^2 LIUS imposed pressure waves of amplitudes 20.1 ± 1.5 and 66.5 ± 1.5 kPa on the cells respectively. Ultrasound intensity is directly proportional to the square of pressure amplitude, thus this 3-fold increase in pressure amplitude corresponded with the 10-fold intensity increase. After the pressure profiles which 30 and 300 mW/cm^2 LIUS would exert on the cells (Figure 5.4) were verified, the LIUS's effects on differentiating ESCs towards cardiomyocytes were then studied.

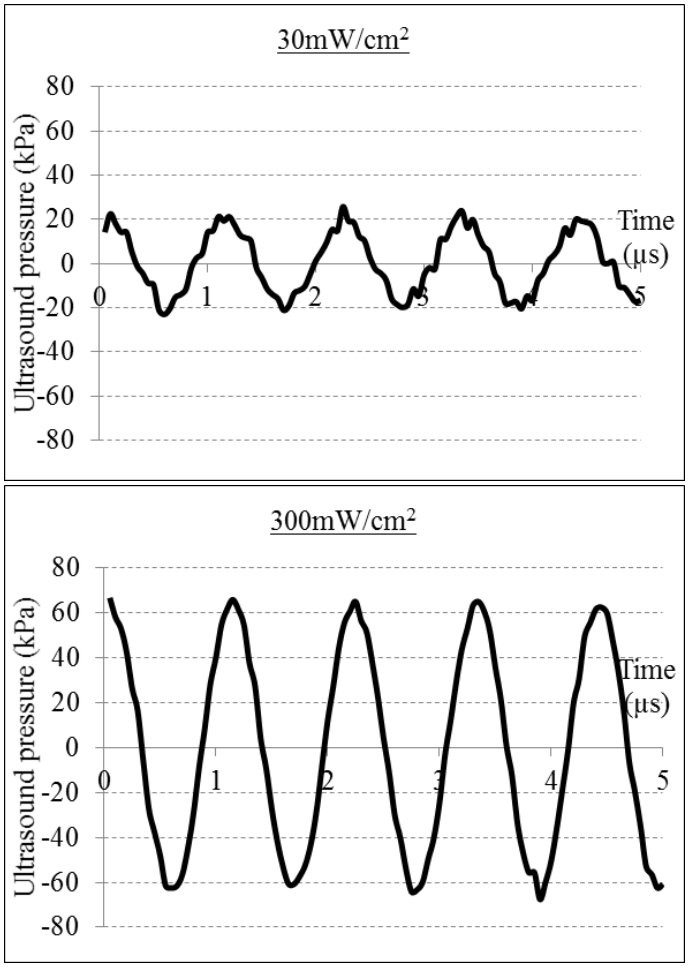

Figure 5-4 Pressure profiles induced on cells by LIUS treatments of intensities at 30 mW/cm^2 and 300 mW/cm^2.

5.3.2 Evaluation of contractile areas in 2D cultures under LIUS treatments

Beating colonies were spotted in 2D cultures after about 18 days. The contractile areas of differentiated mESCs on 2D cultures were evaluated by counting their beating rates on Day 18 and 21. Figure 5.5 shows the average beating rates of contractile areas that were obtained from mESCs under different LIUS treatments. On Day 18, cells under 300cont LIUS treatments gave a beating rate of 41 beats per minute, which was significantly higher than the controls and other treated samples. By Day 21, LIUS treatments managed to give rise to higher beating rates in most of the treated samples when compared to the untreated samples. Samples that were treated with LIUS, with the exception of 30cont

LIUS, produced higher beating rates than controls. These showed that LIUS could generally enhance ESC-differentiated cardiomyocytes' contractile properties.

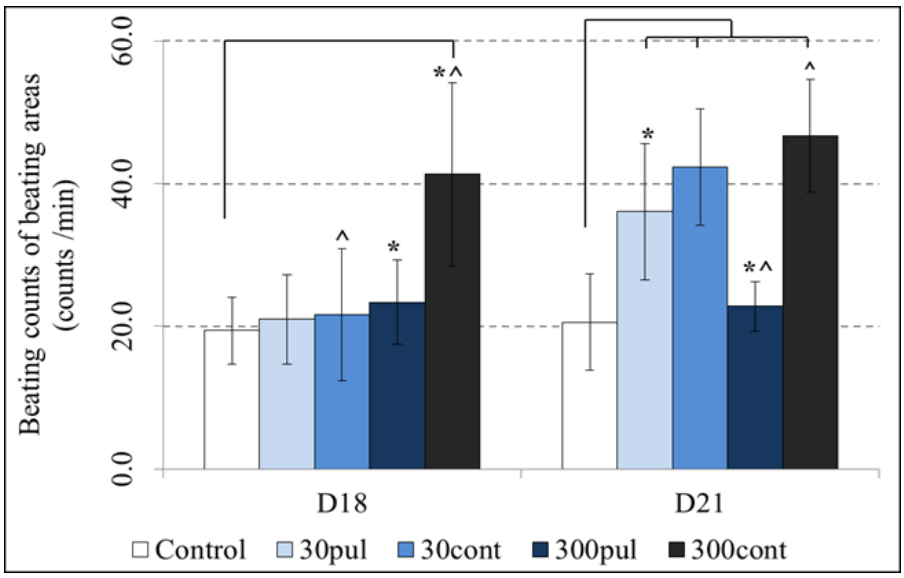

Figure 5-5 Beating counts of contractile areas in 1 minute for different LIUS-treated samples and controls on Day 18 and 21. Scale bar represents significant difference of indicated sample from its respective control. * represents significant difference between the indicated sample and its intensity counterpart (e.g. 30 mW/cm^2 pulsed and 300 mW/cm^2 pulsed LIUS). ^ represents significant difference between the indicated sample and its pulsing counterpart (e.g. 30 mW/cm^2 pulsed and 30 mW/cm^2 continuous LIUS). $p < 0.05$, n = 8 – 12 from 3 independent runs

5.3.3 Cardiac gene expression of mESCs in 2D cultures under different LIUS treatments

Cardiac differentiation was evaluated by comparing cardiac gene expression of cells which were differentiating in 2D cultures and subjected to no LIUS (control) or different LIUS conditions. Their gene expressions were studied after 3, 7 and 10 days of treatment (Day 14, 18 and 21 of culture respectively). Each experiment group was normalised to the genes levels expressed in controls on Day 14. On Day 14, after the cells were subjected to only three days of LIUS, they showed a significant increase of Brachyury T regulation from the controls,

regardless of the LIUS conditions that they were subjected to (Figure 5.6 (a)). This indicated that LIUS produced cues for directed ESCs towards mesodermal commitment, thereby increasing the probabilities for ESCs' cardiomyogenesis. Meanwhile, on Day 14, LIUS with higher intensity (300 mW/cm^2) also caused higher gene expressions of early cardiac progenitor Nkx2.5 than its counterparts with 30 mW/cm^2, regardless of the generation mode (Figure 5.6 (b)).

When expressions of late cardiac markers (i.e. α-MHC, β-MHC and cTNT) were compared, as shown in Figure 5.7, there were gene upregulations that were more pronounced at 30pul and 300cont LIUS than at 30cont and 300pul LIUS. At Day 18, 300cont LIUS produced significant higher upregulation of cardiac myosin heavy chains (both α-MHC and β-MHC) than the controls. Meanwhile, 30pul LIUS did not produce any significant increase in expressions of cardiac genes on Day 18 and actually caused a delayed upregulation. However by Day 21, expressions of cTNT and α-MHC increased in 30pul samples significantly, giving higher expression levels than the controls. This demonstrated a similar enhancement in 30pul LIUS on cardiomyogenesis as that of 300pul LIUS, though the observed effects were delayed.

These results of cardiac gene expressions corresponded to the higher beating rates induced by LIUS treatments, where 300cont LIUS gave rise to higher beating rates since Day 18 and 30pul also produced such effect on Day 21. As such, it could be inferred that LIUS simulation has beneficial effects on cardiomyogenesis.

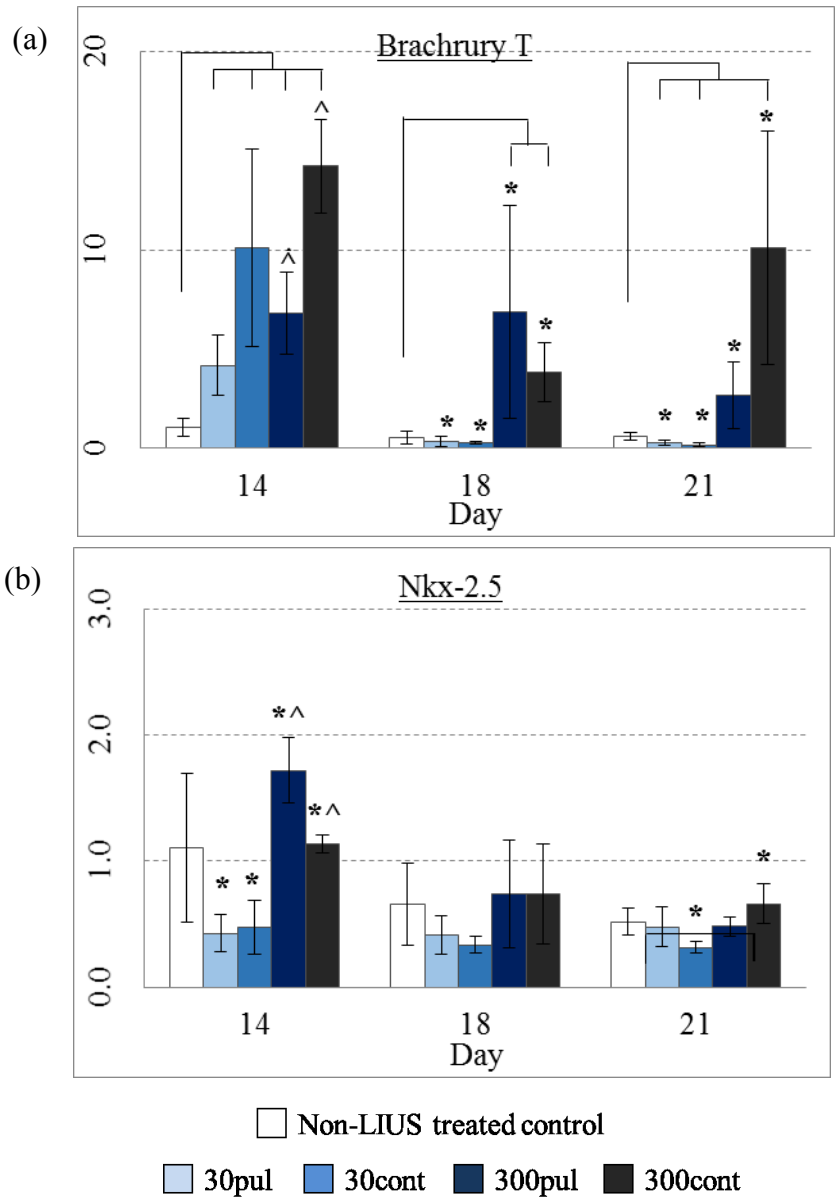

Figure 5-6 Fold changes in expression of (a) mesodermal marker, Brachyury T, and (b) early cardiac progenitor, Nkx-2.5 on Day 14, 18 and 21 of differentiation process for mESCs cultured on 2D plates. Bar represents significant difference of indicated sample from its respective non-treated control. * represents significant difference between the indicated sample and its intensity counterpart. ^ represents significant difference between the indicated sample and its pulsing counterpart. $p < 0.05$, N = 4.

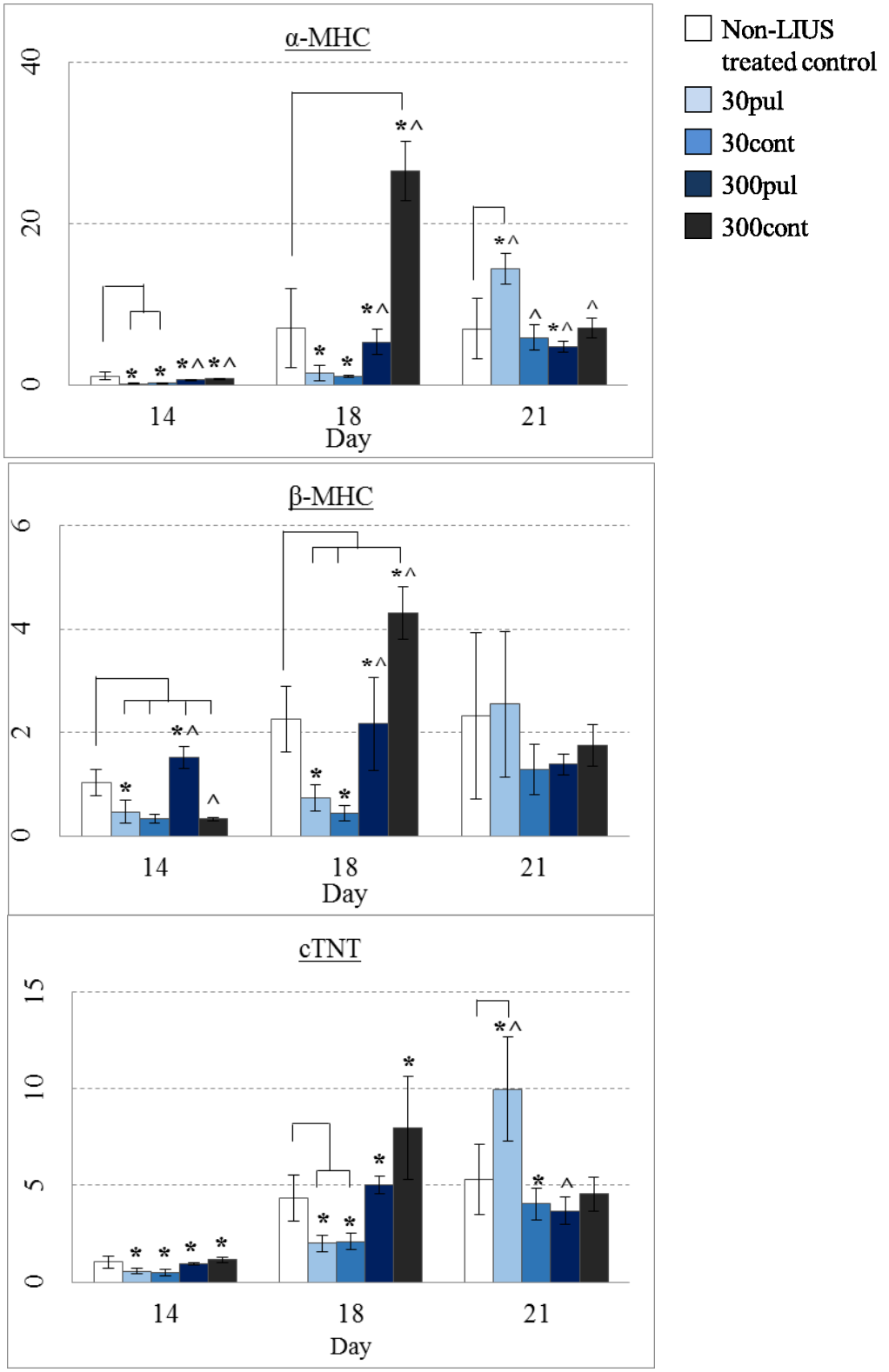

Figure 5-7 Fold changes in expression of late cardiac markers (a) α-MHC, (b) β-MHC and (c) cTnT on Day 14, 18 and 21 for mESCs cultured on 2D plates. Bar represents significant difference of indicated sample from its respective non-treated control. * represents significant difference between the indicated sample and its intensity counterpart. ^ represents significant difference between the indicated sample and its pulsing counterpart. $p < 0.05$, N = 4

5.3.4 Percentage of sacromeric α-actinin cells in 2D mESC cultured differentiated under ultrasound conditions

As observed from the gene expression data, LIUS upregulated cardiomyocyte differentiation of mESCs in 2D cultures. The percentages of differentiated mESCS under different LIUS treatments which were positive for sacromeric α-actinin (ATN) were also determined by flow cytometry. ATN binds actin filament to dense striations to enable contractile motion in cardiomyocytes. Figure 5.8 shows the summary of ATN-positive cell percentages under different LIUS conditions and a representative flow cytometry histogram from each LIUS condition. All LIUS treatments produced differentiated cell populations with 60 – 70% ATN-positive cells, while the control gave rise to only 34.3%. This showed that LIUS had significantly improved cardiomyocyte differentiation regardless of the conditions used. Among the different LIUS conditions, 30pul and 300cont LIUS gave rise to the highest percentage of ATN-positive cells (around 70%) while the other two conditions (30cont and 300pul LIUS) only produced around 60%. This correlated to the gene expression study and further showed the optimal LIUS conditions for cardiomyogenesis of mESCs in the 2D culture setup were 30 mW/cm^2 pulsed and 300 mW/cm^2 continuous US.

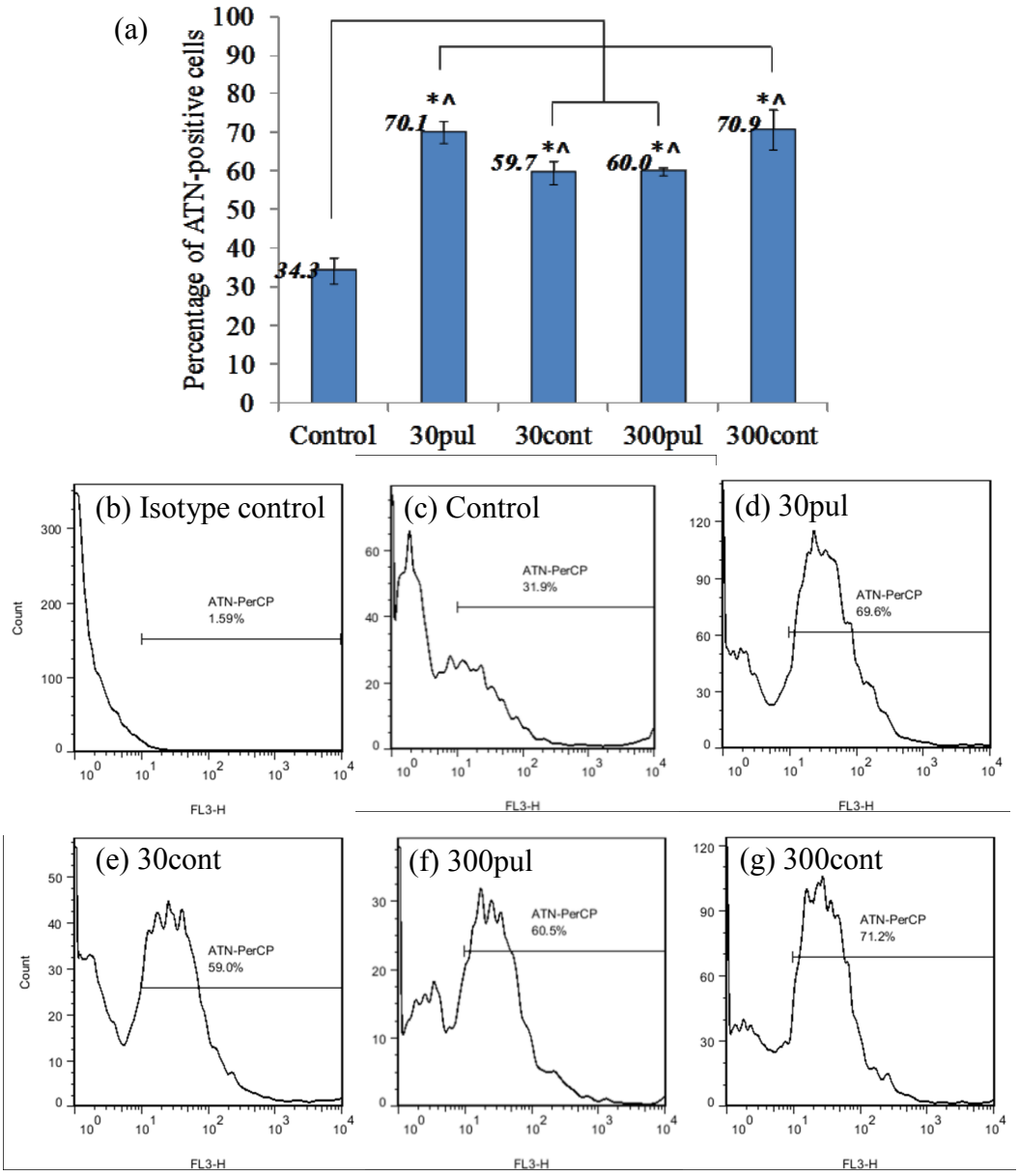

Figure 5-8 Percentage of ATN-positive cells under different LIUS conditions for 2D cultures. (a) Comparison of ATN-positive cells under different LIUS conditions. Bar represents significant difference of indicated sample from the non-treated control. * represents significant difference between the indicated sample and its intensity counterpart. ^ represents significant difference between the indicated sample and its pulsing counterpart. $p < 0.05$, $N = 3$. Flow cytometry histograms of (b) isotype control (a control showing unspecified staining), and of ATN-positive cells under (c) no LIUS treatment (control), (d) 30pul, (e) 30cont, (f) 300pul, and (g) 300cont LIUS treatments.

5.3.5 LIUS's effects on development of structural cardiac proteins in differentiated cells in 2D cultures

To ensure that LIUS was not detrimental to development of structural and cardiac proteins on cell surface, the protein expressions of ATN and cardiac troponin I (cTNI) on Day 21 was evaluated via immunostaining on Day 21 (Figure 5.9). Based on cardiac gene expressions and percentrage of cells positive for sacromeric α-actinin, it was inferred that 30pul and 300cont LIUS gave rise to the highest cardiomyocyte yields. Thus only protein expressions of 30pul and 300cont samples were compared with that in the non-LIUS treated controls.

ATN and cTNI protein expressions are represented by the green and red fluorescence signals respectively in Figure 5.9. Comparing to the nuclei layout of their corresponding nuclei micrographs, these two proteins showed intense, extensive and fairly uniform expressions in 30pul and 300cont samples. Thus LIUS did not pose any detrimental effects to development of cardiac proteins.

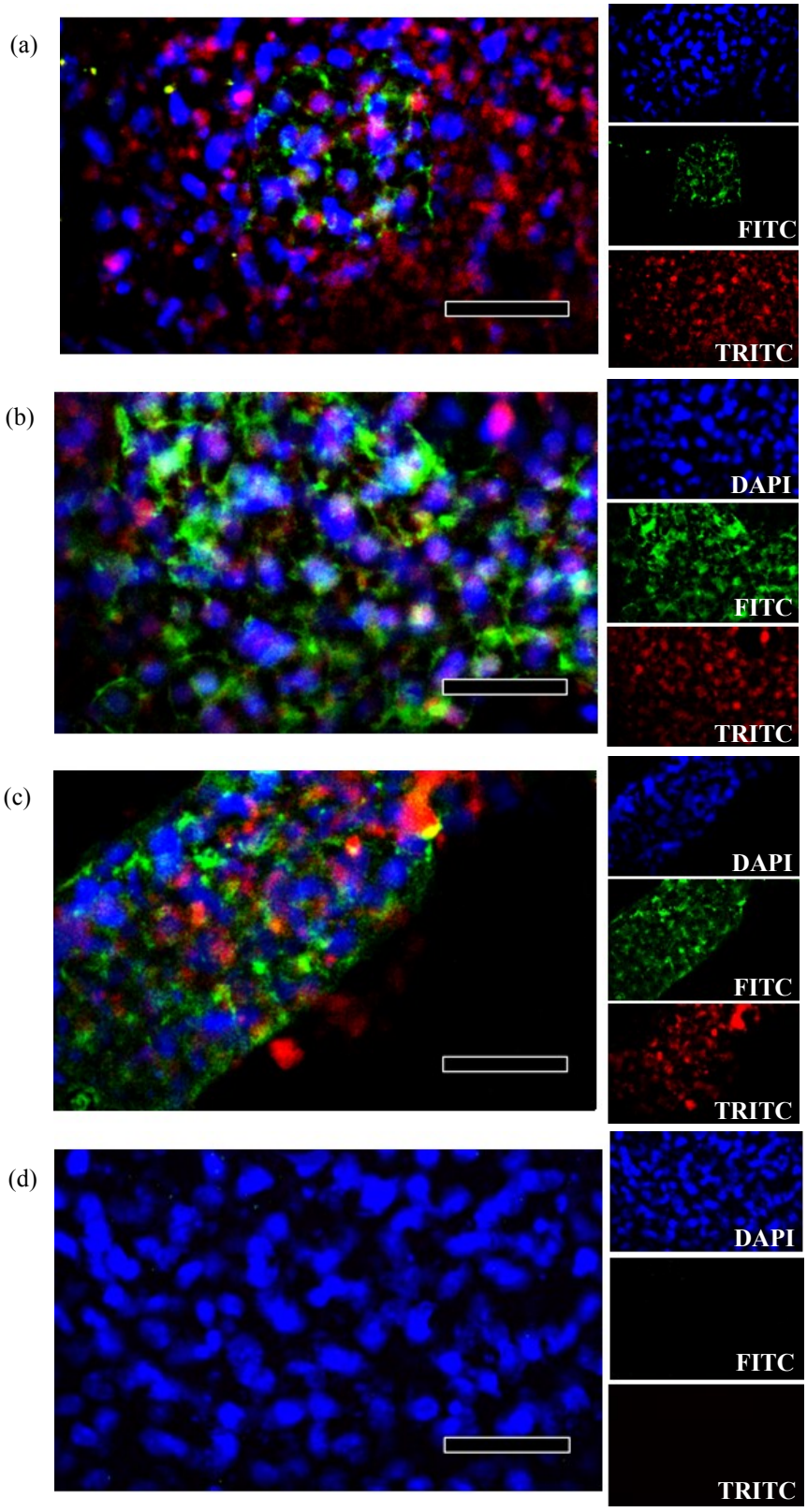

Figure 5-9 Fluorescence micrographs of immunocytochemistry with cardiac markers, ATN (FITC–green) and cTNI (TRITC–red) with their respective nuclei staining (DAPI–blue) after 21 days of 2D culture in (a) non-LIUS treated controls, (b) 30pul samples, (c) 300cont samples, and (d) negative staining controls. Scale bar represent 50 µm.

5.3.6 Spontaneous differentiation towards endodermal and ectodermal lineages under LIUS treatments in 2D cultures

Besides cardiac differentiation of ESCs, spontaneous differentiation towards endodermal and ectodermal lineages was monitored with gene expression levels of alpha-fetoprotein (AFP) and Nestin. In general, there was no significant difference in Nestin expression among the controls and LIUS samples (Figure 5.10 (b)) during the entire culture period, except for the lower expression levels at 30cont on Day 21. In contrast, AFP expressions gave a different observation (Figure 5.10 (a)). Cells under all LIUS treatments produced lower expression levels of AFP than the controls. For instance, the controls gave upregulation of 17 and 31 folds at Day 18 and 21 respectively while that in LIUS-treated samples were only 1.5 – 6 and 8 – 20 folds.

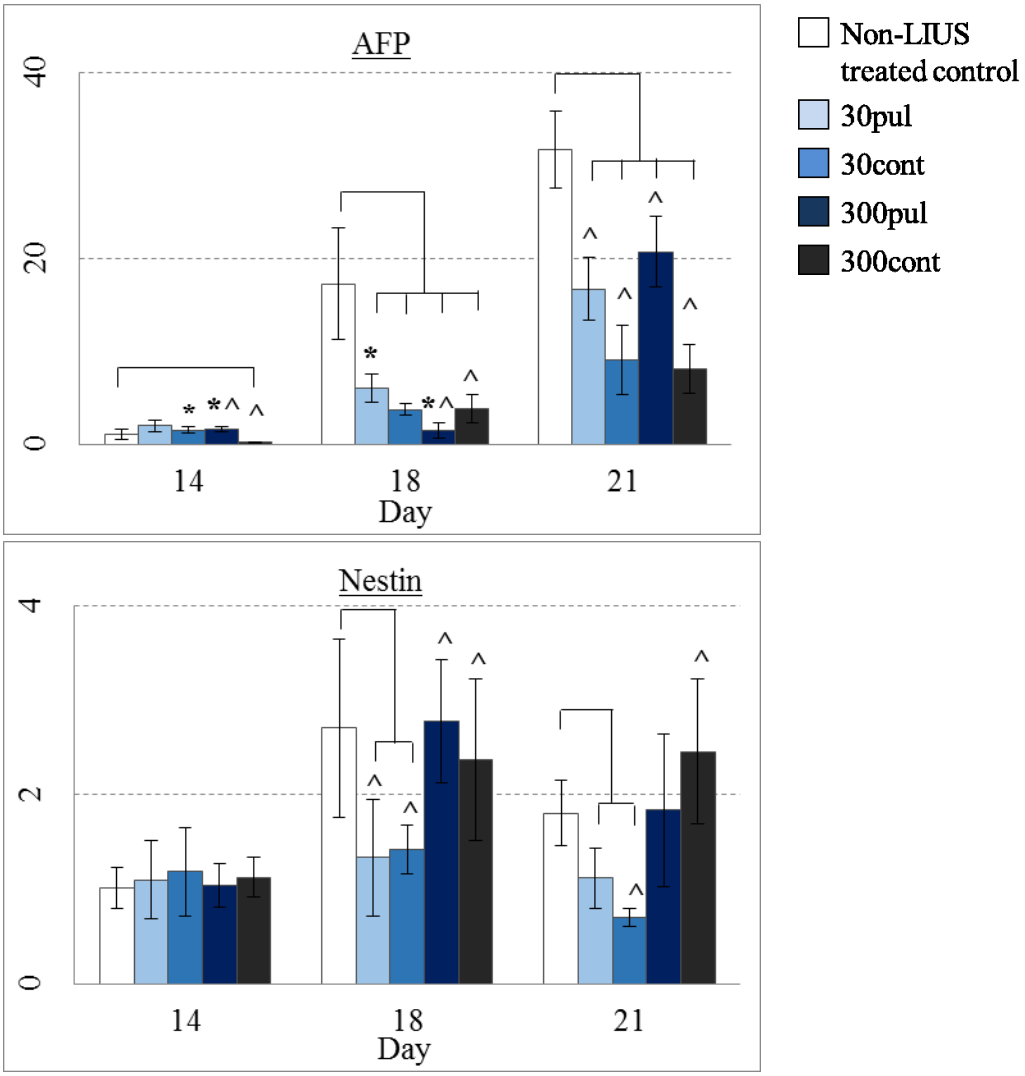

Figure 5-10 Fold changes in expression of (a) endodermal marker, AFP and (b) ectodermal marker, Nestin on Day 14, 18 and 21 of mESCs in 2D culture. Bar represents significant difference of indicated sample from its respective control. * represents significant difference between the indicated sample and its intensity counterpart. ^ represents significant difference between the indicated sample and its pulsing counterpart. $p < 0.05$, $N = 4$.

5.3.7 Evaluation of cell viabilities

The viability of differentiated mESCs in standard 2D flasks was poor at Day 21 (Figure 5.11 (a – c)). Viability ranged 48 – 52% in non-LIUS treated controls treated samples (Table 5.3). The similarities of viabilities in controls and treated samples indicated that there cell death due to stress from LIUS treatments might be insignificant. Substantial cell death observed in the standard 2D culture could be a result of the apoptotic cores during EB formation. During the EB formation, which was prior to the replating step and ultrasound treatment, the cell density and size of suspended EBs might have increased till the extent that the cells faced severe nutrient transport limitations, resulting in apoptotic cores. mESCs were then encapsulated in alginate hydrogel to provide a 3D environment in hope to improve viabilities while enhancing cellular interactions. From the viability staining results, the overall viability of encapsulated mESCs in 3D cultures on Day 21 were significantly better (Figure 5.11 (d – f)) than those observed in standard 2D cultures.

Table 5-3 Viabilities of non-LIUS treated controls and LIUS-treated samples at Day 21 for 2D culture, as quantified by cell enumeration with Trypan blue and hemocytometer. Lack of significant differences as assessed by student t-test of unequal variance. $p < 0.05$, N = 4.

Viability (%)				
Control	30pul	30cont	300pul	300cont
48.8 ± 4.9	48.3 ± 6.8	50.9 ± 7.2	52.0 ± 4.4	50.9 ± 7.0

- No significant difference

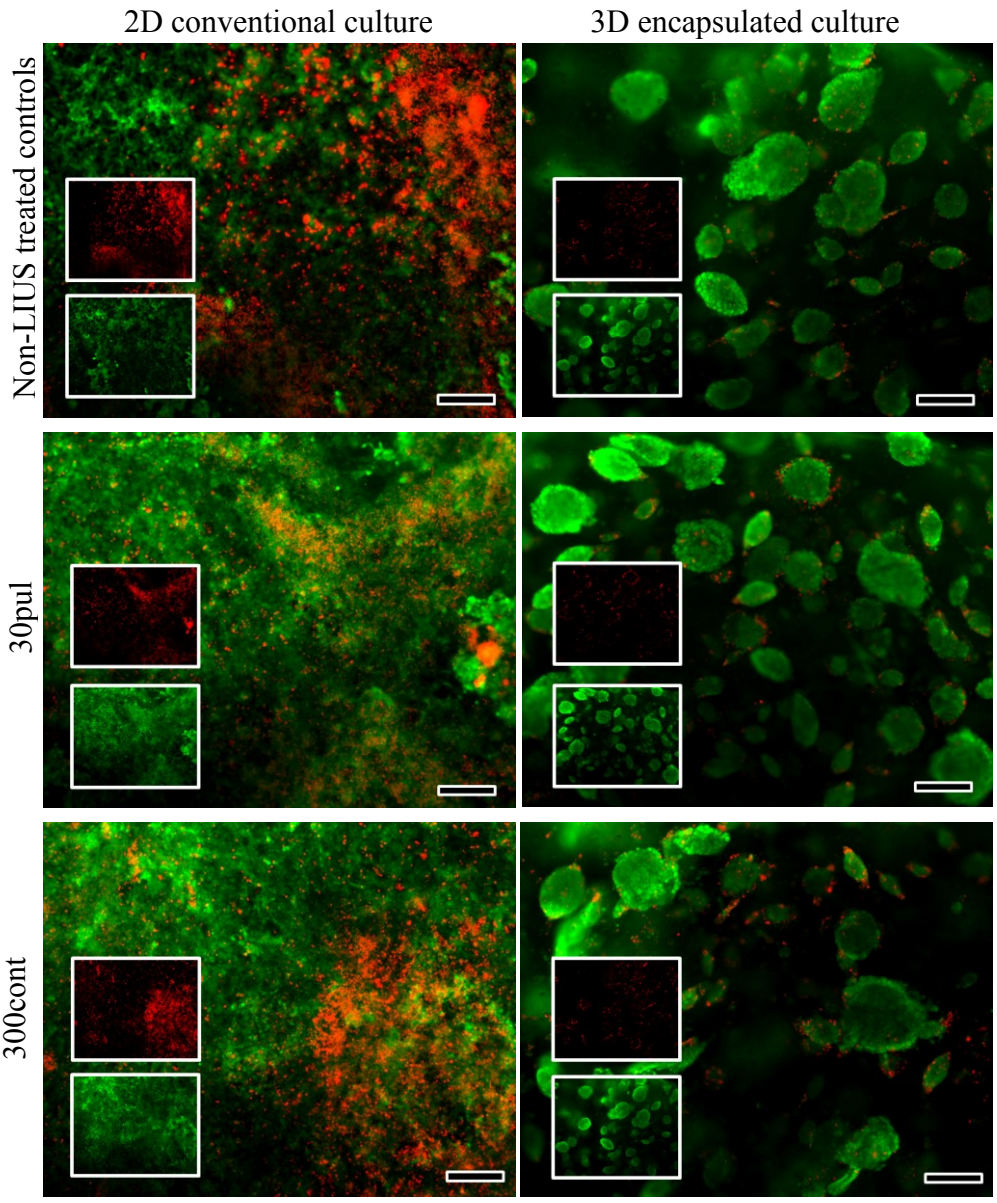

Figure 5-11 Live/dead fluorescence images at of differentiated cells in (a – c) conventional 2D cultures and (d – f) 3D encapsulated aggregates on day 21, where green and red fluorescence represent live and dead cells respectively. Scale bar represents 200 µm.

Furthermore, cell proliferation assay of encapsulated mESCs under 30pul and 300cont LIUS treatments showed no significant differences in the metabolic activities from the controls throughout the entire stimulation period (Figure 5.12). This indicated that these studied LIUS conditions would not cause significant deleterious effects on cell proliferation and viabilities in 3D cultures.

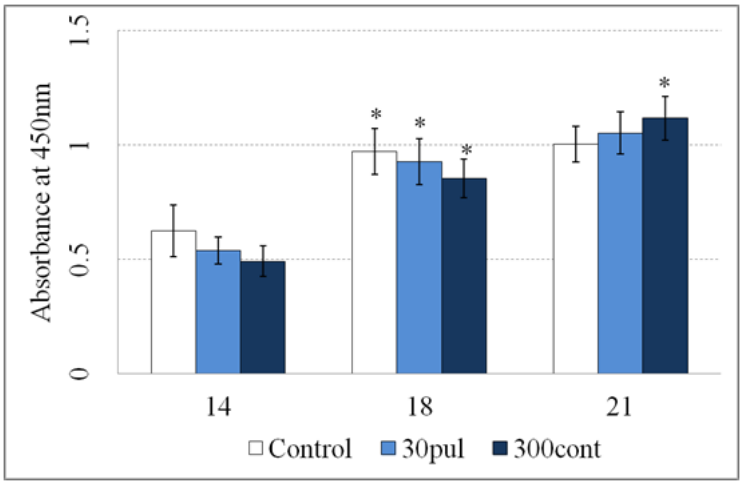

Figure 5-12 Cell proliferation of 3D encapsulated ESCs under control, 30pul and 300cont LIUS conditions. * represents significant difference between the indicated sample and its previous time point. Bar represents significant differences between LIUS conditions. However, the lack of bar indicates there is no cell proliferation differences among the samples at the respective time points. $p < 0.01$, N = 10 from 2 independent runs.

5.3.8 Cardiomyogenesis and spontaneous differentiation of 3D-encapsulated ESCs under 30pul and 300cont LIUS treatments

Since 30pul and 300cont LIUS were found to produce the highest cardiomyocytes yield (Figure 5.7 and Figure 5.8), these two conditions were used to determine if LIUS would have any significant impact in the 3D platform as it had in the 2D platform. Nkx 2.5 and cTNT gene expressions did not show any significant difference between the controls and LIUS-treated samples of encapsulated ESCs (results not shown). However, on Day 14, 300cont LIUS induced a higher upregulation of Brachyury T than the controls and 30pul LIUS samples (Figure 5.13 (a)). At Day 21 (Figure 5.13), there were increased expressions of Brachyury T, α-MHC and β-MHC in 300cont LIUS-treated cells while 30pul LIUS samples showed no significant difference from the control.

Brachyrury T is a marker for mesodermal lineage commitment and is usually a transient marker. However, it showed a second round of upregulation on Day 21. This correspond to the decrease in pluripotent genes' expressions (Nanog and

Oct-4 in Figure 5.14). The second round of Brachyury T's upregulation could be due to further differentiation of the residual pluripotent mESCs.

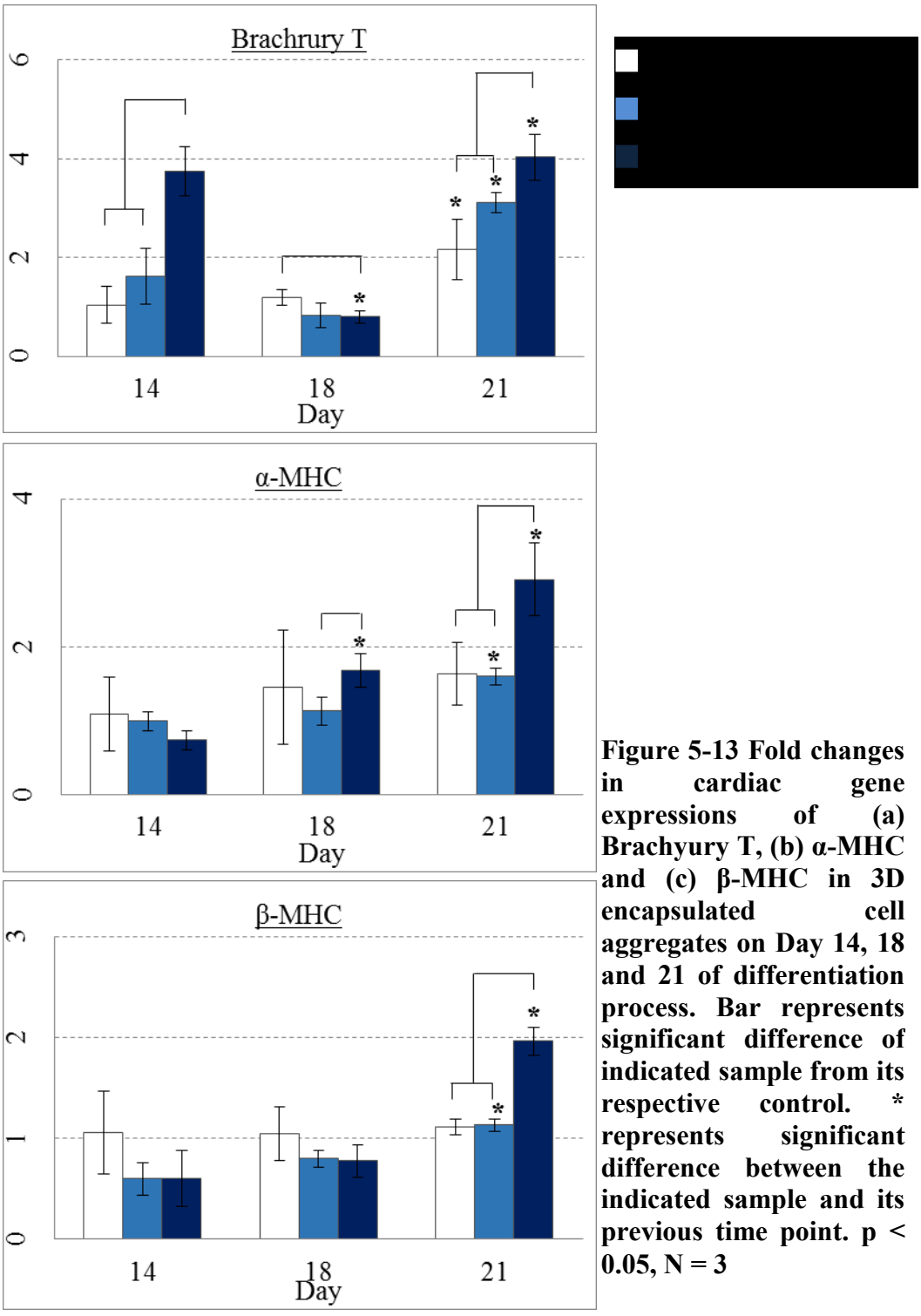

Figure 5-13 Fold changes in cardiac gene expressions of (a) Brachyury T, (b) α-MHC and (c) β-MHC in 3D encapsulated cell aggregates on Day 14, 18 and 21 of differentiation process. Bar represents significant difference of indicated sample from its respective control. * represents significant difference between the indicated sample and its previous time point. $p < 0.05$, N = 3

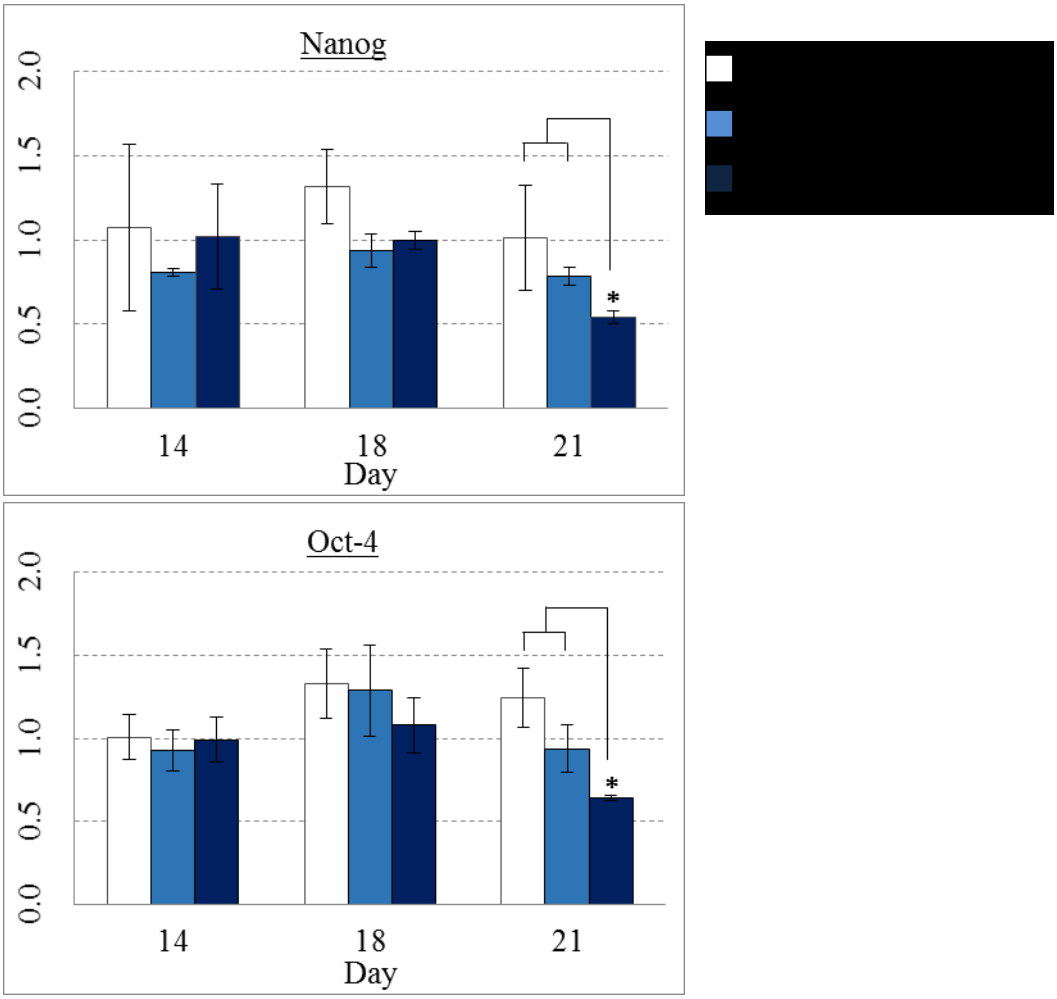

Figure 5-14 Fold changes in pluripotent gene expressions of (a) Nanog, and (b) Oct-4 in 3D encapsulated cell aggregates on Day 14, 18 and 21. Bar represents significant difference of indicated sample from its respective control. * represents significant difference between the indicated sample and its previous time point. $p < 0.05$, $N = 3$

Similar observations in the AFP expression were made in both conventional culture and 3D platform. All LIUS-treated samples in 3D cultures also had lower AFP expressions than the controls (Figure 5.15 (a)). This implied that LIUS also reduced the spontaneous differentiation of mESCs towards endodermal lineage in the 3D platform. Meanwhile, there was no significant difference in Nestin expression among the LIUS-treated samples and the controls (Figure 5.15 (b)). So far, our results on LIUS effects on mESC differentiation in 3D cultures were consistent with those observed in 2D culture.

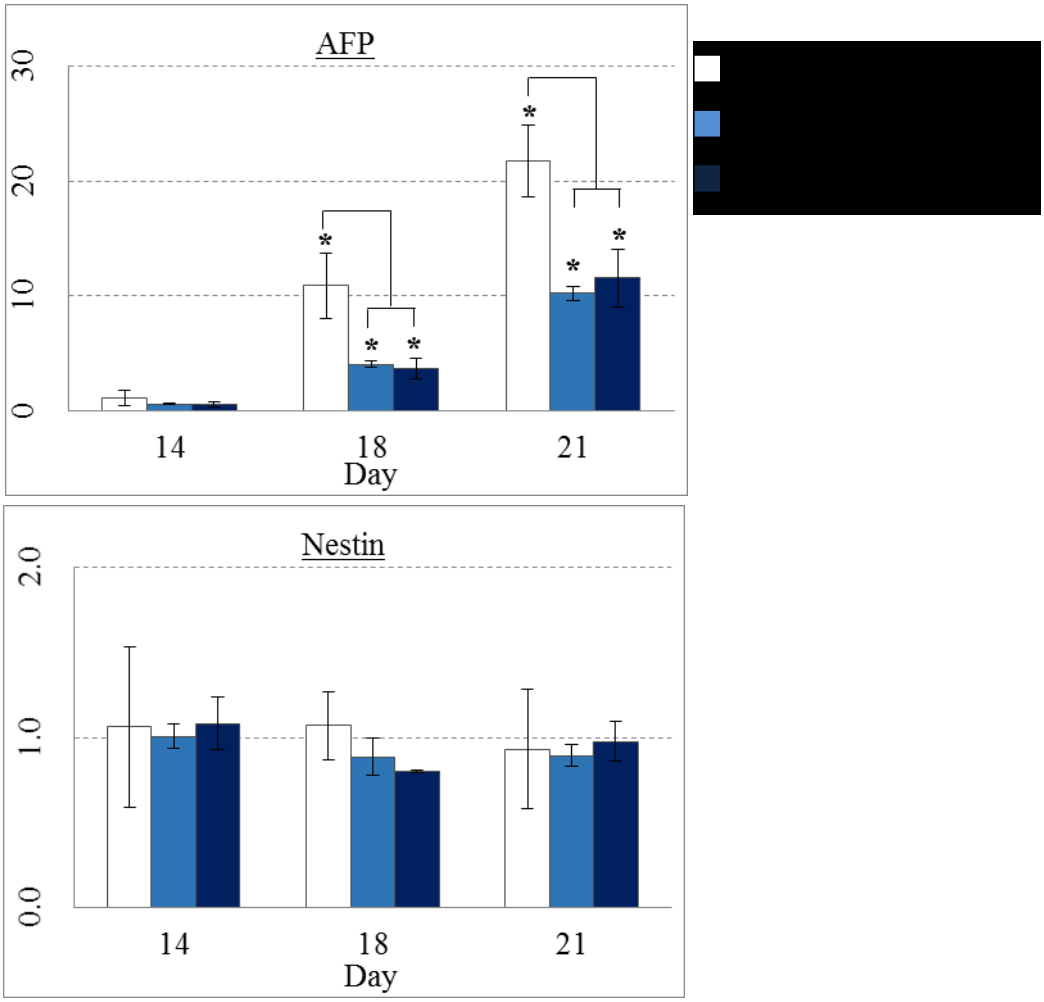

Figure 5-15 Fold changes in cardiac gene expressions of (a) endodermal marker, AFP and (b) ectodermal marker, Nestin in 3D encapsulated cell aggregates on Day 14, 18 and 21 of differentiation process. Bar represents significant difference of indicated sample from its respective control. * represents significant difference between the indicated sample and its previous time point. $p < 0.05$, N = 3

5.4 Discussion

Cardiomyocyte differentiation and maturation from cell sources like neonatal cardiomyocytes, MSCs and ESCs has been shown to improve under mechanical stimulation [8-10]. This chapter demonstrates the feasibility of using LIUS as a novel mechanical stimulation in enhancing cardiomyogenesis of mESCs. The higher percentage of cardiomyocytes obtained and the higher beating rate showed that LIUS could generally increase the extent of mESC differentiation towards cardiomyocytes. One possible explanation is that LIUS generated motions and forces in the culture medium and elicited biophysical effects similar to those from mechanical stimulus on mESCs, resulting in mechanotransduction effects.

Although LIUS is shown to enhance cardiomyogenesis generally, there are different parameters in operating ultrasound stimulation, e.g. intensity, which will affect its efficacy. Different LIUS conditions were used to treat the cells in this chapter and different parameters gave rise to different extent of cardiomyogenesis enhancement. For instance a longer period of treatment and culture was required for 30 mW/cm^2 pulsed LIUS than 300 mW/cm^2 continuous LIUS. This might be attributed to the higher pressure induced by 300 mW/cm^2 continuous LIUS, which might then create a higher mechanical stress and strong mechanotransdiction effects on the mESCs. Such observations indicated the need for optimisation of LIUS for different cell types and cardiogenic conditions.

A distinct effect of LIUS stimulation on mESC differentiation in this study was the reduced spontaneous differentiation towards endodermal lineages. When compared to endodermal commitment, both mESC and hESC commitment towards mesodermal lineages were favoured on stiffer substrates [222, 223].

Zoldan et al. then suggested substrates of different stiffness would exert different levels of counteracting forces on the cells and affect their cellular fate [223]. Hence, a stiffer substrate would impose higher forces on the cells, implying that mesodermal commitment will prefer higher stress environment than endodermal commitment. Similarly, mesodermal commitment in an *in vivo* embryonic development experiences tensional and intercellular forces for migration towards midline of primitive streak and formation of heart tube [224]. These studies substantiate the hypothesis that LIUS stimulation provides mechanical stress as forces that drove ESC commitment away from endodermal lineages and direct it towards the mesoderm lineage in a cardiogenic environment. This could be a useful strategy in minimizing spontaneous differentiation of ESCs towards undesired lineages and increasing the purity and yield of cardiomyocytes from pluripotent stem cells.

Using a 3D substrate for cell culture would make it easier for handling in a dynamic bioreactor, thus enabling an efficient scalable bioprocess. Culturing cells in a 3D environment could achieve higher cell densities and provide a better *in vivo* mimicry, providing advantages over the conventional 2D cultures. For instance, cardiomyogenesis in 3D environment produced cardiomyocytes that bore greater resemblance to those in the myocardium [4, 5]. Moreover, hydrogel encapsulation can enable aggregate size control during proliferation and also support long-term culture, which will be beneficial to cardiomyogenesis [124-126]. In this study, encapsulation of ESCs in Ca-alginate hydrogel has allowed cells to maintain a higher viability than the conventional differentiation method as it eliminates the need for EB formation which can cause a higher apoptotic presence. Hydrogels also have a protective function from any hostile extrinsic

factors [225-227]. Despite the benefits of hydrogel encapsulation on cell viability, LIUS's induction of cardiomyogenesis was not as pronounced in 3D environment as in conventional 2D culture. In 2D culture, 300 mW/cm^2 continuous LIUS could increase cardiac gene expressions as early as Day 18 but such improvements were only observed on Day 21 in the encapsulated cells. Furthermore, upregulated cardiac gene expressions caused by 30 mW/cm^2 pulsed LIUS which were observed in the 2D cultures, were also absent in the encapsulated cells during the experimental period. Nicodemus and Bryant have demonstrated that culture of chondrocytes in hydrogel has built up an endogenous matrix around the cells, which might protect them from sensing the mechanical stimuli [228]. Therefore, one possible reason for the reduced effect of LIUS in 3D environment is that the hydrogel has provided a protective buffer against the mechanical loads of LIUS treatment, thus reducing the effects of mechanotransduction and mechanical stimuli.

5.5 Conclusion

Obtaining cardiomyocytes from cell sources such as pluripotent cells can be enhanced by incorporating biophysical simulations in bioprocess, such as mechanical stimuli. Though LIUS has been studied for bone and cartilage regeneration, its effects had yet to be investigated for cardiomyogenesis. This chapter showed the feasibility and benefits of LIUS utility in driving cardiac differentiation from mESCs. Specific treatments of LIUS could increase cardiac gene expressions and beating rates of contractile areas. Besides conventional 2D culture, improved cardiomyogenesis was also demonstrated in 3D encapsulated mESCs. 3D cultures hold a promising future as a platform for large scale production for obtaining cardiomyocytes with clinical relevant numbers. This chapter demonstrates the feasibility of using LIUS for cardiomyogenesis of mESCs. Once similar studies are also established using human-sourced cells, LIUS stimulation and 3D cultures can create a synergistic platform to obtain cardiomyocytes with translatable quantities and contractile properties for clinical therapies.

6 Conclusion

Cardiovascular diseases are major global mortality causes, especially in developed countries. To date, there is no clinical therapy which can fully regenerate the infarcted myocardium functionality except for heart transplantation. Strategies of ex vivo cardiomyocyte production from stem cells offer promising opportunities for cell transplantation to regenerate the cardiac tissue. However, one should consider the issues and challenges in such strategies, such as the ability to achieve clinically relevant cell numbers efficiently and reproducibly. In this thesis, encapsulated mESCs, an established and pluripotent cell type, was used as a model to investigate the effects of various cell culture / bioprocess considerations that will help to advance the development of 3D stem cell cultures. These factors include the effects of different cell culture platforms, pH environments and mechanical stimulation, in form of US, on obtaining cardiomyocytes for clinical therapies.

For large scale cell culture and reproducibility of cellular products, bioreactors can be developed as a highly feasible platform. Different culture platforms which adopt different mixing and feeding strategies, result in different hydrodynamic flow profiles and thus nutrients' availability to cells will also be affected. A novel bioreactor, which incorporated rotary mixing and perfusion, was used in mESC cardiomyogenesis. The dynamic flow environment provided by rotary mixing is beneficial to cell viability and produces better cell expansion, including that in cardiomyocytes, than a static environment. Moreover, rotary mixing gives rise to low shear stress environment which are more preferentially for cardiomyogenesis and will also eliminate any risk in cell death by high shear stress. Perfusion is a common feeding strategy to provide a continuous exchange of nutrients and metabolites, so as to maintain a consistent environment for cell culture. With a

continuous supply of cardiomyogenic factors and removal of inhibitory factors in this novel bioreactor, cellular fate of ESCs is better controlled and differentiation towards cardiomyocytes is enhanced.

Consistent environment, as provided by perfusion, was shown to enhance cardiomyogenesis of encapsulated mESCs. However, consistency of culture parameters is usually difficult to achieve in conventional TCP and culture platforms, especially when cell numbers are high. A common fluctuating culture parameter is the environmental pH. Due to accumulation of respiratory metabolites, pH tend to decrease and can affect cardiomyogenesis. As from our findings, differentiating mESCs at pH 6.8 will cause a lower yield of cardiomyocytes and higher residual pluripotency than at pH 7.1 and 7.4. Furthermore, cell proliferation and viabilities were compromised when pH decreased to pH 6.8. Though an environment of pH 6.8 is not drastically different from normal culture environments, the impact on cardiomyogenesis was significant. This is an indication of pluripotent cells' sensitivity to pH environments during cardiac differentiation. Thus to ensure reproducibility of cellular products from different culture batches and to increase cardiomyocyte yield, one should consider the importance of pH environment and determine an optimal environment.

Mechanical stimulation is also extensively studied for its effects on cardiomyocyte differentiation and maturation. From its impact on bone and cartilage regeneration, LIUS is a possible candidate in producing mechanical cues to enhance cardiomyogenesis from cell sources. LIUS's complementary effects on cardiomyocyte differentiation of mESCs was demonstrated in both conventional 2D and 3D cultures. In addition, LIUS reduced the likelihood for

mESC spontaneous differentiation towards endodermal lineages significantly. This can be used to increase selectivity of cardiomyocytes from mESC differentiated cell products. A distinct advantage of using LIUS is that incorporation of LIUS stimulation into a culture platform, such as bioreactors, which requires only a simple installation of the ultrasound transducer probes. This makes the application of LIUS probes readily adaptable to a wider range of culture vessel and bioreactor designs. Thus LIUS was shown to be a novel form of mechanical stimulus to complement a 3D bioprocess in obtaining cardiomyocytes for clinical therapies.

In developing a platform to produce cardiomyocytes for clinical therapies, it is important to consider bioprocess design parameters in a cell culture platform. One such parameter is the bioreactor design and its hydrodynamic profile and feeding strategy. A novel rotary perfused bioreactor could successfully enhance cardiomyogenesis as compared to that in conventional static cultures. Another parameter which was found to be important was the ability to control and maintain physiological environment, such as extracellular pH. Cardiomyogenesis is sensitive to slight pH changes and thus uncontrolled environment, which is vulnerable to fluctuations, will make it difficult to ensure reproducibility of cellular products. Last but not least, LIUS was also used as a novel form of mechanical stimulation for cardiomyogenesis of mESCs. It was demonstrated that LIUS was not only feasible but also improved cardiomyocyte yield, showing the ability to use LIUS as a strategy to obtain cardiomyocytes for clinical therapies.

6.1 Recommendation for future works

6.1.1 Translation into clinical practices

Findings in this thesis were primarily based on the mESC model. For clinical translation, studies on human pluripotent stem cells should be conducted in the future roadmap. Bioprocess parameters investigated in this thesis, such as the well-mixed and perfused environment in the novel bioreactor and pH sensitivity, would have similar effects across species. For instance there were studies using mESC as a model for human pluripotent stem cells in large-scale bioreactor platforms. These studies showed the benefits of 3D cultures (on microcarriers and in encapsulation) and bioreactor cultures on the cell expansion and cardiomyogenesis of mESCs [115, 126, 229, 230]. Further development then demonstrated similar findings with human pluripotent stem cells in microcarriers and bioreactor cultures [119, 126, 230-232]. In similar context, the results presented in this thesis could help to evaluate the feasibility of novel bioprocess conditions for the utility of human pluripotent stem cells. However, specific operating conditions such as flow rate or optimal culture pH may differ when culturing human pluripotent stem cell culture and should be optimised independently. Thus more elaborated studies, including assessment of functional properties of the derived cardiomyocytes, should be carried out in the future.

In utilising pluripotent stem cells for producing specific differentiated cells, one major concern is the purity. Differentiated cell populations originating from pluripotent cell sources usually comprise residual pluripotent cells and cells of undesired lineages. The residual pluripotent cells can spontaneously differentiate into other undesired cell types and it takes only a few hundred pluripotent stem cells in transplantation to form teratoma [3]. Therefore, in the application of

ESC-derived products into clinical practice, purification methods used to isolate the desired differentiated cell population is a necessity, and *in vitro* and *in vivo* efficacy and safety must be tested to the most stringent standards set by regulatory authorities. In this thesis, it was observed that there was a substantial amount of pluripotent gene and protein expressions and endodermal gene expression after 21 days of differentiation. Since purity and safety issues have yet been addressed in this thesis, further works are required to address these issues.

To increase cardiomyocyte purity, cardiogenic cells are to be separated from other differentiated cells and residual pluripotent cells prior to transplantation. Purification of cardiomyocytes has been demonstrated by separation on a Percoll density gradient [233] and genetic selection in modified ESC line [234] to a purity level of 71 – 95% and 91.5% respectively. To obtain higher purity levels while avoiding the need for genetic modifications, fluorescence cell-sorting of non-genetic markers such as mitochondrial content [235] or cell surface epitope [236] could be used. Purity greater than 99% have been obtained for such methods. However, fluorescence cell sorting would require single cell suspension and the preparation of a viable cell suspension usually resulted in great loss of cardiomyocytes [236], making it unsuitable for producing cells with clinically relevant numbers. On top of purification, it should also be determined if the purified products is safe for transplantation with teratoma assays performed in animal models.

6.1.2 Ultrasound stimulation

LIUS is found to enhance cardiomyogenesis of mESCs in a cardiogenic environment. One benefit of using LIUS is its versatility to be incorporated into different bioreactor designs. It was also demonstrated that the novel rotary perfused bioreactor can help to increase cardiomyocyte yield from mESCs. Therefore, incorporating LIUS into this novel bioreactor may have synergistic effects, compounding their benefits in producing cardiomyocytes for clinical therapies. One suggestion for future work is to investigate if there is any enhancement in cardiomyocyte differentiation in such rotary perfused bioreactor with LIUS stimulation.

Though LIUS was shown to enhance cardiomyogenesis in both 2D and 3D cultures, its ability to improve cardiomyocyte differentiation was attenuated by the protective barrier of 3D encapsulation. Hence more detailed studies will be needed to determine optimal LIUS operating conditions for cardiomyogenesis of these encapsulated cells. For instance, higher LIUS intensity can be applied to study if there is an earlier onset or higher levels of cardiac gene expression. Moreover, LIUS treatment comprises of various operating parameters, such as ultrasound frequency, intensity, duty cycle and treatment duration. So far ultrasound was shown to be feasible to act as a mechanical stimulation to enhance cardiomyogenesis, and its impact from varying intensity and duty cycle was also demonstrated. However, there are other operating parameters which will also have impact of cardiomyogenesis and further studies are required. Thus, further investigation can be conducted to determine the effects of different parameters on cardiomyogenesis.

Ultrasound is a novel form of mechanical stimulation in mESC cardiomyogenesis and has never been utilised before for this purpose. Hence its effects on specific cellular behaviours are still unknown and will require more extensive studies. For instance AT1, a mechanoreceptor commonly found in cardiomyocytes, was observed to be upregulated in LIUS-treated osteoblasts. This receptor may play an important role in improving cardiac regeneration under LIUS treatment. Therefore, further studies in mechanotransduction can be conducted to enable a better understanding of the molecular mechanism triggered by ultrasound stimulation. Upon studying the molecular mechanism, such understanding can be used as a reference for elucidating ultrasound effects on cardiomyogenesis of human pluripotent cells.

The above suggestions are some future studies which arise from the reported findings in this thesis. However, a 3D bioprocess to produce cardiomyocytes of clinically relevant numbers and functionalities requires many design considerations. Therefore, the list of parameters for investigation and optimisation is not exhaustive. Tissue engineering and regenerative therapies are rapidly advancing fields in the biomedical industry and calls for the amalgamation of different expertise to address the multi-faceted challenges required in translating research outcomes into the clinic.

7 References

1. WHO. *Cardiovascular Diseases (CVDs)*. 2009 September [cited 2010 May 16]; Available from: http://www.who.int/mediacentre/factsheets/fs317/en/index.html.
2. Allen, J. *Heart Disease to cost U.S $503 billion in 2010 | Reuters*. 2009 December 7 [cited 2010 May 16]; Available from: http://www.reuters.com/article/idUSTRE5BG52I20091217.
3. McDevitt, T. and S. Palecek, *Innovation in the culture and derivation of pluripotent human stem cells.* Current Opinion in Biotechnology, 2008. **19**(5): p. 527-533.
4. Zimmermann, W.-H., et al., *Tissue engineering of a differentiated cardiac muscle construct.* Circulation Research, 2002. **90**(2): p. 223-230.
5. Akins, R.E., et al., *Neonatal rat heart cells cultured in simulated microgravity.* In Vitro Cellular & Developmental Biology-Animal, 1997. **33**(5): p. 337-343.
6. Schroeder, M., et al., *Differentiation and lineage selection of mouse embryonic stem cells in a stirred bench scale bioreactor with automated process control.* Biotechnology and Bioengineering, 2005. **92**(7): p. 920-933.
7. Niebruegge, S., et al., *Generation of human embryonic stem cell-derived mesoderm and cardiac cells using size-specified aggregates in an oxygen-controlled bioreactor.* Biotechnology and Bioengineering, 2009. **102**: p. 493-507.

8. Brown, M.A., R.K. Iyer, and M. Radisic, *Pulsatile perfusion bioreactor for cardiac tissue engineering.* Biotechnology Progress, 2008. **24**(4): p. 907-920.

9. Ge, D., et al., *Chemical and physical stimuli induce cardiomyocyte differentiation from stem cells.* Biochemical and Biophysical Research Communications, 2009. **381**(3): p. 317-321.

10. Gwak, S.J., et al., *The effect of cyclic strain on embryonic stem cell-derived cardiomyocytes.* Biomaterials, 2008. **29**(7): p. 844-856.

11. Ginis, I., et al., *Differences between human and mouse embryonic stem cells.* Developmental Biology, 2004. **269**(2): p. 360-380.

12. Greber, B., et al., *Conserved and divergent roles of FGF signaling in mouse epiblast stem cells and human embryonic stem cells.* Cell Stem Cell, 2010. **6**(3): p. 215-226.

13. Tesar, P.J., et al., *New cell lines from mouse epiblast share defining features with human embryonic stem cells.* Nature, 2007. **448**(7150): p. 196-199.

14. Hanna, J., et al., *Human embryonic stem cells with biological and epigenetic characteristics similar to those of mouse ESCs.* Proceedings of the National Academy of Sciences, 2010. **107**(20): p. 9222-9227.

15. Menasché, P., *Skeletal myoblast for cell therapy.* Coronary Artery Disease, 2005. **16**(2): p. 105-110.

16. Léobon, B., et al., *Myoblasts transplanted into rat infarcted myocardium are functionally isolated from their host.* Proceedings of the National Academy of Sciences of the United States of America, 2003. **100**(13): p. 7808-8811.

17. Dib, N., et al., *Safety and feasibility of autologous myoblast transplantation in patients with ischemic cardiomyopathy: four-year follow-up.* Circulation, 2005. **112**(12): p. 1748-1755.

18. Matsuura, K., et al., *Adult cardiac Sca-1-positive cells differentiate into beating cardiomyocytes.* Journal of Biological Chemistry, 2004. **279**(12): p. 11384-11391.

19. Barile, L., et al., *Endogenous cardiac stem cells.* Progress in Cardiovascular Diseases, 2007. **50**(1): p. 31-48.

20. Ott, H.C., et al., *The adult human heart as a source for stem cells: repair strategies with embryonic-like progenitor cells.* Nature Clinical Practice Cardiovascular Medicine, 2007. **4**: p. S27-S39.

21. Bartosh, T., et al., *3D-model of adult cardiac stem cells promotes cardiac differentiation and resistance to oxidative stress.* Journal of Cellular Biochemistry, 2008. **105**(2): p. 612-623.

22. Messina, E., et al., *Isolation and expansion of adult cardiac stem cells from human and murine heart.* Circulation Research, 2004. **95**(9): p. 911-921.

23. Marbán, E. and E. Cingolani, *Heart to Heart: Cardiospheres for Myocardial Regeneration.* Heart Rhythm, 2012. **9**(10): p. 1727-1731.

24. Andersen, D.C., et al., *Murine "cardiospheres" are not a source of stem cells with cardiomyogenic potential.* Stem Cells, 2009. **27**(7): p. 1571-1581.

25. Makino, S., et al., *Cardiomyocytes can be generated from marrow stromal cells in vitro.* Journal of Clinical Investigation, 1999. **103**(5): p. 697-705.

26. Mangi, A.A., et al., *Mesenchymal stem cells modified with Akt prevent remodeling and restore performance of infarcted hearts.* Nature Medicine, 2003. **9**(9): p. 1195-1201.

27. Strom, S.C. and T. Miki, *Placental stem cells and uses thereof*, in *United States Patent Application Publication*. 2005, WO/2005/042703.

28. Aggarwal, S. and M.F. Pittenger, *Human mesenchymal stem cells modulate allogeneic immune cell responses.* Blood, 2005. **105**(4): p. 1815-1822.

29. Di Nicola, M., et al., *Human bone marrow stromal cells suppress T-lymphocyte proliferation induced by cellular or nonspecific mitogenic stimuli.* Blood, 2002. **99**(10): p. 3838-3843.

30. Tse, W.T., et al., *Suppression of allogeneic T-cell proliferation by human marrow stromal cells: implications in transplantation.* Transplantation, 2003. **75**(3): p. 389-397.

31. Le Blanc, K., et al., *Mesenchymal stem cells inhibit and stimulate mixed lymphocyte cultures and mitogenic responses independently of the major histocompatibility complex.* Scandinavian Journal of Immunology, 2003. **57**(1): p. 11-20.

32. Assmus, B., et al., *Transcoronary transplantation of progenitor cells after myocardial infarction.* New England Journal of Medicine, 2006. **355**(12): p. 1222-1232.

33. Janssens, S., et al., *Autologous bone marrow-derived stem-cell transfer in patients with ST-segment elevation myocardial infarction: double-blind, randomised controlled trial.* Lancet, 2006. **367**(9505): p. 113-121.

34. Lunde, K., et al., *Intracoronary injection of mononuclear bone marrow cells in acute myocardial infarction.* New England Journal of Medicine, 2006. **355**(12): p. 1199-1209.

35. Abdel-Latif, A., et al., *Adult bone marrow-derived cells for cardiac repair: a systematic review and meta-analysis.* Archives of Internal Medicine, 2007. **167**(10): p. 989-997.

36. Lipinski, M.J., et al., *Impact of Intracoronary Cell Therapy on Left Ventricular Function in the Setting of Acute Myocardial Infarction:: A Collaborative Systematic Review and Meta-Analysis of Controlled Clinical Trials.* Journal of the American College of Cardiology, 2007. **50**(18): p. 1761-1767.

37. Martin-Rendon, E., et al., *Autologous bone marrow stem cells to treat acute myocardial infarction: a systematic review.* European Heart Journal, 2008. **29**(15): p. 1807-1818.

38. Doetschman, T.C., et al., *The in vitro development of blastocyst-derived embryonic stem cell lines: formation of visceral yolk sac, blood islands and myocardium.* Journal of Embryology and Experimental Morphology, 1985. **87**(1): p. 27-45.

39. Yang, L., et al., *IL-21 and TGF-&bgr; are required for differentiation of human TH17 cells.* Nature, 2008. **454**(7202): p. 350-352.

40. Caspi, O., et al., *Tissue engineering of vascularized cardiac muscle from human embryonic stem cells.* Circulation Research, 2007. **100**(2): p. 263-272.

41. Yamashita, J.K., et al., *Prospective identification of cardiac progenitors by a novel single cell-based cardiomyocyte induction.* FASEB Journal, 2005. **19**(11): p. 1534-1536.

42. Bauwens, C., et al., *Development of a perfusion fed bioreactor for embryonic stem cell-derived cardiomyocyte generation: oxygen-mediated enhancement of cardiomyocyte output.* Biotechnology and Bioengineering, 2005. **90**(4): p. 452-461.

43. Chang, M.G., et al., *Proarrhythmic potential of mesenchymal stem cell transplantation revealed in an in vitro coculture model.* Circulation, 2006. **113**(15): p. 1832-1841.

44. Schenke-Layland, K., et al., *Reprogrammed mouse fibroblasts differentiate into cells of the cardiovascular and hematopoietic lineages.* Stem Cells, 2008. **26**(6): p. 1537-1546.

45. Narazaki, G., et al., *Directed and systematic differentiation of cardiovascular cells from mouse induced pluripotent stem cells.* Circulation, 2008. **118**(5): p. 498-506.

46. Mauritz, C., et al., *Generation of functional murine cardiac myocytes from induced pluripotent stem cells.* Circulation, 2008. **118**(5): p. 507-517.

47. Zhang, J., et al., *Functional cardiomyocytes derived from human induced pluripotent stem cells.* Circulation Research, 2009. **104**(4): p. e30-e41.

48. Moretti, A., et al., *Patient-specific induced pluripotent stem-cell models for long-QT syndrome.* New England Journal of Medicine, 2010. **363**(15): p. 1397-1409.

49. Kaji, K., et al., *Virus-free induction of pluripotency and subsequent excision of reprogramming factors.* Nature, 2009. **458**(7239): p. 771-775.

50. Zhou, H., et al., *Generation of induced pluripotent stem cells using recombinant proteins.* Cell Stem Cell, 2009. **4**(5): p. 381-384.

51. Kim, D., et al., *Generation of human induced pluripotent stem cells by direct delivery of reprogramming proteins.* Cell Stem Cell, 2009. **4**(6): p. 472-476.

52. Plews, J.R., et al., *Activation of pluripotency genes in human fibroblast cells by a novel mRNA based approach.* PloS One, 2010. **5**(12): p. e14397.

53. Huangfu, D., et al., *Induction of pluripotent stem cells from primary human fibroblasts with only Oct4 and Sox2.* Nature Biotechnology, 2008. **26**(11): p. 1269-1275.

54. Keller, G.M., *In vitro differentiation of embryonic stem cells.* Current opinion in Cell Biology, 1995. **7**(6): p. 862-869.

55. Schöler, H.R., T. Ciesiolka, and P. Gruss, *A nexus between Oct-4 and E1 A: Implications for gene regulation in embryonic stem cells.* Cell, 1991. **66**(2): p. 291-304.

56. Yeom, Y.I., et al., *Germline regulatory element of Oct-4 specific for the totipotent cycle of embryonal cells.* Development, 1996. **122**(3): p. 881-894.

57. Nichols, J., et al., *Formation of pluripotent stem cells in the mammalian embryo depends on the POU transcription factor Oct4.* Cell, 1998. **95**(3): p. 379-391.

58. Palmieri, S.L., et al., *Oct-4 transcription factor is differentially expressed in the mouse embryo during establishment of the first two extraembryonic cell lineages involved in implantation.* Developmental Biology, 1994. **166**: p. 259-267.

59. Niwa, H., J.-i. Miyazaki, and A.G. Smith, *Quantitative expression of Oct-3/4 defines differentiation, dedifferentiation or self-renewal of ES cells.* Nature Genetics, 2000. **24**(4): p. 372-376.

60. Rathjen, P.D., et al., *Properties and uses of embryonic stem cells: prospects for application to human biology and gene therapy.* Reproduction, Fertility, and Development, 1997. **10**(1): p. 31-47.

61. Tam, P.P. and D.A. Loebel, *Gene function in mouse embryogenesis: get set for gastrulation.* Nature Reviews Genetics, 2007. **8**(5): p. 368-381.

62. Lawson, A. and G.C. Schoenwolf, *Epiblast and primitive-streak origins of the endoderm in the gastrulating chick embryo.* Development, 2003. **130**(15): p. 3491-3501.

63. Srivastava, D. and K.N. Ivey, *Potential of stem-cell-based therapies for heart disease.* Nature, 2006. **441**(7097): p. 1097-1099.

64. Rajala, K., M. Pekkanen-Mattila, and K. Aalto-Setälä, *Cardiac differentiation of pluripotent stem cells.* Stem Cells International, 2011. **2011**: p. DOI: 10.4061/2011/383709.

65. Bondue, A., et al., *Mesp1 acts as a master regulator of multipotent cardiovascular progenitor specification.* Cell Stem Cell, 2008. **3**(1): p. 69-84.

66. Lindsley, R.C., et al., *Mesp1 coordinately regulates cardiovascular fate restriction and epithelial-mesenchymal transition in differentiating ESCs.* Cell Stem Cell, 2008. **3**(1): p. 55-68.

67. Cheung, C. and S. Sinha, *Human embryonic stem cell-derived vascular smooth muscle cells in therapeutic neovascularisation.* Journal of Molecular and Cellular Cardiology, 2011. **51**(5): p. 651-664.

68. Azhar, M., et al., *Transforming growth factor beta in cardiovascular development and function.* Cytokine & Growth Factor reviews, 2003. **14**(5): p. 391-407.

69. Zhang, H. and A. Bradley, *Mice deficient for BMP2 are nonviable and have defects in amnion/chorion and cardiac development.* Development, 1996. **122**(10): p. 2977-2986.

70. Kumar, D. and B. Sun, *Transforming growth factor-β2 enhances differentiation of cardiac myocytes from embryonic stem cells.* Biochemical and Biophysical Research Communications, 2005. **332**(1): p. 135-141.

71. Schuldiner, M., et al., *Effects of eight growth factors on the differentiation of cells derived from human embryonic stem cells.* Proceedings of the National Academy of Sciences of the United States of America, 2000. **97**(21): p. 11307-11312.

72. Monzen, K., et al., *Bone morphogenetic proteins induce cardiomyocyte differentiation through the mitogen-activated protein kinase kinase kinase TAK1 and cardiac transcription factors Csx/Nkx-2.5 and GATA-4.* Molecular and Cellular Biology, 1999. **19**(10): p. 7096-7105.

73. Bin, Z., et al., *Efficient cardiomyocyte differentiation of embryonic stem cells by bone morphogenetic protein-2 combined with visceral endoderm-like cells.* Cell Biology International, 2006. **30**(10): p. 769-776.

74. Yao, S., et al., *Long-term self-renewal and directed differentiation of human embryonic stem cells in chemically defined conditions.* Proceedings of the National Academy of Sciences of the United States of America, 2006. **103**(18): p. 6907-6912.

75. Asashima, M., T. Michiue, and A. Kurisaki, *Elucidation of the role of activin in organogenesis using a multiple organ induction system with amphibian and mouse undifferentiated cells in vitro.* Development, Growth & Differentiation, 2008. **50**(s1): p. S35-S45.

76. Mummery, C.L., et al., *Visceral-endoderm-like cell lines induce differentiation of murine P19 embryonal carcinoma cells.* Differentiation, 1991. **46**(1): p. 51-60.

77. Mummery, C., et al., *Differentiation of human embryonic stem cells to cardiomyocytes role of coculture with visceral endoderm-like cells.* Circulation, 2003. **107**(21): p. 2733-2740.

78. Xu, X.Q., et al., *Chemically defined medium supporting cardiomyocyte differentiation of human embryonic stem cells.* Differentiation, 2008. **76**(9): p. 958-970.

79. Lake, J.-a., et al., *Reversible programming of pluripotent cell differentiation.* Journal of Cell Science, 2000. **113**(3): p. 555-566.

80. Hwang, Y.S., et al., *Enhanced derivation of osteogenic cells from murine embryonic stem cells after treatment with HepG2-conditioned medium and modulation of the embryoid body formation period: application to*

skeletal tissue engineering. Tissue Engineering, 2006. **12**(6): p. 1381-1392.

81. Xu, C., et al., *Characterization and enrichment of cardiomyocytes derived from human embryonic stem cells.* Circulation Research, 2002. **91**(6): p. 501-508.

82. Choi, S.-C., et al., *5-azacytidine induces cardiac differentiation of P19 embryonic stem cells.* Experimental & Molecular Medicine, 2004. **36**(6): p. 515-523.

83. Wobus, A.M., et al., *Retinoic acid accelerates embryonic stem cell-derived cardiac differentiation and enhances development of ventricular cardiomyocytes.* Journal of Molecular and Cellular cardiology, 1997. **29**(6): p. 1525-1539.

84. Zandstra, P., et al., *Scalable production of embryonic stem cell-derived cardiomyocytes.* Tissue Engineering, 2003. **9**(4): p. 767-778.

85. Takahashi, T., et al., *Ascorbic acid enhances differentiation of embryonic stem cells into cardiac myocytes.* Circulation, 2003. **107**(14): p. 1912-1916.

86. Wu, X., et al., *Small molecules that induce cardiomyogenesis in embryonic stem cells.* Journal of the American Chemical Society, 2004. **126**(6): p. 1590-1591.

87. Yau, W.W.Y., et al., *Cardiogenol C can induce Mouse Hair Bulge Progenitor Cells to Transdifferentiate into Cardiomyocyte-like Cells.* Proteome Science, 2011. **9**(1): p. 3.

88. Ueno, S., et al., *Biphasic role for Wnt/ -catenin signaling in cardiac specification in zebrafish and embryonic stem cells.* Proceedings of the

National Academy of Sciences of the United States of America, 2007. **104**(23): p. 9685-9690.

89. Dang, S.M., et al., *Controlled, scalable embryonic stem cell differentiation culture.* Stem Cells, 2004. **22**(3): p. 275-282.

90. Sargent, C.Y., G.Y. Berguig, and T.C. McDevitt, *Cardiomyogenic differentiation of embryoid bodies is promoted by rotary orbital suspension culture.* Tissue Engineering Part A, 2009. **15**(2): p. 331-342.

91. Gerecht-Nir, S., S. Cohen, and J. Itskovitz-Eldor, *Bioreactor cultivation enhances the efficiency of human embryoid body (hEB) formation and differentiation.* Biotechnology and Bioengineering, 2004. **86**(5): p. 493-502.

92. Consolo, F., et al., *Computational modeling for the optimization of a cardiogenic 3D bioprocess of encapsulated embryonic stem cells.* Biomechanics and Modeling in Mechanobiology, 2011. **11**(1): p. 261-277.

93. Dvir, T., et al., *Activation of the ERK1/2 cascade via pulsatile interstitial fluid flow promotes cardiac tissue assembly.* Tissue Engineering, 2007. **13**(9): p. 2185-2193.

94. Carrier, R.L., et al., *Perfusion improves tissue architecture of engineered cardiac muscle.* Tissue Engineering, 2002. **8**(2): p. 175-188.

95. Radisic, M., et al., *Mathematical model of oxygen distribution in engineered cardiac tissue with parallel channel array perfused with culture medium containing oxygen carriers.* American Journal of Physiology - Heart and Circulatory Physiology, 2005. **288**(3): p. H1278-H1289.

96. Hoerstrup, S.P., et al., *New pulsatile bioreactor for in vitro formation of tissue engineered heart valves.* Tissue Engineering, 2000. **6**(1): p. 75-79.

97. Sodian, R., et al., *New pulsatile bioreactor for fabrication of tissue-engineered patches.* Journal of Biomedical Materials Research, 2001. **58**(4): p. 401-405.

98. Rabkin, E. and F.J. Schoen, *Cardiovascular tissue engineering.* Cardiovascular Pathology, 2002. **11**(6): p. 305-317.

99. Vunjak-Novakovic, G., M. Radisic, and B. Obradovic, *Cardiac tissue engineering: effects of bioreactor flow environment on tissue constructs.* Journal of Chemical Technology & Biotechnology, 2006. **81**(4): p. 485-490.

100. Papadaki, M., et al., *Tissue engineering of functional cardiac muscle: molecular, structural, and electrophysiological studies.* American Journal of Physiology - Heart and Circulatory Physiology, 2001. **280**(1): p. H168-H178.

101. Zhang, H., et al., *Computational-fluid-dynamics (CFD) analysis of mixing and gas–liquid mass transfer in shake flasks.* Biotechnology and Applied Biochemistry, 2005. **41**(1): p. 1-8.

102. Kwon, O., et al., *Oxygen transport and consumption by suspended cells in microgravity: a multiphase analysis.* Biotechnology and Bioengineering, 2008. **99**(1): p. 99-107.

103. Carrier, R.L., et al., *Cardiac tissue engineering: cell seeding, cultivation parameters, and tissue construct characterization.* Biotechnology and Bioengineering, 1999. **64**(5): p. 580-589.

104. Bursac, N., et al., *Cardiac muscle tissue engineering: toward an in vitro model for electrophysiological studies.* American Journal of Physiology, 1999. **277**(2): p. H433-H444.

105. Sumaru, K. and T. Kanamori, *Optimal design of bio-hybrid systems with a hollow fiber scaffold: model analysis of oxygen diffusion/consumption.* Biochemical Engineering Journal, 2004. **20**(2): p. 127-136.

106. Curcio, E., et al., *Mass transfer and metabolic reactions in hepatocyte spheroids cultured in rotating wall gas-permeable membrane system.* Biomaterials, 2007. **28**(36): p. 5487-5497.

107. Coletti, F., S. Macchietto, and N. Elvassore, *Mathematical modeling of three-dimensional cell cultures in perfusion bioreactors.* Industrial & Engineering Chemistry Research, 2006. **45**(24): p. 8158-8169.

108. Lim, M., A. Teo, and A. Mantalaris, *Hydrodynamics and bioprocess considerations in designing bioreactors for cardiac tissue engineering.* Journal of Regenerative Medicine and Tissue Engineering, 2012. **1**(1): p. 4.

109. Radisic, M., et al., *Biomimetic approach to cardiac tissue engineering.* Philosophical Transactions of the Royal Society B: Biological Sciences, 2007. **362**(1484): p. 1357-1368.

110. Matsuura, K., et al., *Fabrication of Mouse Embryonic Stem Cell-Derived Layered Cardiac Cell Sheets Using a Bioreactor Culture System.* PloS One, 2012. **7**(12): p. e52176.

111. Hecker, L., et al., *Novel bench-top perfusion system improves functional performance of bioengineered heart muscle.* Journal of Bioscience and Bioengineering, 2009. **107**(2): p. 183-190.

112. Radisic, M., et al., *Medium perfusion enables engineering of compact and contractile cardiac tissue.* American Journal of Physiology - Heart and Circulatory Physiology, 2004. **286**(2): p. H507-H516.

113. Kenar, H., et al., *A 3D aligned microfibrous myocardial tissue construct cultured under transient perfusion.* Biomaterials, 2011. **32**: p. 5320-5329.

114. Chen, V.C., et al., *Scalable GMP compliant suspension culture system for human ES cells.* Stem Cell Research, 2012. **8**(3): p. 388-402.

115. He, W., et al., *Stirred Suspension Culture Improves Embryoid Body Formation and Cardiogenic Differentiation of Genetically Modified Embryonic Stem Cells.* Biological and Pharmaceutical Bulletin, 2012. **35**(3): p. 308-316.

116. Shafa, M., et al., *Impact of stirred suspension bioreactor culture on the differentiation of murine embryonic stem cells into cardiomyocytes.* BMC Cell Biology, 2011. **12**(1): p. 53.

117. Rungarunlert, S., et al., *Enhanced cardiac differentiation of mouse embryonic stem cells by use of the slow-turning, lateral vessel (STLV) bioreactor.* Biotechnology Letters, 2011. **33**(8): p. 1565-1573.

118. Lü, S., et al., *Bioreactor cultivation enhances NTEB formation and differentiation of NTES cells into cardiomyocytes.* Cloning and Stem Cells, 2008. **10**(3): p. 363-370.

119. Lecina, M., et al., *Scalable platform for human embryonic stem cell differentiation to cardiomyocytes in suspended microcarrier cultures.* Tissue Engineering Part C: Methods, 2010. **16**(6): p. 1609-1619.

120. Li, Z., et al., *High Efficiency Matrix Modulus-Induced Cardiac Differentiation of Human Mesenchymal Stem Cells inside a*

Thermosensitive Hydrogel. Acta Biomaterialia, 2012. **8**(10): p. 3586-3595.

121. Moshaverinia, A., et al., *Alginate hydrogel as a promising scaffold for dental-derived stem cells: an in vitro study.* Journal of Materials Science: Materials in Medicine, 2012. **23**(12): p. 3041-3051.

122. Liu, J., et al., *Human umbilical cord stem cell encapsulation in novel macroporous and injectable fibrin for muscle tissue engineering.* Acta Biomaterialia, 2012. **9**(1): p. 4688-4697.

123. Ye, K.Y., K.E. Sullivan, and L.D. Black, *Encapsulation of cardiomyocytes in a fibrin hydrogel for cardiac tissue engineering.* Journal of Visualized Experiments: JoVE, 2011. **19**(55): p. 3251.

124. Gerecht-Nir, S., et al., *Three-dimensional porous alginate scaffolds provide a conducive environment for generation of well-vascularized embryoid bodies from human embryonic stem cells.* Biotechnology and Bioengineering, 2004. **88**(3): p. 313-320.

125. Siti-Ismail, N., et al., *The benefit of human embryonic stem cell encapsulation for prolonged feeder-free maintenance.* Biomaterials, 2008. **29**(29): p. 3946-3952.

126. Jing, D., A. Parikh, and E.S. Tzanakakis, *Cardiac cell generation from encapsulated embryonic stem cells in static and scalable culture systems.* Cell Transplantation, 2010. **19**(11): p. 1397-1412.

127. Lakshmanan, R., U.M. Krishnan, and S. Sethuraman, *Living cardiac patch: the elixir for cardiac regeneration.* Expert Opinion on Biological Therapy, 2012. **12**(12): p. 1623-1640.

128. Engler, A.J., et al., *Embryonic cardiomyocytes beat best on a matrix with heart-like elasticity: scar-like rigidity inhibits beating.* Journal of Cell Science, 2008. **121**(22): p. 3794-3802.

129. Li, R.K., et al., *Construction of a bioengineered cardiac graft.* Journal of Thoracic and Cardiovascular Surgery, 2000. **119**(2): p. 368-375.

130. Dar, A., et al., *Optimization of cardiac cell seeding and distribution in 3D porous alginate scaffolds.* Biotechnology and Bioengineering, 2002. **80**(3): p. 305-312.

131. Bai, X., et al., *Fabrication of engineered heart tissue grafts from alginate/collagen barium composite microbeads.* Biomedical Materials, 2011. **6**: p. 045002.

132. Prabhakaran, M., et al., *Electrospun biocomposite nanofibrous patch for cardiac tissue engineering.* Biomedical Materials, 2011. **6**: p. 055001.

133. Kai, D., et al., *Guided orientation of cardiomyocytes on electrospun aligned nanofibers for cardiac tissue engineering.* Journal of Biomedical Materials Research Part B: Applied Biomaterials, 2011. **98B**(2): p. 379-386.

134. Marsano, A., et al., *Scaffold stiffness affects the contractile function of three-dimensional engineered cardiac constructs.* Biotechnology Progress, 2010. **26**(5): p. 1382-1390.

135. Schussler, O., et al., *Use of arginine–glycine–aspartic acid adhesion peptides coupled with a new collagen scaffold to engineer a myocardium-like tissue graft.* Nature Clinical Practice Cardiovascular Medicine, 2009. **6**(3): p. 240-249.

136. Aubin, H., et al., *Directed 3D cell alignment and elongation in microengineered hydrogels.* Biomaterials, 2010. **31**(27): p. 6941-6951.

137. Engelmayr, G.C., et al., *Accordion-like honeycombs for tissue engineering of cardiac anisotropy.* Nature Materials, 2008. **7**(12): p. 1003-1010.

138. Fujita, A., et al., *Control of cardiomyocyte orientation on a microscaffold fabricated by photopolymerization with laser beam interference.* Journal of Biomedical Optics, 2006. **11**(2): p. 021015.

139. Bienaimé, C., J.N. Barbotin, and J.E. Nava-Saucedo, *How to build an adapted and bioactive cell microenvironment? A chemical interaction study of the structure of Ca-alginate matrices and their repercussion on confined cells.* Journal of Biomedical Materials Research Part A, 2003. **67**(2): p. 376-388.

140. Chia, S.-M., et al., *Hepatocyte encapsulation for enhanced cellular functions.* Tissue Engineering, 2000. **6**(5): p. 481-495.

141. Uludag, H., P. De Vos, and P.A. Tresco, *Technology of mammalian cell encapsulation.* Advanced Drug Delivery Reviews, 2000. **42**(1): p. 29-64.

142. Simpson, N.E., et al., *The role of the CaCl2-guluronic acid interaction on alginate encapsulated betaTC3 cells.* Biomaterials, 2004. **25**(13): p. 2603-2610.

143. Awad, H.A., et al., *Chondrogenic differentiation of adipose-derived adult stem cells in agarose, alginate, and gelatin scaffolds.* Biomaterials, 2004. **25**(16): p. 3211-3222.

144. Dahlmann, J., et al., *Fully defined in situ cross-linkable alginate and hyaluronic acid hydrogels for myocardial tissue engineering.* Biomaterials, 2013. **34**(4): p. 940 - 951.

145. Shachar, M., et al., *The effect of immobilized RGD peptide in alginate scaffolds on cardiac tissue engineering.* Acta Biomaterialia, 2011. **7**(1): p. 152-162.

146. Dvir, T., et al., *Nanowired three-dimensional cardiac patches.* Nature Nanotechnology, 2011. **6**(11): p. 720-725.

147. Shachar, M., N. Benishti, and S. Cohen, *Effects of mechanical stimulation induced by compression and medium perfusion on cardiac tissue engineering.* Biotechnology Progress, 2012. **28**(6): p. 1551-1559.

148. Dvir, T., et al., *A novel perfusion bioreactor providing a homogenous milieu for tissue regeneration.* Tissue Engineering, 2006. **12**(10): p. 2843-2852.

149. Kim, B.S., et al., *Cyclic mechanical strain regulates the development of engineered smooth muscle tissue.* Nature Biotechnology, 1999. **17**(10): p. 979-983.

150. Kim, B.S. and D.J. Mooney, *Scaffolds for engineering smooth muscle under cyclic mechanical strain conditions.* Journal of Biomechanical Engineering, 2000. **122**(3): p. 210-215.

151. Fink, C., et al., *Chronic stretch of engineered heart tissue induces hypertrophy and functional improvement.* The FASEB Journal, 2000. **14**(5): p. 669.

152. Parsons, M., et al., *Mechanical load enhances procollagen processing in dermal fibroblasts by regulating levels of procollagen C-proteinase.* Experimental Cell Research, 1999. **252**(2): p. 319-331.

153. Salameh, A., et al., *Cyclic mechanical stretch induces cardiomyocyte orientation and polarization of the gap junction protein connexin43.* Circulation Research, 2010. **106**(10): p. 1592-1602.

154. Huang, Y., et al., *Effect of cyclic strain on cardiomyogenic differentiation of rat bone marrow derived mesenchymal stem cells.* PloS One, 2012. **7**(4): p. e34960.

155. Guan, J., et al., *The stimulation of the cardiac differentiation of mesenchymal stem cells in tissue constructs that mimic myocardium structure and biomechanics.* Biomaterials, 2011. **32**(24): p. 5568-5580.

156. Kensah, G., et al., *A novel miniaturized multimodal bioreactor for continuous in situ assessment of bioartificial cardiac tissue during stimulation and maturation.* Tissue Engineering Part C: Methods, 2011. **17**(4): p. 463-473.

157. Neef, K., et al., *Mechanical preconditioning enables electrophysiologic coupling of skeletal myoblast cells to myocardium.* The Journal of Thoracic and Cardiovascular Surgery, 2012. **144**(5): p. 1176-1184.

158. Hotary, K. and K. Robinson, *Endogenous electrical currents and the resultant voltage gradients in the chick embryo.* Developmental Biology, 1990. **140**(1): p. 149-160.

159. Winkel, G. and R. Nuccitelli, *Large ionic currents leave the primitive streak of the 7.5-day mouse embryo.* The Biological Bulletin, 1989. **176**(2S): p. 110-117.

160. Sauer, H., et al., *Effects of electrical fields on cardiomyocyte differentiation of embryonic stem cells.* Journal of Cellular Biochemistry, 1999. **75**(4): p. 710-723.

161. Chen, M., et al. *Cardiac differentiation of embryonic stem cells with point-source electrical stimulation*. in *30th Annual International IEEE EMBS Conference*. 2008. Vancouver, Canada.

162. Serena, E., et al., *Electrical stimulation of human embryonic stem cells: Cardiac differentiation and the generation of reactive oxygen species.* Experimental Cell Research, 2009. **315**(20): p. 3611-3619.

163. Radisic, M., et al., *Functional assembly of engineered myocardium by electrical stimulation of cardiac myocytes cultured on scaffolds.* Proceedings of the National Academy of Sciences of the United States of America, 2004. **101**(52): p. 18129-18134.

164. Tandon, N., et al. *Alignment and Elongation of Human Adipose-Derived Stem Cells in Response to Direct-Current Electrical Stimulation*. in *31st Annual International Conference of the IEEE EMBS*. 2009. Minneapolis, USA: NIH Public Access.

165. Inoue, N., et al., *Rapid electrical stimulation of contraction modulates gap junction protein in neonatal rat cultured cardiomyocytes: involvement of mitogen-activated protein kinases and effects of angiotensin II-receptor antagonist.* Journal of the American College of Cardiology, 2004. **44**(4): p. 914-922.

166. McDonough, P. and C. Glembotski, *Induction of atrial natriuretic factor and myosin light chain-2 gene expression in cultured ventricular*

myocytes by electrical stimulation of contraction. Journal of Biological Chemistry, 1992. **267**(17): p. 11665-11668.

167. Barash, Y., et al., *Electric Field Stimulation Integrated into Perfusion Bioreactor for Cardiac Tissue Engineering.* Tissue Engineering Part C: Methods, 2010. **16**(6): p. 1417-1426.

168. Boheler, K.R., et al., *Differentiation of pluripotent embryonic stem cells into cardiomyocytes.* Circulation Research, 2002. **91**(3): p. 189-201.

169. Czyz, J. and A.M. Wobus, *Embryonic stem cell differentiation: the role of extracellular factors.* Differentiation, 2001. **68**(4-5): p. 167-174.

170. Ma, C.Y.J., et al., *A combined fluid dynamics, mass transport and cell growth model for a three-dimensional perfused biorector for tissue engineering of haematopoietic cells.* Biochemical Engineering Journal, 2007. **35**(1): p. 1-11.

171. Yeo, D., et al., *Improving embryonic stem cell expansion through the combination of perfusion and bioprocess model design.* PloS One, 2013. **8**(12): p. e81728.

172. Guan, K., D.O. Fürst, and A.M. Wobus, *Modulation of sarcomere organization during embryonic stem cell-derived cardiomyocyte differentiation.* European Journal of Cell Biology, 1999. **78**(11): p. 813-823.

173. Schmittgen, T.D. and K.J. Livak, *Analyzing real-time PCR data by the comparative CT method.* Nature protocols, 2008. **3**(6): p. 1101-1108.

174. Antin, P.B., et al., *Precocious expression of cardiac troponin T in early chick embryos is independent of bone morphogenetic protein signaling.* Developmental Dynamics, 2002. **225**(2): p. 135-141.

175. Stefanovic, S. and M. Pucéat, *Oct-3/4: not just a gatekeeper of pluripotency for embryonic stem cell, a cell fate instructor through a gene dosage effect.* Cell Cycle, 2007. **6**(1): p. 8-10.

176. Mossman, A.K., et al., *Mixl1 and oct4 proteins are transiently co-expressed in differentiating mouse and human embryonic stem cells.* Stem Cells and Development, 2005. **14**(6): p. 656-663.

177. Ai, Z., et al., *Wnt-1 regulation of connexin43 in cardiac myocytes.* Journal of Clinical Investigation, 2000. **105**(2): p. 161-171.

178. Effros, R., et al., *In vivo myocardial cell pH in the dog. Response to ischemia and infusion of alkali.* Journal of Clinical Investigation, 1975. **55**(5): p. 1100.

179. Bountra, C. and R. Vaughan-Jones, *Effect of intracellular and extracellular pH on contraction in isolated, mammalian cardiac muscle.* The Journal of Physiology, 1989. **418**(1): p. 163-187.

180. Oshita, S., et al., *Contractile force and resting tension in the presence of halothane and increased extracellular potassium or decreased extracellular pH in isolated guinea pig atria.* Canadian Journal of Anaesthesia, 1994. **41**(6): p. 534-541.

181. Fuller, S., C. Gaitanaki, and P. Sugden, *Effects of increasing extracellular pH on protein synthesis and protein degradation in the perfused working rat heart.* Biochemical Journal, 1989. **259**(1): p. 173.

182. Gaitanaki, C.J., P.H. Sugden, and S.J. Fuller, *Stimulation of protein synthesis by raised extracellular pH in cardiac myocytes and perfused hearts.* FEBS Letters, 1990. **260**(1): p. 42-44.

183. Hirayama, Y., et al., *Calcium-activated CL-current is enhanced by acidosis and contributes to the shortening of action potential duration in rabbit ventricular myocytes.* The Japanese Journal of Physiology, 2002. **52**(3): p. 293-300.

184. Yamamoto, S. and T. Ehara, *Acidic extracellular pH-activated outwardly rectifying chloride current in mammalian cardiac myocytes.* American Journal of Physiology-Heart and Circulatory Physiology, 2006. **290**(5): p. H1905-H1914.

185. Zhou, Q. and G.C. Bett, *Regulation of the voltage-insensitive step of HERG activation by extracellular pH.* American Journal of Physiology-Heart and Circulatory Physiology, 2010. **298**(6): p. H1710-H1718.

186. Chiu, P.W., et al., *Esophageal pH exposure and epithelial cell differentiation.* Diseases of the Esophagus, 2009. **22**(7): p. 596-599.

187. Isfort, R.J., et al., *Calcium functions as a transcriptional and mitogenic repressor in Syrian hamster embryo cells: roles of intracellular pH and calcium in controlling embryonic cell differentiation and proliferation.* Experimental Cell Research, 1996. **226**(2): p. 363-371.

188. Yang, H., W. Miller, and E. Papoutsakis, *Higher pH promotes megakaryocytic maturation and apoptosis.* Stem Cells, 2002. **20**(4): p. 320-328.

189. McAdams, T.A., W.M. Miller, and E.T. Papoutsakis, *Variations in culture pH affect the cloning efficiency and differentiation of progenitor cells in ex vivo haemopoiesis.* British Journal of Haematology, 1997. **97**(4): p. 889-895.

190. Boussouf, A. and S. Gaillard, *Intracellular pH changes during oligodendrocyte differentiation in primary culture.* Journal of Neuroscience Research, 2000. **59**(6): p. 731-739.

191. Isfort, R.J., et al., *Induction of protein phosphorylation, protein synthesis, immediate-early-gene expression and cellular proliferation by intracellular pH modulation.* European Journal of Biochemistry, 1993. **213**(1): p. 349-357.

192. Tapper, H. and R. Sundler, *Cytosolic pH regulation in mouse macrophages. Characteristics of HCO3 (-)-dependent mechanisms.* Biochemical Journal, 1992. **281**(Pt 1): p. 239-244.

193. Hjelmeland, A.B., et al., *Acidic stress promotes a glioma stem cell phenotype.* Cell Death & Differentiation, 2010. **18**(5): p. 829-840.

194. Stathopoulou, K., I. Beis, and C. Gaitanaki, *MAPK signaling pathways are needed for survival of H9c2 cardiac myoblasts under extracellular alkalosis.* American Journal of Physiology-Heart and Circulatory Physiology, 2008. **295**(3): p. H1319-H1329.

195. Endo, T., et al., *Significance of pH on differentiation of human erythroid cell lines.* Leukemia Research, 1994. **18**(1): p. 49-54.

196. LeBoeuf, R.A. and G.A. Kerckaert, *The induction of transformed-like morphology and enhanced growth in Syrian hamster embryo cells grown at acidic pH.* Carcinogenesis, 1986. **7**(9): p. 1431-1440.

197. Veraitch, F.S., et al., *The impact of manual processing on the expansion and directed differentiation of embryonic stem cells.* Biotechnology and Bioengineering, 2008. **99**(5): p. 1216-1229.

198. Pagano, G., et al., *pH-Induced changes in mitotic and developmental patterns in sea urchin embryogenesis. I. Exposure of embryos.* Teratogenesis, Carcinogenesis, and Mutagenesis, 1985. **5**(2): p. 101-112.

199. Teo, A., et al., *A novel perfused rotary bioreactor for cardiomyogenesis of embryonic stem cells.* Biotechnology Letters, 2014. **36**(5): p. 947-960.

200. Li, H., et al., *Acidic pH conditions mimicking degenerative intervertebral discs impair the survival and biological behavior of human adipose-derived mesenchymal stem cells.* Experimental Biology and Medicine, 2012. **237**(7): p. 845-852.

201. Chen, M., et al., *Mitogen-activated protein kinase in endothelin-1-induced cardiac differentiation of mouse embryonic stem cells.* Journal of Cellular Biochemistry, 2010. **111**(6): p. 1619-1628.

202. Barruet, E., et al., *p38 mitogen activated protein kinase controls two successive-steps during the early mesodermal commitment of embryonic stem cells.* Stem Cells and Development, 2010. **20**(7): p. 1233-1246.

203. Kempf, H., et al., *Distinct regulation of mitogen-activated protein kinase activities is coupled with enhanced cardiac differentiation of human embryonic stem cells.* Stem Cell Research, 2011. **7**(3): p. 198-209.

204. Yeghiazarians, Y., et al., *Myocardial improvement with human embryonic stem cell-derived cardiomyocytes enriched by p38MAPK inhibition.* Cytotherapy, 2012. **14**(2): p. 223-231.

205. Wu, J., et al., *p38 Mitogen-activated protein kinase controls a switch between cardiomyocyte and neuronal commitment of murine embryonic stem cells by activating myocyte enhancer factor 2C-dependent bone*

morphogenetic protein 2 transcription. Stem Cells and Development, 2010. **19**(11): p. 1723-1734.

206. Das, B., et al., *HIF-2α Suppresses p53 to Enhance the Stemness and Regenerative Potential of Human Embryonic Stem Cells.* Stem Cells, 2012. **30**(8): p. 1685-1695.

207. Yoon, J.H., et al., *Introducing pulsed low-intensity ultrasound to culturing human umbilical cord-derived mesenchymal stem cells.* Biotechnology Letters, 2009. **31**(3): p. 329-335.

208. Lee, H.J., et al., *Low-intensity ultrasound inhibits apoptosis and enhances viability of human mesenchymal stem cells in three-dimensional alginate culture during chondrogenic differentiation.* Tissue Engineering, 2007. **13**(5): p. 1049-1057.

209. Cheung, W.-H., et al., *Applications of Exogenous Mesenchymal Stem Cells and Low Intensity Pulsed Ultrasound Enhance Fracture Healing in Rat Model.* Ultrasound in Medicine & Biology, 2013. **39**(1): p. 117-125.

210. Jiang, T., et al., *Osteogenic effect of low intensity pulsed ultrasound on rat adipose-derived stem cells in vitro.* Journal of Huazhong University of Science and Technology-Medical Sciences, 2012. **32**(1): p. 75-81.

211. Ikeda, K., et al., *Effects of low-intensity pulsed ultrasound on the differentiation of C2C12 cells.* Life Sciences, 2006. **79**(20): p. 1936-1943.

212. Hasegawa, T., et al., *Osteogenic activity of human fracture haematoma-derived progenitor cells is stimulated by low-intensity pulsed ultrasound in vitro.* Journal of Bone & Joint Surgery, British Volume, 2009. **91**(2): p. 264-270.

213. Choi, J.W., et al., *Mechanical Stimulation by Ultrasound Enhances Chondrogenic Differentiation of Mesenchymal Stem Cells in a Fibrin-Hyaluronic Acid Hydrogel.* Artificial Organs, 2013. **37**(7): p. 648-655.

214. Lee, H.J., et al., *Low-intensity Ultrasound Stimulation Enhances Chondrogenic Differentiation in Alginate Culture of Mesenchymal Stem Cells.* Artificial Organs, 2006. **30**(9): p. 707-715.

215. Schumann, D., et al., *Treatment of human mesenchymal stem cells with pulsed low intensity ultrasound enhances the chondrogenic phenotype in vitro.* Biorheology, 2006. **43**(3): p. 431-443.

216. Cui, J.H., et al., *Effects of low-intensity ultrasound on chondrogenic differentiation of mesenchymal stem cells embedded in polyglycolic acid: an in vivo study.* Tissue Engineering, 2006. **12**(1): p. 75-82.

217. Lai, C.-H., et al., *Effects of low-intensity pulsed ultrasound, dexamethasone/TGF-β1 and/or BMP-2 on the transcriptional expression of genes in human mesenchymal stem cells: chondrogenic vs. osteogenic differentiation.* Ultrasound in Medicine & Biology, 2010. **36**(6): p. 1022-1033.

218. Cui, J.H., et al., *Preconditioning of mesenchymal stem cells with low-intensity ultrasound for cartilage formation in vivo.* Tissue Engineering, 2007. **13**(2): p. 351-360.

219. Park, H., et al., *Indirect Low-Intensity Ultrasonic Stimulation for Tissue Engineering.* Journal of Tissue Engineering, 2010. **1**(1): p. DOI: 10.4061/2010/973530.

220. Bandow, K., et al., *Low-intensity pulsed ultrasound (LIPUS) induces RANKL, MCP-1, and MIP-1β expression in osteoblasts through the angiotensin II type 1 receptor.* Journal of Cellular Physiology, 2007. **211**(2): p. 392-398.

221. O'Brien Jr, W.D., *Ultrasound - biophysics mechanisms.* Progress in Biophysics and Molecular Biology, 2007. **93**(1-3): p. 212-255.

222. Jaramillo, M., et al., *Inducing endoderm differentiation by modulating mechanical properties of soft substrates.* Journal of Tissue Engineering and Regenerative Medicine, 2012: p. DOI: 10.1002/term.1602.

223. Zoldan, J., et al., *The influence of scaffold elasticity on germ layer specification of human embryonic stem cells.* Biomaterials, 2011. **32**(36): p. 9612-9621.

224. Ingber, D.E., *Mechanical control of tissue morphogenesis during embryological development.* International Journal of Developmental Biology, 2006. **50**(2): p. 255-266.

225. Shah, K., *Encapsulated stem cells for cancer therapy.* Biomatter, 2013. **3**(1): p. e24278.

226. Aguado, B.A., et al., *Improving viability of stem cells during syringe needle flow through the design of hydrogel cell carriers.* Tissue Engineering Part A, 2011. **18**(7-8): p. 806-815.

227. Weir, M.D., H.H. Xu, and C.G. Simon, *Strong calcium phosphate cement-chitosan-mesh construct containing cell-encapsulating hydrogel beads for bone tissue engineering.* Journal of Biomedical Materials Research Part A, 2006. **77**(3): p. 487-496.

228. Nicodemus, G. and S. Bryant, *The role of hydrogel structure and dynamic loading on chondrocyte gene expression and matrix formation.* Journal of Biomechanics, 2008. **41**(7): p. 1528-1536.

229. Fernandes-Platzgummer, A., et al., *Scale-up of mouse embryonic stem cell expansion in stirred bioreactors.* Biotechnology Progress, 2011. **27**(5): p. 1421-1432.

230. Storm, M.P., et al., *Three-dimensional culture systems for the expansion of pluripotent embryonic stem cells.* Biotechnology and Bioengineering, 2010. **107**(4): p. 683-695.

231. Badenes, S.M., et al., *Scalable Expansion of Human-Induced Pluripotent Stem Cells in Xeno-Free Microcarriers.* Methods in Molecular Biology, 2014: p. DOI: 10.1007/7651_2014_106.

232. Ting, S., et al., *Differentiation of human embryonic stem cells to cardiomyocytes on microcarrier cultures.* Current Protocols in Stem Cell Biology, 2012: p. 21:D:1D.7:1D.7.1–1D.7.14.

233. Laflamme, M.A., et al., *Cardiomyocytes derived from human embryonic stem cells in pro-survival factors enhance function of infarcted rat hearts.* Nature Biotechnology, 2007. **25**(9): p. 1015-1024.

234. Anderson, D., et al., *Transgenic enrichment of cardiomyocytes from human embryonic stem cells.* Molecular Therapy, 2007. **15**(11): p. 2027-2036.

235. Hattori, F., et al., *Nongenetic method for purifying stem cell–derived cardiomyocytes.* Nature Methods, 2009. **7**(1): p. 61-66.

236. Van Hoof, D., et al., *Identification of cell surface proteins for antibody-based selection of human embryonic stem cell-derived cardiomyocytes.* Journal of Proteome Research, 2010. **9**(3): p. 1610-1618.

Appendix: List of Publications

Journal papers:

1. A. Teo, A. Mantalaris, Y.F. Zhou, J.-C. Wang, M. Chong, M. Lim, Low intensity pulsed ultrasound stimulation enhances cardiac differentiation of embryonic stem cells. In submission to PLOS One.

2. A. Teo, A. Mantalaris, M. Lim, Influence of culture pH on proliferation and cardiac differentiation of murine embryonic stem cells. Biochemical Engineering Journal, 2014. 90: 8-15

3. A. Teo, A. Manatalaris, K. Song, M. Lim. A novel perfusion bioreactor for cardiomyogenesis of embryonic stem cells. Biotechnology Letters, 2014. 36 (5): 947-960

4. A. Teo, A. Mantalaris, M. Lim, Hydrodynamics and bioprocess considerations in designing bioreactors for cardiac tissue engineering, Journal of Regenerative Medicine & Tissue Engineering, 2012. 1: 4.

Conference presentations:

1. A Teo, A Mantalaris, Y Zhou, M Lim, Ultrasound Stimulation For Cardiomyogenesis From Embryonic Stem Cells. TERMIS Eu 2013, Istanbul, Turkey, 2013.

2. A Teo, M Lim, A Mantalaris. A novel perfusion bioreactor in cardiomyogenesis. TERMIS World Congress, Vienna, Austria, 2012